Characterization of avian reovirus recombination groups C, F, and G temperature-sensitive mutants

By

Anh Thuy Tran

A Thesis
Submitted to the Faculty of Graduate Studies
In Partial Fulfillment of the Requirements for the Degree of

Master of Science

Department of Medical Microbiology and Infectious Diseases
University of Manitoba
Winnipeg, Manitoba
Canada

THE UNIVERSITY OF MANITOBA

FACULTY OF GRADUATE STUDIES

*****

COPYRIGHT PERMISSION

Characterization of avian reovirus recombination Groups C, F, and G temperature-sensitive mutants

BY

Anh Thuy Tran

A Thesis/Practicum submitted to the Faculty of Graduate Studies of The University of Manitoba in partial fulfillment of the requirement of the degree

MASTER OF SCIENCE

CONTENTS

LIST OF FIGURES

LIST OF TABLES

LIST OF ABBREVIATIONS

ARV	avian reovirus
ATP	adenosine triphosphate
ATPase	adenosine triphosphatase
Ab	antibody
BRV	baboon reovirus
CPE	cytopathic effect
CSF	cerebrospinal fluid
CNS	central nervous system
d.p.i	days post infection
ddH_2O	double-distilled water
ds	double-stranded
DNA	deoxyribonucleic acid
eIF-2	early initiation factor 2
EOP	efficiency of plating
EOY	efficiency of yield
EM	electron microscope(y)
h	hour(s)
ISVP	intermediate (infectious) subviral particle
Ig	immunoglobulin
JAM	junction adhesion molecule
kDa	kilo-Daltons
LB	Luria-Bertani media
mRNA	messenger ribonucleic acid
MOI	multiplicity of infection
MW	molecular weights
MRV	mammalian reovirus virus

NTPase	nucleoside triphosphatase
NTP	nucleoside triphosphate
NBV	Nelson bay virus
OD	optical density
ORF	open reading frame
PBS	phosphate buffered saline
PCR	polymerase chain reaction
PKR	cellular dsRNA-binding protein
PFU	plaque forming unit
RBD	dsRNA-binding domain
QM5	continuous quail fibrosarcoma cell line
RT-PCR	reverse-transcription polymerase chain reaction
RNA	ribonucleic acid
RdRp	RNA-dependent-RNA-polymerase
REO	respiratory enteric orphan
RNA^+	indication of genomic dsRNA production
RNA^-	indication of inability to produce genomic dsRNA
Sf9	*Spodoptera frugiperda* 21 cell clone
ss	single-stranded
SDS	sodium dodecyl sulfate
SDS-PAGE	sodium dodecyl sulfate polyacrylamide gel electrophoresis
T3D	mammalian reovirus serotype 3 Dearing
TEM	transmission electron microscope
ts	temperature-sensitive
UTR	untranslated region

ACKNOWLEDGEMENTS

I would like to express my deepest gratitude to my advisor, Dr. Kevin M. Coombs, an exemplary figure of a compassionate and devoted mentor. He has shown me that research consists not only of the arduous work but also the consideration, devotion, and attention to those working with and around us. His guidance and encouragement is eternally appreciated.

I extend my thanks to past and present members of the Coombs' lab for their companionship, support, and advice. In no particular order, they are: Ita Hadžisejdić, Lindsay Noad, Laura Hermann, Wanhong Xu, Jieyuan Jing, Trina Racine, Chris Lindquist, and Jason Sneath.

A special thank you to Dr. Paul Hazelton for his friendship, advice, and help throughout my studies. His sense of humour is always a joy to encounter in the department. I extend my thanks to Dr. Deborah Court; although not directly involved in my studies, her friendship is greatly valued.

A sincere thank you goes to my Committee members Dr. Heinz Feldmann and Dr. Lorrie Kirshenbaum for their guidance and insightful discussions. I would especially like to thank Dr. Heinz Feldmann for his support and help both inside and outside of my work.

Last but certainly not least, I would like to thank my parents and sister most of all. They are the very reasons that keep me going after each and every challenge I face, both academically and in life.

DEDICATION

To the three people that mean the world to me,

my parents and sister.

A promise made is a promise kept.

ABSTRACT

Reovirus infection has long been a classical experimental system for studying the role of individual viral genes and the proteins they encode during distinct stages of viral replication and assembly. Avian reoviruses (ARV) are ubiquitous in commercial poultry and are frequently isolated from the gastrointestinal and respiratory tracts of chickens with acute infections such as viral arthritis/tenosynovitis and gastroenteritis. Despite the fact that ARV pathogenesis has been extensively described, and has a significant impact on the economy, the basic aspects of its biology such as viral factors that influence ARV-host cell interactions and pathogenesis remain poorly understood. However, through the use of temperature-sensitive mutants, significant progress is being made into understanding the processes of replication and assembly in avian reoviruses. A cross-infection was carried out using the wild-type of a different serotype ARV176 with mutant *tsC37* at three different MOI ratios. dsRNA was extracted from isolated clones to obtain electropherotype profiles from which reassortants were identified. The temperature-sensitivty of each reassortant was determined by efficiency of plating (EOP) at permissive temperature and non-permissive temperatures. *tsC37*, prototype of recombination group C mutants, was mapped to the S3 gene, which encodes for the major outer capsid protein σB. Both *tsC37* and *tsC287* S3 genes were sequenced to locate a missense mutation at nucleotide position 871 and 872, respectively, which resulted in an amino acid

transition from Pro_{281}-to-Thr and Pro_{281}-to-Leu, respectively. This amino acid Pro_{281} was found to be highly conserved among ortheoreoviruses and orbiviruses. Mutated ARV amino acids were placed into the homologous MRV σ3 crystal structures to infer effects. Preliminary electron microscopy of *tsC37* infection at nonpermissive temperature suggested primary production of core-like structures that lack genomic content. Thus, recombination group C *ts* mutants represent novel orthoreovirus clones defective at late stage of assembly. Two additional ARV mutants, *tsF206* and *tsG247* were recently mapped to the L3 and S4 genes, respectively. These *ts* mutants are excellent tools to delineate ARV assembly and replication mechanisms.

PART I | INTRODUCTION

1.1 *Reoviridae:* A Perspective

Viruses with double-stranded (ds) RNA genomes represent one of the marvels of evolution in their ability to exploit unique strategies for genome organization and replication. The dsRNA viruses include several human pathogens, most notably the human rotaviruses and Colorado tick fever virus in addition to numerous pathogens of other organisms including mammals, birds, fish, insects, and plants. More significantly, studies of the dsRNA viruses have contributed a number of fundamental concepts to the fields of virology and molecular biology.

The family *Reoviridae* is a significant group of dsRNA viruses since it is the only family (out of six dsRNA virus families) known to infect mammals (Nibert and Schiff 2001). Reoviruses provided one of the first systems for *in vitro* studies of RNA synthesis (Borsa *et al.* 1968; Skehel and Joklik 1969; Shatkin and Brody 1990) and evidence for the 5′ cap structure on eukaryotic messenger RNAs (mRNAs), its mechanism of synthesis, and its importance in mRNA translation (Furuichi *et al.* 1975). Early evidence for the consensus sequence for translation initiation in eukaryotic mRNAs also was obtained from work on reoviruses (Kozak and Shatkin 1978). The use of reassortant genetics to identify allelic differences in reovirus genome segments, that segregate with phenotypic

differences between reovirus strains (Sharpe and Fields 1981), demonstrated the value of genetic approaches to virology at a time when such approaches were not yet developed for many other animal viruses. Moreover, several of these early genetic studies with reoviruses concerned the basis of viral pathogenesis and yielded some of the first evidence for the role of animal virus receptor-binding proteins in tropism and/or virulence (Weiner *et al.* 1980). Studies with reoviruses also provided early evidence for the role of M cells in viral penetration of the mucosal barrier during entry into an animal host (Wolf *et al.* 1981).

Reovirus infection has long been a classical experimental system for studying the role of individual viral genes and the proteins they encode during distinct stages of viral pathogenesis *in vivo* (reviewed in Tyler 2001). Although many *Reoviridae* are important pathogens, most of the work on their molecular biology has been carried out on the mammalian reoviruses, the prototype of the genus *Orthoreovirus.* Mammalian reoviruses are a good model for studies on viral replication and pathogenesis, primarily because they were the first to be discovered (Stanley *et al.* 1953) and because they grow best in cultured cells. Other significant genera of this virus family are the *Orbivirus*, to which some important animal pathogens like bluetongue virus are classified (Roy 2001), and the *Rotavirus*, which includes the important human infantile gastroenteritis viruses (Estes 2001). Additionally, new genera have been proposed such as *Mycoreovirus* (Enebak 1992; Osaki *et al.* 2002; Hillman *et al.* 2004) and

Dinovernavirus (Attoui *et al.* 2005). Of interest is the *Orthoreovirus* genus, which is divided into 3 subgroups: mammalian reovirus (MRV) species (subgroup 1), avian reovirus and nelson bay virus (NBV) species (subgroup 2), and baboon reovirus (BRV) species (subgroup 3) (Chappell *et al.*, 2005).

The avian orthoreoviruses remain less well characterized at the molecular level than the mammalian isolates. Presently, studies once carried out on MRV have now been extended to ARV, because both avian and mammalian reoviruses have similar features in their structures and molecular compositions (Zhang *et al.* 2005). Despite certain similarities, they differ in host range and in biological and serological properties (Spandidos and Graham 1976; Schnitzer 1985). Most avian orthoreoviruses promote the formation of multinucleated syncytia within infected cultures and are thus said to be fusogenic. Unlike the nonfusogenic mammalian orthoreoviruses, they lack the capacity to agglutinate red blood cells (Ni and Ramig 1993; Fields 1996) and thus may lack the capacity to bind the cellular carbohydrate receptors that have been implicated in hemagglutination by the nonfusogenic mammalian orthoreoviruses (Fields 1996).

1.2 Reovirus pathogenesis

Reoviruses were originally called respiratory enteric orphans (REO) on the basis of their repeated isolation from respiratory and enteric tracts of asymptomatic children (Sabin 1959; Tai *et al.* 2005). Currently, prototypic mammalian orthoreoviruses have not been definitively confirmed to cause any

illnesses from its infection of the respiratory and intestinal tracts of humans and other vertebrate animals. Nevertheless, Tyler *et al.* (2004) reported an association of serotype 3 reoviruses as a cause of meningitis in humans. The novel reovirus strain was isolated from a 6.5-week-old child with meningitis. Designated T3/Human/Colorado/1996 (T3C/96), it was found to be capable of systemic spread in newborn mice after peroral inoculation and produces lethal encephalitis. Moreover, four other studies have described the isolation of reovirus directly from cerebrospinal fluid (CSF) or neural tissue samples obtained from individuals with meningitis or encephalitis (Krainer and Aronson 1959; Joske *et al.* 1964; Johansson *et al.* 1996; Hermann 2005). In addition to reovirus, other members of the *Reoviridae* family have been associated with the central nervous system (CNS) disease in humans. Rotavirus, an important cause of gastroenteritis in children (reviewed in Kapikian *et al.* 2001) has been implicated in a few cases of encephalitis (Wong *et al.* 1984; Lynch *et al.* 2001), as has Colorado tick fever virus, a member of the *Coltivirus* genus of the *Reoviridae* (Klasco 2002).

In contrast to human reovirus infection, infection of newborn mice is highly pathogenic. After oral inoculation in mice, reovirus is taken up by intestinal M cells (Wolf *et al.* 1981; Amerongen *et al.* 1994) and undergoes primary replication in lymphoid tissue of Peyer's patches. Reoviruses can either spread to the CNS hematogenously and infect ependymal cells (Weiner *et al.* 1980; Tyler *et al.* 1986), which results in hydrocephalus (Weiner *et al.* 1977), or spread to the

CNS neurally and infect neurons (Weiner *et al.* 1980; Tyler *et al.* 1986; Morrison *et al.* 1991), leading to lethal encephalitis (Weiner *et al.* 1977; Tardieu *et al.* 1983). The pathways of viral spread in the host (Tyler *et al.* 1986) and pattern of neurotropism (Weiner *et al.* 1980; Dichter and Weiner 1984) segregate with the viral S1 gene, which encodes the viral attachment protein (Weiner *et al.* 1980a; Lee *et al.* 1981). The σ1 protein determines the CNS cell types that are specifically targeted during reovirus infection, presumably by its capacity to bind receptors expressed on specific CNS cells (Tyler 2004).

Avian reoviruses, on the other hand, have been directly implicated in the pathogenesis of a range of disease states, including viral arthritis/tenosynovitis (van der Heide 1977; Olson 1978; Rosenberger *et al.* 1989a), gastroenteritis, hepatitis, myocarditis, and respiratory illness (Olson 1978) in chickens and infectious enteritis in turkeys (Gershowitz and Wooley 1973). Other illnesses reported include the pale bird syndrome and malabsorption or runting-stunting syndrome (Kouwenhoven *et al.* 1978). Avian reoviruses are ubiquitous in commercial poultry and are frequently isolated from the gastrointestinal and respiratory tracts of chickens with acute infections (Rosenberger and Olson 1991). ARV infections spread through the fecal-oral route via contaminated food and water sources (Jordan and Pattison 1996). On the basis of neutralization, there are at least 11 ARV serotypes (Glass *et al.* 1973; Heironymus *et al.* 1983; Rosenberger *et al.* 1989).

Viral arthritis/tenosynovitis in chickens, first recognized in 1959 (Olson 1959), continues to be a major focus for researchers in the poultry industry. Young birds infected with this disease usually show a general lack of performance that includes decreasing weight and poor feed conversion rates, leading to poor health conditions that in the end add up to low marketability of the bird.

Another aspect in ARV pathogenesis deals with the virus' ability to replicate in macrophages (O'Hara *et al.* 2001). Recently, ARV has been reported to perhaps cause immunosuppression in chickens (Neelima *et al.* 2003), which may predispose the host to other infectious agents and stresses present in the environment. Chickens infected with reovirus in the field were seen to be more vulnerable to secondary bacterial infections with *Staphylococcus aureus* (Neelima *et al.* 2003). Although the occurrence is well documented, the molecular mechanism of ARV immunsuppression in chickens is still poorly defined.

In general, the diseases caused by ARV in chickens, although associated with low mortality, often produce high morbidity rates resulting in significant economic losses (Olson and Solomon 1968; Glass *et al.* 1973; Calnek *et al.* 1997). Therefore attempts at producing vaccines to combat these illnesses in chickens continue to be a major objective. Despite the fact that ARV pathogenesis has been extensively described, and has a significant impact on the economy, the basic aspects of its biology such as viral factors that influence ARV-host cell interactions and pathogenesis remain poorly understood.

1.3 Avian Reovirus Structure

Like mammalian reovirus, ARV is a non-enveloped virus with 10 linear double-stranded RNA gene segments surrounded by a double concentric icosahedral capsid shell (inner shell or core and the outer shell) of 70-80 nm diameter (Spandidos and Graham 1976; Nibert and Schiff 2001). The genomic segments of avian reovirus can be resolved into three size classes based on their electrophoretic mobility, designated L (large), M (medium), and S (small) (Spandidos and Graham 1976; Gouvea and Schnitzer 1982). In total, the genomic composition includes 3 large segments (Ll, L2, L3), 3 medium sized segments (Ml, M2, M3), and 4 small segments (S1, S2, S3, S4). Nine of the gene segments are monocistronic and encode a single different protein (Gouvea and Schnitzer 1982) while S1 is tricistronic with partially overlapping open reading frames (ORFs) that encode for three proteins (Bodelón *et al.* 2001; Shmulevitz *et al.* 2002) (Figure 1A).

Three λ polypeptides are encoded by the L genes (λA, λB and λC; molecular weights (MW) 130–150 kDa), three μ polypeptides by the M genes (μA, μB and μNS; MW 70–80 kDa) and four σ polypeptides by the S genes (σA, σB, σNS and σC; MW 30–50 kDa) (Schnitzer 1985; Varela and Benavente 1994). Two small non-structural proteins, p10 and p17, also are encoded by the avian reovirus genome segment S1 (Bodelon *et al.* 2001; Shmulevitz *et al* 2002), and a smaller version of the non-structural protein μNS, termed μNSC, is expressed by

A.

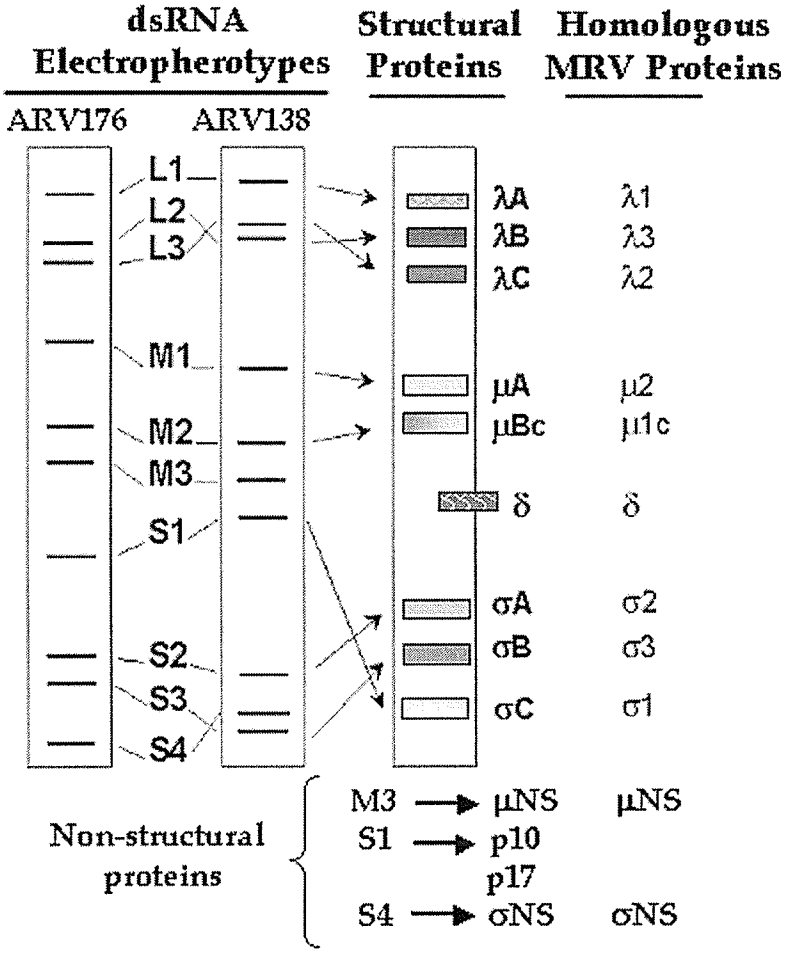
dsRNA Electropherotypes
Structural Proteins
Homologous MRV Proteins
ARV176
ARV138
L1
L2
L3
M1
M2
M3
S1
S2
S3
S4
λA
λB
λC
μA
μBc
δ
σA
σB
σC
λ1
λ3
λ2
μ2
μ1c
δ
σ2
σ3
σ1
Non-structural proteins
M3 → μNS
S1 → p10
p17
S4 → σNS
μNS
σNS

B.

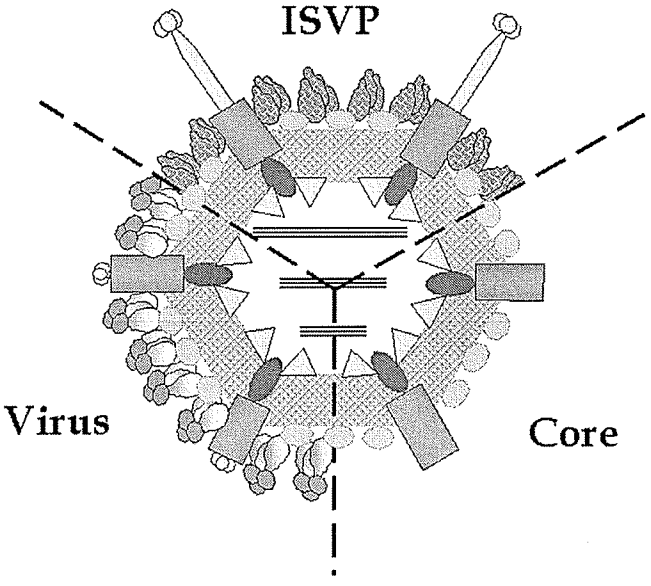
ISVP
Virus
Core

Figure 1. Diagrammatic representation of avian reovirus structure, electropherotype, and protein profile. (A) electropherotypes of ARV176 and ARV138, with corresponding proteins encoded by each gene segment. (B) Composite diagram of reovirus particle types: virus, infectious subviral particle (ISVP), and core. Proteins in (A) are coloured in correlation to its position in the virion cartoon in (B).

the M3 gene in both infected and transfected cells (Touris-Otero *et al.* 2004). Therefore, the previously reported coding capacity of the avian reovirus genome is now expanded to 13 proteins of which 8 are structural. The avian reovirus structural proteins λA, λB, μA and σA are core components, while μB, μBC, σB and σC are present in the outer virion shell. Finally, the core spike protein λC, which is the avian reovirus guanylyltransferase (Hsiao 2002), extends from the inner core to the outer capsid (Martínez-Costas *et al.* 1997) (Table 1).

Although the mammalian reovirus S1 genome segment has two overlapping, out-of-phase ORFs that express one structural (σ1) and one non-structural protein (σ1s) (Ernst and Shatkin 1985; Jacobs and Samuel 1985; Duncan *et al.* 1990; Nibert *et al.* 1990), the S1 segment of ARV has recently been reported to contain three partially overlapping ORFs, which are highly conserved in all ARV strains (Bodelón *et al.* 2001; Shmulevitz *et al.* 2002). The three ORFs encode for the structural protein σC and two small non-structural proteins, p10 and p17 (Bodelón *et al.* 2001). The fact that these proteins are specified by out-of-phase reading frames suggests that p10, p17, and σC are structurally and functionally unrelated to each other (Shmulevitz *et al.* 2002).

The p17 polypeptide has no significant sequence similarity to other known proteins, so its amino acid sequence offers no clues about its function. On the other hand, the fact that the p17 ORF is conserved in every avian reovirus S1 gene sequence reported so far suggests that p17 plays an important function in virus-host interactions (Costas *et al.* 2005). One study demonstrated that p17 is a

Table 1. Properties of Avian Reovirus.

Gene segment	Protein	Location in virion	Location[a]	Function or property	References
L1	λA	Inner capsid	V, I, C	Unknown	
L2	λB	Inner capsid	V, I, C	Unknown	
L3	λC	Inner capsid, core spike	V, I, C	Guanylyltransferas, methyltransferases, Caps mRNA	• Hsiao 2002; • Martínez-Costas *et al.* 1995
M1	μA	Inner capsid	V, I, C	unknown	
M2	μBc	Outer capsid	V	cleaved into fragments, role in cytosol entry	• Duncan 1996
M3	μNS	Non-structural	–	Role in inclusion body formation	• Tourís-Otero *et al.* 2004
S1	σC	Outer capsid	V, I	Promote attachment to host cell	• Martinez-Costas 1997; • Shapouri *et al.*, 1996
	p10	Non-structural	–	Involved in syncytia formation	• Duncan *et al.* 1990
	p17	Non-structural	–	Role in cell growth inhibition?	• Liu *et al.* 2005
S2	σA	Inner capsid	V, I, C	Binds dsRNA; NTPase activity	• Gonziález-López *et al.* 2003 • Yin *et al.* 2002
S3	σB	Outer capsid	V	Unknown	
S4	σNS	Non-structural	–	Binds ssRNA, unknown role in RNA assortment	• Touris-Otero *et al.* 2005

[a]V, virion; I, ISVP; C, core

nuclear targeting protein, which shuttles between the nucleus and the cytoplasm in a transcription-dependent manner and that exits the nucleus via a CRM1-independent pathway (Costas *et al.* 2005). Additionally, p17 has been implicated with cell growth retardation via the activation of p53 pathway (Liu *et al.* 2005). The functions for p10 and σC proteins will be discussed later.

ARV can be found to exist in 4 morphological states, similar to MRV: virion, ISVP, core, and top component (Figure 1B). The mature virion consists of the inner and outer capsid layers as mentioned above. The proteolytic degradation of certain outer capsid proteins (namely σB is degraded, μBc is cleaved to δ, and σC lengthens) *in vitro* or during infection yields an intermediate (infectious) subviral particle (ISVP). Next, ISVP loses σC; μBc gets cleaved further to yield the δ′ protein, believed to be an intermediate step which leads to the generation of the core (Duncan 1996), the final uncoated form found within the host cytoplasm. The fourth structure, top component, obtained its name because of its low buoyant density in cesium chloride gradients relative to a mature virus. The top component is a defective particle produced during infection that retains the double capsid but lacks the dsRNA genome; hence the lower buoyant density.

Previously, ARV structure and protein distribution were based on correlation to the MRV crystal structure. In regards to this model, basic structural analyses have noted only small differences from MRV. Hence, recent cryoelectron microscopy imaging obtained for the avian orthoreovirus ARV138

revealed a virion with structure very closely related to MRV and only minor differences (Zhang *et al.* 2005). Nevertheless, the details of ARV composition, as well as the mechanisms of assembly, require a lot more investigation.

Despite increasing interest in avian orthoreoviruses, knowledge about ARV remains relatively behind that of MRV. Most of what is known about ARV replication and protein functions are speculations from studies conducted on the mammalian reovirus. Hence, much, but not all, of the biological viral structures and functions discussed in the latter part of this introduction will be assumptions derived from mammalian reovirus studies based on its similarity to avian reoviruses, where known differences will be indicated.

1.3.1 The Core Structure

Structural proteins ARV λA, λB, λC, μA, and σA are the core proteins with λA and σA as the major core proteins (Figure 1A). λC pentamers (spikes), λB and μA minor internal proteins are associated only at the vertices. The complete core is formed with spike proteins ARV λC that protrude from the 12 vertices. Moreover, λC protein of the inner capsid crosses the outer layer to be exposed at the surface of the virion (Martínez-Costas *et al.* 1997). Structural studies have indicated that all members of the *Reoviridae* family contain an icosahedral core with $T = 1$ symmetry; which, in the case of ARV, consists of 120 inner capsid

protein subunits λA organized as 60 assymmetric dimers surrounding the genome (Nibert and Schiff 2001; Zhang *et al.* 2005).

Crystallographic and cryoelectron microscopic analysis of several MRV have indicated the dsRNA genome is organized in partially ordered concentric layers within the core (Reinisch *et al.* 2000); recent cryoelectron microscopy of ARV138 revealed a similar genome packaging structure in avian reoviruses (Zhang *et al.* 2005). It is suggested each segment may exist as a tightly wound spiral around one of the 12 RdRp-capping complexes at the fivefold-axes of the core. Also associated with the fivefold-channels are one or more copies of the viral protein responsible for capping viral messenger RNAs, which may extend through the core and contact a surrounding capsid shell of the virion. The fact that the icosahedral nature of the core restricts the number of RdRp-capping complexes to 12, may explain why no reovirus has been isolated which contains more than 12 genome segments. On the other hand, there are reoviruses with less than 12 genomic segments, which indicate not all of the 12 potential sites in the core may be occupied by dsRNA (Patton and Spencert 2000).

1.3.2 Outer Capsid Structure

The outer capsid plays a significant role in recognizing host cells and allowing the release of the viral core into the cytoplasm. X-ray crystallography has been determined for all the MRV outer capsid proteins (Olland *et al.* 2001;

Chappell *et al.* 2002; Liemann *et al.* 2002), while crystallography for ARV outer capsid proteins remains to be ascertained. Therefore, the following discussions will mainly involve evidence established for MRV, from which understanding for ARV proteins are inferred.

The outer capsid consists mainly of MRV μ1 (ARV μB equivalent) and MRV σ3 (ARV σB) at 600 copies each (Dryden *et al.* 1993; Zhang *et al.* 2005) and up to 36 copies of the cell attachment protein MRV σ1 (ARV σC) (Weiner *et al.* 1980a; Lee *et al.* 1981; Strong *et al.* 1991). Similar to MRV μ1 protein cleavage to yield μ1C, a major μ class structural protein, ARV μB (present in minor amounts relative to its cleavage product) is cleaved to yield μBc, also a major μ class structural protein, thus adding to the similarities between avian and mammalian reoviruses in protein composition (Ni *et al.* 1993). In both MRV and ARV virions, outer capsid proteins, ARV μB (MRV μ1) and ARV σB (MRV σ3), are arranged in an incomplete $T = 13$ (*laevo*) lattice (Dryden *et al.* 1993; Zhang *et al.* 2005).

The outer capsid proteins MRV μ1 (μB in ARV) and MRV σ3 (σB in ARV) associate with each other, which causes important conformational changes to both proteins (Mabrouk and Lemay 1994; Shepard *et al.* 1996), to form heterohexamers ((MRV μ1/σ3)$_3$) complexes (Dryden *et al.* 1993; Liemann *et al.* 2002) that are essential for assembly of the outer shell onto nascent cores (Fields *et al.* 1971; Shepard *et al.* 1995; Shing and Coombs 1996).

1.3.2.1 The ARV σB/ MRV σ3 Protein

Encoded by the S3 genome, ARV σB is 367 amino acids in length with a molecular weight of 40 kDa (Schnitzer 1985; Varela and Benavente 1994); compared to MRV σ3, which is 365 amino acids in length, 41 kDa and encoded by the S4 genome segment (Giantini *et al.* 1984; Mendez *et al.* 2003). Both proteins are believed to be N-terminally acetylated proteins and also contain a tightly bound zinc ion (Huismans and Joklik 1976; Yue and Shatkin 1997). The monomer of the major outer capsid protein is a bi-lobed structure, organized around a central helix spanning the length of the protein. Currently, the crystal structure for ARV σB is unavailable; however, MRV σ3 crystal structure revealed a protein with an overall dimension of ~76 x 35 x 35 Å, which narrows at the center to give a smaller and a larger lobe. Although the N-terminal residue is in the small lobe and the C-terminal residue is in the large lobe, the two lobes in MRV σ3 do not strictly correspond to the sequential N- and C-terminal sections of the protein. Additionally, the joint between the lobes is believed to confer some flexibility to the protein (Olland *et al.* 2001).

The small lobe consists of two segments (residues 1-90 and 287-336) of approximately 140 residues and a CCHC zinc-binding motif. Similarly, the large lobe also is constituted of two separate segments (residues 91-286 and 337-365) approximately 225 residues in total (Figure 2). Additionally, the extended loops observed in the large lobe are speculated to be the sites of proteolysis (Olland *et*

Figure. 2. Crystal structure cartoon presentation of the four different segments that constitute the large and small lobe of a MRV σ3 monomer (PDB # 1FN9), as determined by Olland *et al.* (2001). ARV σB structure is believed to be similar. In the large lobe, colours ruby and yellow highlight residues 91-286 and residues 337-365, respectively. In the small lobe, colours green and wheat highlight residues 1-90 and residues 287-336, respectively. Images created with PyMOL (DeLano 2004).

al. 2001), a significant process that occurs during reovirus entry. These characteristics are expected to be similar in ARV σB.

1.3.2.2 dsRNA-binding

MRV σ3 is a dsRNA-binding protein that targets RNA duplexes of approximately 32-45 bp in a manner independent of RNA sequence (Huismans and Joklik 1976; Yue and Shatkin 1997). σ3 has a tendency to dimerize in solution, which suggests that the dsRNA-binding form of the protein is dimeric (Figure 3). Site-directed mutagenesis has implicated several basic amino acids in dsRNA binding, including Lys_{293} (Denzler and Jacobs 1994; Mabrouk *et al.* 1995). Lys_{293} protrudes from the surface and makes no contacts with other atoms in the structure (Olland *et al.* 2001). A map of surface electrostatic potential in the MRV σ3 dimer shows a large positively charged patch that spans the two subunits on one of the broad surfaces. This patch is speculated to act as a surface for dsRNA binding, which might involve non-specific interaction with the backbone of the RNA duplex. Residue Lys_{293} is part of this patch (Olland *et al.* 2001).

MRV μ1 plays a regulatory role with regards to dimer/RNA binding. When sufficient μ1 is present, formation of MRV μ1-σ3 complexes will compete with MRV σ3 dimer formation and inhibit σ3 binding of dsRNA (Olland *et al.* 2001). dsRNA-binding activities also have been shown for both MRV λ1 and σ2

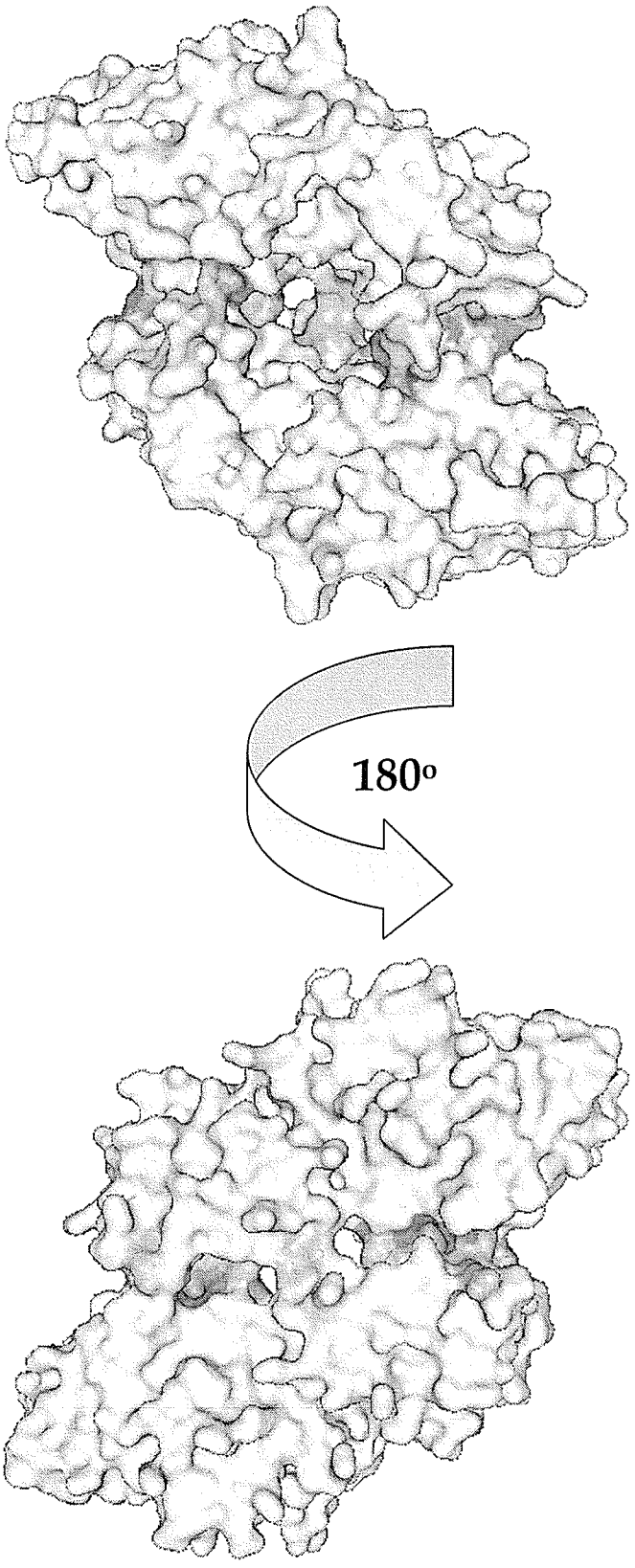
180o

Figure 3. Speculated dimer-binding sites (determined by Olland *et al.* 2001) seen in MRV σ3 dimer crystal structure (PDB # 1FN9). ARV σB dimer binding is believed to be similar. Green and blue colours highlight specific interface residues in the small and large lobes, respectively, involved in dimer binding. Images created with PyMOL (DeLano 2004).

(Schiff *et al.* 1988; Lemay and Danis 1994). In the case with avian reoviruses, σA has been shown to exhibit dsRNA-binding as well (Gonziález-López *et al.* 2003).

At present, the region on MRV σ3 specifically involved in dsRNA-binding has not been decisively determined; however, studies of σ3 structure so far clearly indicate that it is quite different from previously characterized dsRNA-binding domains (RBDs) of other dsRNA-binding proteins such as the cellular PKR (Nanduri *et al.* 1998), the *Xenopus laevis* RNA-binding protein A (Ryter and Schultz 1998), and *Escherichia coli* RNase III (Kharrat *et al.* 1995). Unlike the RBDs of these proteins, which are composed of a three-stranded anti-parallel β-sheet flanked by two helices, MRV σ3 do not form any type of domain or homologous structure (Olland *et al.* 2001).

Like many viral proteins, MRV σ3 (likewise, ARV σB) has multifunctional roles, one of which involves the regulation of cellular antiviral mechanisms. Reoviruses activate host antiviral defense mechanisms by inducing synthesis and secretion of interferon and other cytokines. It has been demonstrated that the dsRNA-dependent protein kinase (PKR) is the main factor acting to restrict reovirus replication upon cell treatment with interferon (Miyamoto and Samuel 1980; De Beneditti *et al.* 1985). The mechanism of PKR inhibition is briefly as follows: in the presence of dsRNA, interferon induces PKR, leading to the phosphorylation of the initiation factor eIF-2 that results in the shut-off of the translational initiation (Hovanessian 1991; Clemens 1996), which in turn inhibits protein synthesis thereby limiting viral spread (Mathews 1996). Studies have

implicated mammalian reovirus protein σ3's ability to bind dsRNA to its role in blocking the dsRNA-dependent activation of PKR and to stimulate translation (Lloyd and Shatkin 1992; Beattie *et al.* 1995; Yue and Shatkin 1997; Bergeron *et al.* 1998). When not in association with MRV μ1, σ3 negates the interferon-induced shutdown of host protein synthesis in the cytoplasm of infected cells by preventing PKR activation via dsRNA-binding (Lloyd and Shatkin 1992; Beattie *et al.* 1995; Schmechel *et al.* 1997; Yue and Shatkin 1997). As with many other biological characteristics and functions shared between these two orthoreovirus species, similar structure and functionality observed in MRV σ3 also are expected to be seen in ARV σB.

1.3.2.3 The μ1-σ3 (ARV μB-σB) Interface

MRV σ3 (ARV σB) association with MRV μ1 (ARV μB) to form the heterohexameric complex is a significant step in both avian and mammalian reovirus replication (Figure 4). Each MRV σ3 contacts two μ1 subunits. The entire complex consists of 3 σ3 and 3 μ1 subunits. The three MRV μ1 molecules are coiled around each other with a right-handed twist, winding from bottom to top of the complex (Liemann *et al.* 2002). The μ1 polypeptide consists of four distinct domains: I, II, and III are predominantly α-helical domains, which constitute the lower part of the μ1 trimer in the heterohexamer complex; a jelly-roll β-barrel forms Domain IV, which makes up the outward facing "head" in the

Figure 4. MRV μ1-σ3 heterohexameric crystal structure (PDB # 1JMU). Each colour (blue, green, and orange) highlights one μ1 subunit. The σ3 subunits are shown in wheat. Images created with PyMOL (DeLano 2004).

complex (Liemann *et al.* 2002). Of particular interest are Domains III and IV, which interact directly with σ3 in the heterohexameric complex. Two discontinuous polypeptide chain segments (279–305 and 515–640), a summation of 125 residues, in Domain III forms a cradle for the base of σ3 (Nibert and Fields 1992), and residues 581–583 anchor σ3 residues 69–71 in a small β sheet—a structure not observed in the dimer (Olland *et al.* 2001). Domain IV (residues 306–514) is a jelly-roll β barrel (Harrison 2001) with three additional β hairpin insertions speculated to participate in MRV μ1-σ3 or μ1-μ1 interactions within the heterohexamer (Liemann *et al.* 2002). Two long β hairpins (approximately at residues 342-350 and 355-360) flank the five-stranded β sheet on the $\mu1_3\sigma3_3$ surface and interact with the large and small lobes, respectively, of two different σ3 molecules. Two additional β hairpins (approximately at residues 502-504 and 507-509) interact with the small lobe of a σ3 subunit (Liemann *et al.* 2002) (Figure 5). Currently, ARV σB and ARV μB structure and heterohexamer complex formation are speculated from data observed in MRV studies.

On the virion, the large lobe of both MRV σ3 and ARV σB forms the knobs visible in cryoelectron microscopy reconstructions of the respective viruses (Dryden *et al.* 1993; Zhang *et al.* 2005). MRV σ3 is thought to undergo a conformational change upon binding to MRV μ1, as demonstrated by heightened protease sensitivity; however that change is believed not to involve major tertiary structural alterations as suggested by the observation that both free and μ1-

Figure 5. Proposed residues in MRV μ1 involved in σ3 binding. One each of MRV μ1 (orange) and σ3 (wheat) subunits from the heterohexameric crystal structure (PDB # 1JMU). Blue and Green β-sheets and pink helices represent proposed residues involved in σ3 interactions. Images created with PyMOL (DeLano 2004).

bound forms of σ3 react with conformation-dependent antibodies (Shepard *et al.* 1995). The smaller, zinc binding lobe of MRV σ3 rests between two MRV μ1 Domain IV (Liemann *et al.* 2002). It remains to be seen whether this characteristic is similar in avian reoviruses.

1.4 Reovirus Attachment and Entry

Specific attachment of viruses to cell-surface receptors is the critical initial step that governs whether an infection will occur or not. Despite the substantial diversity in the types of receptors recognized and the mechanisms of entry employed, overall the strategy to penetrate the cell membrane is the same (reviewed in Stehle and Dermody 2003).

In MRV, several proteins have been identified as possible receptors with which σ1 interacts, but a definitive answer remains to be determined. One such recently identified protein is the junction adhesion molecule (JAM) (Barton *et al.* 2001; Prota *et al.* 2003), where sialic acid appears to be an important component of the receptor(s). A domain in the fibrous tail of serotype 3 Dearing (T3D) σ1 binds to α-linked sialic acid (Barton *et al.* 2001; Prota *et al.* 2003), whereas the head binds to junction adhesion molecule 1 (JAM1) (Barton *et al.* 2001a). JAM1 is an Ig-superfamily member expressed by a variety of cells including dendritic cells (Rescigno *et al.* 2001), epithelial, and endothelial cells (Martin-Padura *et al.* 1998; Liu *et al.* 2000). After receptor binding, virions are taken up into endocytic

compartments, where endosomal proteases digest MRV σ3 (Chang and Zweerink 1971). This proteolytic step can be mimicked *in vitro* by chymotryptic digestion of purified virions (Joklik 1972; Shatkin and LaFiandra 1972), where studies have found that cleavage initiates in a central specific "Hypersensitive Region" (Jané-Valbuena *et al.* 2002) and then proceeds bidirectionally towards the protein's termini (Mendez *et al.* 2003; Hadzisejdić 2005). Similarly, ARV attachment of the mature virion to the target cell, mediated by the σC cell attachment protein (Shapouri *et al.* 1996; Martinez-Costas 1997), facilitates entry via the receptor-mediated endocytosis pathway. However, the specific cellular receptor for ARV σC binding is unknown.

Like most animal viruses, reoviruses are activated for infection by proteolytic cleavages. The acidic environment of the endosome is required to process ARV outer capsid proteins to produce ISVP during viral entry. However, ISVPs of MRV can be generated by extracellular proteolysis in some situations, and the entry of such particles is acid independent and may not require endocytosis (Chang and Zweerink 1971; Nibert and Schiff 2001), thereby allowing it to bypass receptor-mediated endocytosis entry and to fuse directly with the cell membrane. Nevertheless, similar to MRV, cleavage of the avian reovirus major outer capsid protein μBc into δ reveals hydrophobic residues that promote interaction with the endosomal membrane and entry into the cytoplasm (Duncan 1996). Unlike MRV entry, ARV has an additional delayed cleavage of μBc that acts independent of the other cleavage process (where μBc cleaves to δ).

This cleavage gives rise to δ′. The functional significance of undergoing two independent cleavages of μBc is unknown; however, this suggests that δ′ may be an intermediate entry step or a by-product of an unproductive entry pathway (Duncan 1996). Avian reovirus infection can be inhibited by group and serotype specific antibodies, which bind to σB major outer capsid proteins and the cell attachment proteins (σC), respectively (Theophilus *et al.* 1995).

The proteolytic and conformational change to the structure of MRV $\mu1_3\sigma3_3$ heterohexamer indicate likely steps in the molecular mechanism of endosomal penetration. Mammalian reovirus protein σ3 is tightly packed between adjacent μ1 subunits in the heterohexamer, which insinuates that the removal of σ3 will destabilize the μ1 trimer and suggests why proteolysis is required to extract σ3. Although proteolytic removal of σ3 and autolytic cleavage of μ1 render the μ1 trimer metastable, it is believed that some property of the endosome from which the virus escapes must catalyze rearrangement to a penetration-active conformation (Liemann *et al.* 2002). Thus, the structure of the $\mu1_3\sigma3_3$ complex suggests it plays an active role in inserting a reovirus core across cellular or endosomal membrane through major conformational rearrangements and multiple membrane interactions. Proteolytic removal of σ3, in the intestinal lumen or in an endosome, and autolytic cleavage of μ1 primes this complex for penetration, but interactions within the surface lattice of the ISVP hold it in a primed conformation (Liemann *et al.* 2002). The avian reovirus σB protein is

believed to undergo similar proteolytic processes that also lead to conformation changes significant for viral penetration into the cell (i.e. extracellular ISVP) or from the endosome.

1.5 Reovirus Replication

Currently, little is known about ARV replication in contrast to the extensively characterized mechanisms of MRV replication and assembly. Similarities between ARV and MRV viral compositions, such as protein distributions and functions (Zhang *et al.* 2005), suggest they may possess a common replication cycle. Both ARV and MRV replicate in the cytoplasm of infected cells. From studies with MRV, it is established that the segmented dsRNA genomes of reoviruses are never detected free in the cytoplasm but are transcribed and replicated within viral capsids by RdRp (Patton and Spencert 2000). Hence, the uncoating of reoviruses is incomplete where the final entry product is the core, which carries all enzymes for transcription of positive (+) sense mRNAs (Patton and Spencert 2000).

1.5.1 The Core: An Active Transcriptional Complex

From mammalian reovirus studies, it is known that upon infection the RNA-dependent-RNA-polymerase (RdRp) of the core is activated to synthesize mRNAs that are capped and released into the cytoplasm via channels at the five-

fold axes of the core. During transcription, channels penetrating the core and the overlaying protein layer allow entry of the nucleoside-triphosphate substrates for the RdRp. Essentially, the core may be viewed as a collection of 12 polymerase units, where each represents one of the core pentamers, which operate independently yet simultaneously to transcribe the genome segments. Due to the structural organization of the transcriptionally-active particle, only a single type of mRNA can pass through any one of the fivefold channels of the core. Studies have noted that mRNAs are not made in equimolar amounts, which suggests the polymerase units of the core function independently of one another—contrary to the production of genome segments that are produced in equimolar levels during RNA replication (Patton and Spencert 2000).

Collectively, RdRp, helicase, and RNA trisphosphatase activities are found within the MRV λ3 (ARV λB) and cofactor MRV μ2 (ARV μA). Biochemical studies have demonstrated that the ARV core protein λC (equivalent to MRV λ2) possesses guanylyltransferase (Hsiao *et al.* 2002) and methyltransferase activities (Spandidos and Graham 1976; Martínez-Costas *et al.* 1995). This ARV protein also catalyzes the addition of a type-1 5′ methylated cap to mRNA transcripts (Martínez-Costas *et al.* 1995). Most of the avian reovirus mRNAs are monocistronic and begin translation from the AUG codon closest to the 5′-terminal cap. Viral mRNAs and the positive strand of dsRNA segment lack a poly(A) tail at their 3′ end. However, there is evidence of oligoadenylates

within ARV to suggest the virion has poly(A) polymerase activity (Spandidos and Graham 1976).

In addition to transcription and capping activities, mammalian reovirus cores have been proposed to possess two other functions: an RNA helicase activity (Rankin *et al.* 1989) and a nucleoside triphosphate (NTPase) activity (Kapuler *et al.* 1970). It was later suggested that the NTPase activity represents the capping-associated RNA triphosphatase (Furuichi *et al.* 1976). However, the NTPase in cores was found to exhibit a preference for ATP (Noble and Nibert 1997), whereas the substrate for this RNA triphophatase, the 5'-terminal nucleotide in each of the 10 reovirus mRNAs, is a guanosine (Antczak *et al.* 1982). This suggests that the NTPase may present a separate activity from the RNA triphosphatase. ATPase activity in mammalian reovirus cores is genetically associated with λ1 major core shell protein (Noble and Nibert 1997). Studies have suggested that the ATPase activity remains latent in reovirus virions and ISVPs but is activated when MRV μ1 undergoes protease-mediated degradation that occurs during production of cores, suggesting that μ1 may play a role in regulating the ATPase (Noble and Nibert 1997).

ARV core protein σA, similar to its counterpart σ2 of MRV, is a dsRNA-binding protein. The σA protein binds dsRNA in a sequence non-specific manner, and its association with the viral genome segments prevents activation of host dsRNA-dependent enzymes that inhibit protein synthesis (Gonziález-López *et al.* 2003), a function also carried out by ARV σB. Because σA is one of

the core proteins of ARV, it is also suspected that this protein may contain enzymatic activities, including NTP hydrolysis activity. σA was shown to contain the active site of the nucleotidyl phosphatase activity, but the functions of the nucleotidyl phosphatase activities of σA in ARV infection are unknown. It is believed the hydrolysis of NTPs by σA may be important for generating energy that is used for transcription and replication of the viral genome (Yin *et al.* 2002). Since ARV cores are structurally and functionally similar to MRV cores, it is possible that other ARV core proteins are also associated with NTPase activity in addition to σA.

Previous studies demonstrated that avian reovirus is highly resistant to the antiviral effects of interferon and suggested that the dsRNA-binding σA protein, in addition to σB, might play an important role in that resistance (Gonziález-López *et al.* 2003). σA has been observed to have the ability to reverse the interferon-induced antiviral state of the infected cell by down-regulating PKR activity in a manner similar to other virus-encoded dsRNA-binding proteins (Gonziález-López *et al.* 2003).

1.5.2 Stages in Replication: An Overview

Presently, the specific mechanisms of ARV assembly and replication have yet to be fully elucidated; however, ongoing studies have suggested its stages of replication are similar to that deduced in MRV; therefore, an overview of the

mammalian reovirus replication cycle may illuminate mechanisms involved in avian reovirus replication. MRV replication occurs in three stages (Figure 6): primary transcription, secondary transcription, and encapsidation. During the first stage, MRV genes L1, M3, S3, and S4 are initially transcribed from the parental negative (-) RNA template to produce 5′ capped mRNAs, which are translated by host translational machinery to give early proteins λ3, μNS, σNS, and σ3, respectively. These proteins stimulate primary transcription from all 10 template (-) RNAs. These 5′ capped mRNAs also act as templates for the synthesis of genomic dsRNA later in the replication cycle. A single copy of each (+) RNA strand is assorted into a transcriptase/assortment complex where synthesis of the complementary negative strand occurs (Silverstein *et al.* 1976).

Next is secondary transcription, which results in the production of uncapped viral mRNAs from newly synthesized (-) RNA strand template (Patton and Spencert 2000). The switch from cap-dependent to cap-independent mRNA synthesis is suspected to involve the intracellular distribution of MRV σ3 and its interaction with μ1c in addition to certain cellular interferon-regulated gene products that include PKR and RNase-L (Schmechel *et al.* 1997; Smith *et al.* 2005). Nevertheless, defined mechanisms in this switch remain to be elucidated. However, the majority of the transcription occurs at this stage. Ultimately, structural proteins encapsidate the progeny dsRNA genomes to complete the replication cycle (Patton and Spencert 2000). The mature virions are enclosed in

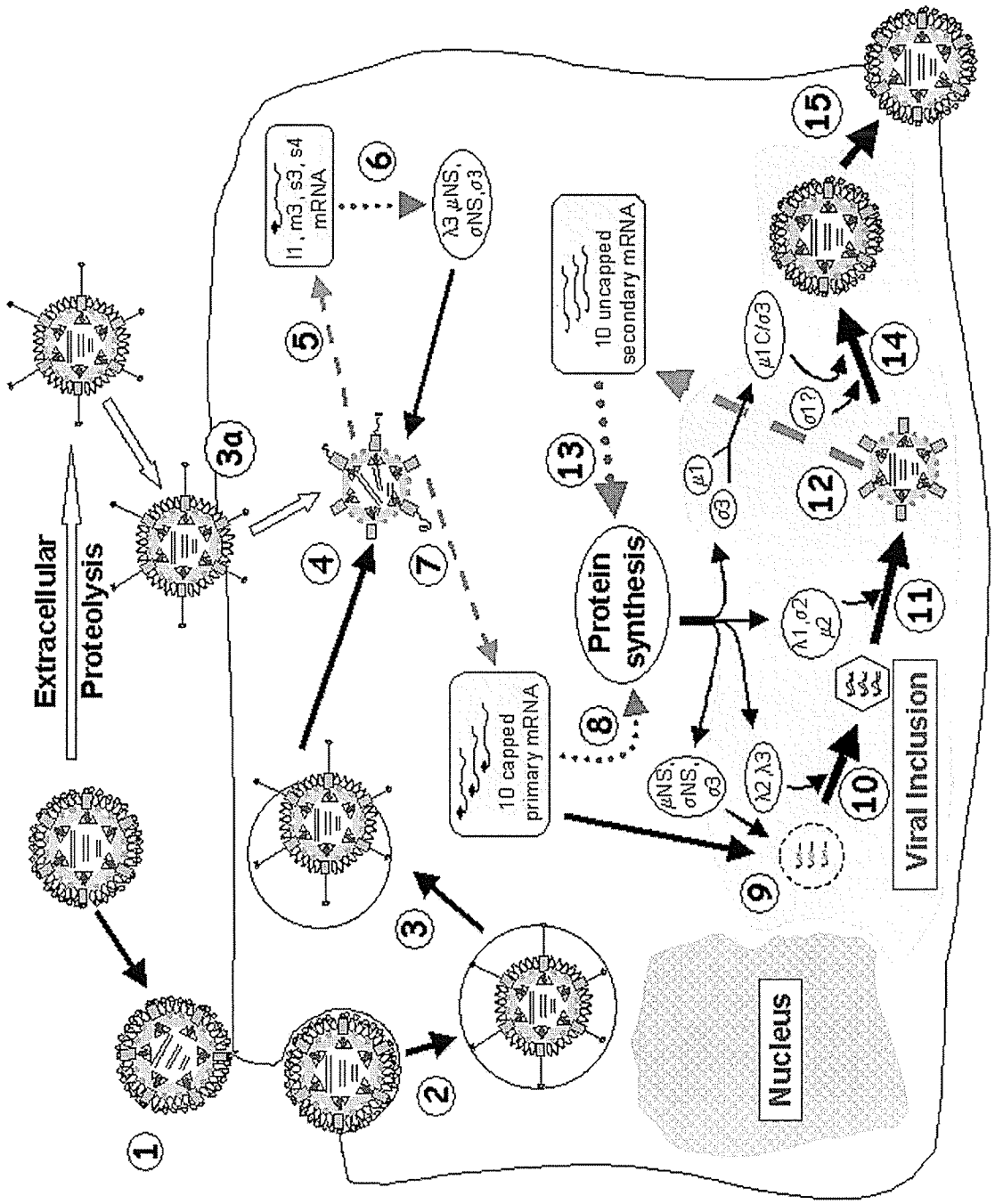
Extracellular
Proteolysis
Nucleus
Viral Inclusion
Protein synthesis
10 capped primary mRNA
10 uncapped secondary mRNA
l1, m3, s3, s4 mRNA
λ3 μNS, σNS, σ3
μNS, σNS, σ3
λ2, λ3
λ1, σ2 μ2
μ1
σ3
μ1C/σ3
σ1?
1
2
3
3a
4
5
6
7
8
9
10
11
12
13
14
15

Figure 6. Mammalian reovirus replicative cycle. Avian reovirus replicative cycle is presumed to be similar. (1) receptor-mediated virus attachment (upper left), (2) entry via endocytosis into endosomes where acid-mediated proteolysis removes outer capsid protein σB and σC extension results, (3) intermediate subviral particles (ISVP) escapes endosome, (4) uncoating of ISVP results in transciptionally active core particle released into cytoplasm, (5) early capped transcription, (6) translation of early capped transcripts, (7) primary capped transcription, (8) primary translation, (9) assortment of mRNA segments suspected to be mediated by σB and non-structural proteins; this is believed to occur within viral inclusion bodies, (10) synthesis of negative RNA strands to generate progeny dsRNA, which then associate with core proteins, (11) generation of transcriptase (replicase) complex, (12) secondary uncapped transcription, (13) secondary translation, (14) assembly of outer capsid, and (15) progeny virus release (lower right). Dashed green arrows indicate transcription events, dotted red arrows indicate translation, and black arrows indicate movement of proteins and viral complexes. Arrow thickness represent relative amounts of various components. Step 3a shows an alternate route of entry for reovirus in the form of ISVPs, which are capable of direct membrane penetration.

non-membranous inclusion bodies in the cell cytoplasm as paracrystalline arrays (Broering *et al.* 2005).

The genome segments of reoviruses contain 5′- and 3′-untranslated regions (UTRs) that vary considerably in length. The extent of nucleotide homology between all the genome segments of any particular reovirus is limited to only short stretches (< 10 nucleotides) at their 5′- and 3′-termini, termed the 5′- and 3′-consensus sequences, which allow discrimination of viral RNA from host RNA. The conserved terminal 5′-GCUAA--//--UCAUC-3′ sequences can be found on ARV S-class genomic segments (Patton and Spencert 2000), which suggest they may function as the virus-host RNA recognition signals. Individual mammalian reovirus RNA species also possess segment specific signals that allow the assortment complex to sequester all different RNA species. Similar to the homologous MRV protein σNS, ARV non-structural protein (σNS) binds single-stranded (ss) RNA in a sequence independent manner (Touris-Otero *et al.* 2005), but unlike MRV, its role in RNA assortment remains to be determined. MRV μNS may also associate with the cell cytoskeleton and perhaps play a role in genome packaging. Conversely, the function of ARV μNS has not been described in this regard.

1.6 Reovirus Assembly

Presently, the avian reovirus assembly process has not been fully resolved. However, ongoing work with a recently generated panel of temperature-

sensitive mutants is slowly shedding light on this virus group's mechanisms of replication (Patrick *et al.* 2001; Xu *et al.* 2004; Xu *et al.* 2005), which appears to behave quite similar to corresponding MRV *ts* mutants. In contrast, the use of temperature-sensitive mutants have long played a significant role in deducing the MRV life-cycle (reviewed in Coombs 1998), which has been a major focus of the majority of studies carried out relative to avian reoviruses.

A dodecahedral assembly model was proposed for the assembly of MRV (refer to Hazelton and Coombs 1999), to which ARV is speculated to have great similarity. Based upon this model, a five-sided apical complex forms the dodecahedron base unit upon which the primary core particles are built up. This base unit consists of 1 central copy of λ3 (ARV λB), 5 dimers of λ1 (ARV λA) and 10 copies of σ2 (ARV σA), in which λ3 interacts with the λ1 amino termini (Xu *et al.* 1993). The addition of the pentameric spike protein λ2 (ARV λC), the association of μ2 (ARV μA) and the cell attachment protein σ1 (ARV σC) at each of the 12 vertices produces the complete core particle. Electron cryomicroscope reconstructions further suggest that λ2 and μ2 interact with λ3 at the apices of the primary core particle (Dryden *et al.* 1998;). Virion assembly is complete when the σ3 (ARV σB) and μ1/μ1c (ARV μB/μBc) outer shell proteins associate together and then pack onto the core around the λ2 spikes (Dryden *et al.* 1993; Hazelton and Coombs 1999). Assembly of MRV core and outer shell structures can occur independently of one another.

1.6.1 Genome Packaging

Despite the relatively detailed report of the specific steps of virion assembly in MRV, the selective packaging mechanism that leads to the presence of equimolar genome segments within reovirus remains to be ascertained. It appears certain the packaging of the mRNA precedes dsRNA synthesis and that dsRNA synthesis takes place within $T = 1$ cores. As a consequence, the cis-acting signals for selective packaging are present on the mRNA template. Many of the reovirus proteins exhibit RNA-binding activity, some specifically and some non-specifically, as previously mentioned, but it has been reasoned that the ability to distinguish between the different viral RNAs during selective packaging may be driven by more than simply a number of viral proteins. Instead, it is speculated that selective packaging is more likely mediated by RNA-RNA interactions occurring *in trans* between the viral mRNA templates. The RNA-binding proteins may function in this process to stabilize the RNA-RNA interactions or to alter the structure of the mRNA templates in a manner that makes the RNA packaging sites sterically accessible (Patton and Spencer 2000).

1.6.2 Viral Inclusion Bodies

It has been established that avian reovirus morphogenesis is a temporally controlled process, which occurs exclusively within globular viral factories (or inclusion bodies) that are not microtubule-associated (Tourís-Otero *et al.* 2004a).

In contrast, MRV inclusion bodies have been determined to associate with cellular microtubules (Broering *et al.* 2002). Little is known about the establishment and expansion of viral inclusions. However, studies have shown that the M3-encoded avian reovirus non-structural protein μNS forms viral-like inclusions when expressed in transfected cells, and is present within viral inclusions in infected cells. (Tourís-Otero *et al.* 2004). These findings suggest that ARV μNS is the minimal viral protein required for the formation of these inclusions. Furthermore, μNS associates with the other major non-structural avian viral protein σNS in both infected and transfected cells, and mediates its recruitment into factories (Tourís-Otero *et al.* 2004); all of which suggests that core assembly and core coating take place exclusively within viral factories of infected cells, in a temporally coordinated fashion, and also indicate that viral morphogenesis starts with μNS forming reovirus inclusion bodies after which ARV proteins σNS and λA are seen recruited to these structures. Tourís-Otero *et al.* (2004a) also have demonstrated that μNS mediates the association of the major core protein λA, but not of σA or σC, with inclusions, indicating that the recruitment of viral proteins into avian reovirus factories has specificity. Thus, some proteins appear to be initially recruited to factories by association with ARV μNS, whereas others are recruited subsequently through interaction with as-yet unknown factors (Tourís-Otero *et al.* 2004a).

The avian reovirus non-structural protein σNS has previously been shown to bind ssRNA *in vitro* in a sequence-independent manner. The results of a

recent study further revealed that σNS binds poly(A), poly(U) and ssDNA, but not poly(C), poly(G) or duplex nucleic acids. This suggests that ARV σNS binding of ssRNA is specific to certain nucleotide sequences. Furthermore, studies have found σNS RNA-binding activity is conformation-dependent. The minimum RNA size for σNS binding has been observed to be between 10 and 20 nucleotides. On the contrary, ARV σNS does not have preference for viral mRNA sequences. Additionally, these findings show that σNS is present in large ribonucleoprotein complexes in the cytoplasm of avian reovirus-infected cells, indicating that it exists in intimate association with ssRNAs *in vivo*. Removal of RNA from the complexes generates a σNS protein that tends to associate in small oligomers. Moreover, it also has been observed that RNA-free σNS exists as homodimers and homotrimers (Tourís-Otero *et al.* 2005).

1.7 Syncytia Formation

All non-enveloped viruses capable of inducing syncytia belong to the *Reoviridae* family, where ARV serves as the prototypic fusogenic virus (Chappell *et al.*, 2005). Cell-to-cell fusion, a property typical of ARVs, is not associated with MRVs. There are, however, two atypical MRV isolates (Nelson bay virus and baboon reovirus) and two isolated from snakes that share the syncytium-inducing properties of the avian subgroup. The ARV S1-encoded protein, p10 (10 kDa), induces this fusion. Proteins with similar function and important

conserved motifs also were identified in NBV and BRV (Duncan *et al.* 1990). Although it is membrane-associated, the protein p17, encoded on the same genomic segment as p10, is not associated with syncytia formation (Bodelón *et al.* 2001).

1.8 Assortment and Reassortment

In 1969, irrefutable evidence surfaced that reovirus genomes consist not of one but of ten molecules of double-stranded RNA (Skehel and Joklik 1969). It soon became apparent that the mechanism for genome packaging in reovirus is not a case of a "headful" mechanism such as that observed in bacteriophage (reviewed in Poranen and Tuma 2004) or influenza virus (reviewed in Mikulasova *et al.* 2000). Each of the ten reovirus gene segments may be resolved in polyacrylamide gels, and the resulting pattern of gene migrations is known as the viral electropherotype. Different viral serotypes possess different characteristic electropherotypes; for example, the different electropherotypes of two different strains ARV138 and ARV176 are illustrated in Figure 1A. Note the different distance of migration of each gene within the strain relative to the other strain. The segmented nature of these genomes is extensively exploited via reassortant analysis in ARV, MRV, and *Rotavirus* (another genus within the *Reoviridae* family) for genetic studies (reviewed in Ramig and Ward 1991).

When cells are infected with a mixture of two different strains, the genes from the two parents are capable of mixing (in a process called "assortment") with each other to generate novel electropherotypes. The progeny viruses, which arise from this mixed infection, with genetic combinations from both parents, are known as reassortants (reviewed in: Joklik and Roner 1995; Coombs 1998; Joklik 1998). Figure 7 illustrates this concept.

The properties of the new virus strains will depend on which segments are inherited from which parent and the functional behavior of each particular constellation of segments and their protein products. Since the parental electropherotypes are known, gel analyses of the parents and each reassortant clone may be used to determine the parental origin of every gene in any given reassortant quite easily.

In *Reoviridae*, reassortment from mixed infections is limited to species level. In a cross-infection, the two parent reoviruses each contribute 10 gene segments, resulting in 2^{10}, or 1024, potential gene combinations in the resulting progeny virions (Fields 1971; Fields 1973). If assortment was completely random, then of the 2^{10} possibilities, two are parental and the rest are reassortants. However, 3-30% reassortant progeny in total are generally produced; that suggests assortment is a non-random event. It is postulated that nucleotide signals may direct this non-random reassortment of certain gene segments. On the other hand, random reassortment may occur where certain hybrid genotypes are less favourable and are undetected or a physical separation

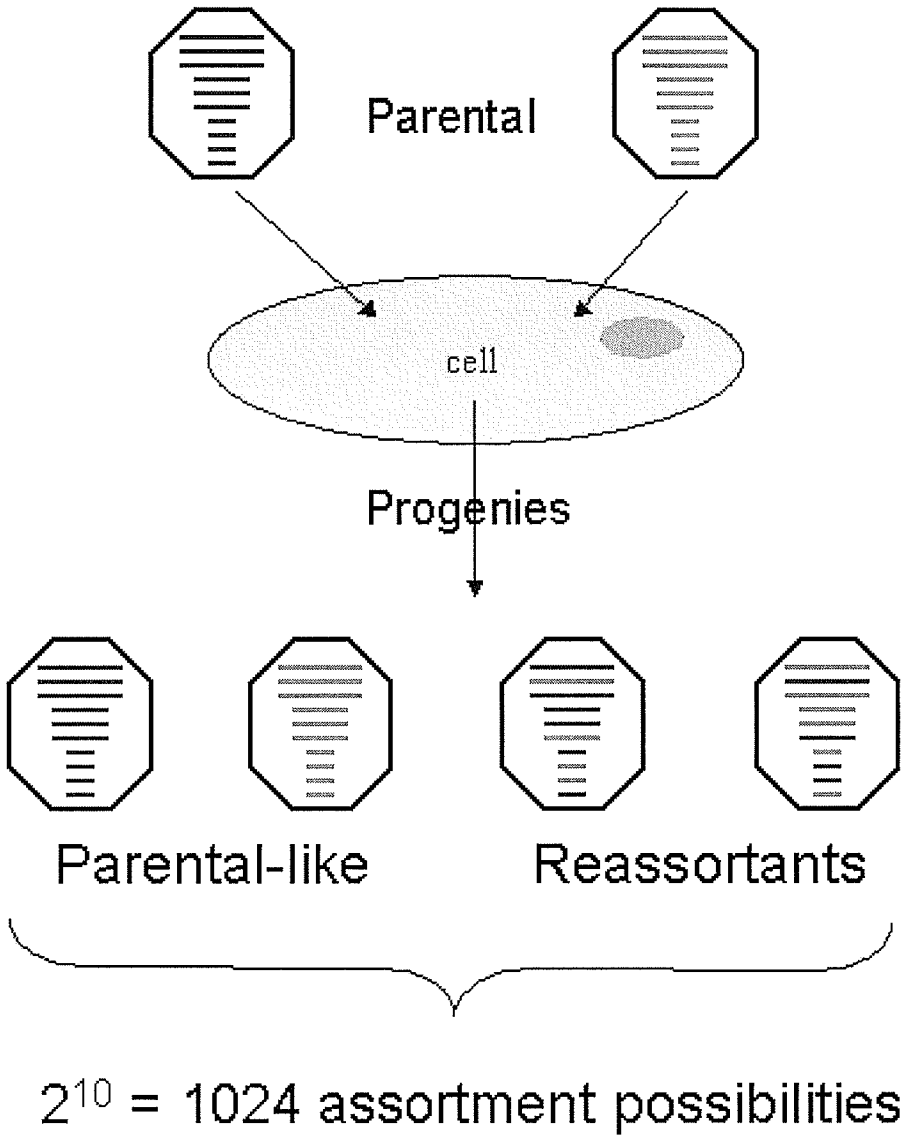

Figure 7. Schematic representation of assortment in reoviruses. Co-infection of two different serotypes leads to assortment of parental genomic segments, which gives progenies (reassortants) with mixed genomic background.

of inclusion bodies within the infected cell prevents complete mixing of progeny gene segments (Nibert *et al.* 1996).

1.9 Temperature-sensitive Mutants

Previously, the development of a reverse-genetic system for the study of reovirus protein functions had been hindered by the nature of the viral genome and its mode of replication. Nevertheless, persistent work led to a recent breakthrough in the generation of a reovirus reverse genetic system (Roner and Joklik 2001; Roner *et al.* 2004); however, the process and system are not efficient and rather cumbersome. On the other hand, the segmented nature of the genome remains a significant aspect that allows the generation of reassortant viruses and facilitates the assignment of temperature-sensitive (*ts*) mutations to specific genes (reviewed in Coombs 1998). As a result, reovirus temperature-sensitive mutants pose as an attractive alternate approach to studying the functional roles of viral proteins.

The term "temperature-sensitive" implies a defective replication of an organism (to which the term is referred) by a change in temperature. This is commonly applied to higher temperatures under which the defect is phenotypically expressed. However, it can equally represent effects at lower temperatures, which in turn are known as "cold sensitive." The observed temperature-sensitive effect on replication is usually a sum of the virus and the

cell in which it infects, because in dealing with *ts* ARV clones, the defective phenotype is expressed upon incubation of the infected cells at the elevated temperatures. A virus clone's *ts* phenotype may be expressed mathematically as a ratio of the ability of the virus to grow at the non-permissive temperature to its ability to grow at the lower permissive temperature. Non-permissive refers to the temperature at which a defect in viral replication is phenotypically expressed; the opposite is true at the permissive temperature. This mathematical ratio is obtained by dividing the non-permissive viral titer by the permissive titer to generate an efficiency of plating (EOP) value. The EOP values for wild-type reoviruses usually remains within an order of magnitude of 1.0, which indicates replication at higher temperatures show only a slight reduction compared to replication at the lower temperature. By contrast, a *ts* clone, when examined by the same analysis, will normally generate a value significantly lower than 0.1 (reviewed in Coombs 1998).

Alternative methods are available to test the temperature sensitivity of potential *ts* mutants. The EOP plaque assay is only one method to measure viral replication. Although the EOP plaque assay is commonly used since it is relatively simple and rapid, it does not usually accurately reflect viral replication, because the plaque assay's success requires cell killing. Therefore, an alternative strategy was developed to more directly measure viral replication by determining the amount of virus produced by an infected cell. This alternative method is the efficiency of yield (EOY) assay, where cells infected with a virus

clone are incubated at non-permissive temperatures and, mathematically similar to EOP, the yield of virus produced at the restrictive temperature is compared to the amount of that virus produced at the permissive temperature (this is the EOY ratio). As seen in EOP assays, wild-type virus grows equally well at both temperatures and usually generates EOY values of approximately 1.0. EOY assay not only confirms *ts* status of clones identified by EOP, but this assay also indicates *ts* phenotypes of clones which EOP could not determine. Therefore, EOY may be considered more sensitive than EOP. However, EOY assays are extremely labour intensive, which is a major disadvantage compared to the EOP assay (Patrick *et al.* 2001; Patrick 2001).

A large understanding of MRV replication and assembly, as well as viral protein functions, stemmed from studies of *ts* mutants, which was initiated in two different laboratories (Ikegami and Gomatos 1968; Fields and Joklik 1969; Cross and Fields 1972; Hazelton and Coombs 1995; Zou and Brown 1996; Roner *et al.* 1997; Keirstead and Coombs 1998; Hazelton and Coombs 1999; Mbisa *et al.* 2000; Becker *et al.* 2001). A brief history of *ts* mutants studies in MRV should be mentioned here. Chemical mutagenesis of wild-type reovirus stocks generated the original group of MRV *ts* mutants (Ikegami and Gomatos 1968; Fields and Joklik 1969), and sets the stage for their use in MRV biological studies. Ikegami treated stocks of reovirus serotype 3, strain Dearing (T3D), with nitrous acid, nitrosoguanidine, or 5-fluorouracil. Six *ts* clones were identified, two each from the nitrous acid-treated, 5-fluorouracil-treated, and nontreated samples (Ikegami

and Gomatos 1968). Fields also treated stocks of reovirus T3D with nitrous acid, nitrosoguanidine, or proflavin, from which 35 *ts* clones were initially identified (16 from nitrous acid-treated, 14 from the nitrosoguanidine-treated, and five from the proflavin-treated stocks) (Fields and Joklik 1969). Each clone is placed into one of five groups (designated groups A to E) based on genetic analysis (Ikegami and Gomatos 1968; Fields and Joklik 1969). Subsequent clones were discovered, which gave a total of 10 groups with the inclusion of groups F to J (Cross and Fields 1972; Ramig and Fields 1979; Ahmed et al 1980; Coombs *et al.* 1994).

The initiative to develop avian reovirus *ts* mutants was undertaken a few years prior to the work described in this dissertation. Megan Patrick (2001) generated a panel of ARV *ts* mutants by infecting cells with ARV138 in the presence of nitrosoguanidine. A total of seven recombination groups (A to G) were clearly identified, indicating each had their *ts* mutations in different genes; that 7 of the 10 ARV138 dsRNA gene segments have representative *ts* mutations (Table 2). Six *ts* mutants failed to recombine with numerous mutants in more than one recombination group and suggested that they have multiple gene segments with *ts* lesions (Patrick *et al.* 2001; Patrick 2001). Genetic recombination in reoviruses occurs through reassortment of individual gene segments rather than strand breakage and rejoining (Joklik and Roner 1995).

Of these seven groups, three prototypic members have been mapped to their respective gene segments: *tsA12* mapped to S2 (σA), *tsB31* mapped to M2

Table 2. Recombination groups of avian reovirus temperature-sensitive mutants, chemically generated from ARV138 via nitrosoguanidine treatment*.

Groups	Clone	References
A	tsA12	• Xu *et al.* 2004; Patrick *et al.* 2001
	tsA146	
B	tsB31	• Xu *et al.* 2005
C	tsC37	• Xu *et al.* 2005; *also reported in this dissertation*
	tsC287	
D	tsD46	• Xu *et al.* 2005
	tsD195	
	tsD219	
E	tsE158	
F	tsF206	
G	tsG247	

* Refer to Patrick *et al.* 2001; Patrick 2001.

(μB), *tsD46* mapped to L2 (λB) (Patrick *et al.* 2001; Xu *et al* 2004; Xu *et al.* 2005). Here, I report the complete mapping of three other mutants in recombination groups C (prototype *tsC37*), F (*tsF206*), and G (*tsG247*).

1.10 The Concept of Mapping Temperature-sensitivity

Mapping of *ts* mutations, or other markers with identifiable phenotype, requires some means of identifying the parental origin of each genome segment within a putative reassortant virus. In segmented viruses, this means of identification has been the polymorphic electrophoretic migration rates of the genome segments of different viral strains. This technique, referred to as reassortant mapping, has been applied to both reoviruses and rotaviruses (Ramig and Ward 1991). This approach relies on the generation of reassortant progeny from mixed infections that involve a *ts* mutant clone and non-*ts* wild-type virus (parental) of a different strain. Reassortant electropherotypes and *ts* status (EOP value) are determined. The reassortants are then grouped into two panels; one panel consists of clones that retained the temperature-sensitive phenotype while reassortants that behave as non-*ts* are placed in a separate panel. All *ts* reassortants should share a gene segment that originated from its mutant parent, while non-*ts* reassortants should share the corresponding gene segment of wild-type origin. All other segments should be randomly assorted with respect to

temperature-sensitivity. This combination of results allows the gene segment associated with the *ts* phenotype to be identified (reviewed in Coombs 1998).

Reassortment mapping in this study involved the use of ARV176, which was the wild-type crossed with *tsC37* in a cross-infection to generate reassortants. Since ARV138 and ARV176 play critical roles in the work to be discussed in this thesis, a brief background of these two viruses is warranted. It has been demonstrated that ARV176 is highly pathogenic relative to ARV138 in an embryonated egg model, a feature associated with the different degree of fusogenic capability harboured by each virus (Duncan and Sullivan 1998). Both viruses infect and replicate with equal efficiency in cultured fibroblast cells, and all 10 of their individual genome segments can be resolved by electrophoretic analysis (Duncan and Sullivan 1998). Furthermore, the two strains exhibit approximately 94% to 98% amino acid sequence identity in the three sequenced S-class genome segment-encoded proteins (Duncan 1999) and 97.7% to 99% amino acid identity in the recently sequenced M-class genes (Noad 2004); hence, these two strains make ideal parental virus candidates for genetic and molecular approaches to identify viral determinants of host interaction and pathogenicity.

1.11 Study Objectives

As mentioned earlier, the molecular biology of ARV remains relatively understudied despite the economic significance avian reoviruses pose. Most

knowledge about ARV assembly was conjectured from the studies of MRV, which has been investigated in greater detail. There are similarities between both MRV and ARV, but there are also important distinctions, which serve as a good reason for further analysis of ARV. Moreover, avian reovirus is regarded to have a relatively simple structure, making it a useful model in studies involving more complex viruses and as a tool in other areas of research.

The complete assignment of lesions in all ARV *ts* mutants to gene segments will be a significant progressive step toward the understanding of the molecular nature of ARV. Hence, this study reports the characterization of 1 of the 7 reported *ts* mutant panels, specifically recombination group C mutants. The investigation reported here is based on three general hypotheses: (1) We hypothesized that *tsC37* mutant represents 1 of 7 novel assembly-defective agents that can be used to delineate assembly of the reovirus core particle and replication processes; (2) therefore, we hypothesized that the conformational alterations of *tsC37* mutant protein affects the later stage of capsid assembly or viral release; (3) we hypothesized that expression of the wild-type gene corresponding to the mutated gene in quail fibrosarcoma (QM5) cells will complement the defect in *tsC37*. Hence, the objectives of this study were to: (i) determine which viral genomic segment contains the lesion promoting the temperature-sensitive phenotype observed in the ARV *ts* mutants, (ii) determine the precise mutation within the gene and protein for recombination group C mutants, (iii) deduce the step in viral replication inhibited by the mutation

determined in objective (ii), and (iv) develop an expression system for both the mutant gene and its wild-type genomic counterpart. Later into the project, characterizations of recombination groups F and G were added to objective (i).

The completion of recombination groups C (*tsC37*), F (*tsF206*), and G (*tsG247*) genetic maps have pinpointed the lesions to genes S3, S4, and L3, respectively. Further sequencing of *tsC37* and *tsC287* S3 genes revealed missense mutations at adjacent nucleotide positions 871 and 872, respectively, which led to the same amino acid substution at position 281 in the major outer capsid protein ARV σB. The specific amino acid mutation determined in recombination group C mutants was placed into the crystal structure of the homologous MRV protein σ3 to deduce possible structural effects that would give rise to the temperature-sensitivity observed at the non-permissive temperature. Concurrently, several attempts were made to develop an expression system of recombinat mutant and complement wild-type proteins in baculovirus. Unfortunately, these efforts were unsuccessful. Hence, the methods used in objective (4) were included as an appendix.

PART II | MATERIALS AND METHODS

2.1 Stock QM5 Cells and Avian Reoviruses

Viruses were passaged in QM5 continuous quail cell line (Quail fibrosarcoma). ARV strains 138 and 176 are prototypic lab stocks originally donated by Dr. R. Duncan of Dalhousie University, Halifax, Canada. *tsC37, tsC287, tsF206,* and *tsG247* are mutants obtained by infecting QM5 cells with ARV138 in the presence of nitrosoguanidine (refer to Patrick 2001). Cells were maintained in completed 1x Medium199 (7.5% fetal calf serum (Gibco BRL), 2 mM L-glutamine, and 0.0525% $NaHCO_3$) and grown in the presence of 5% CO_2 at 37°C. Confluent cell monolayers were routinely passaged by standard trypsinization procedures: media is removed, cells are washed with phosphate buffered saline/ethylenediamine tetraacetate (PBS/EDTA: 137 mM NaCl, 0.3 mM KCl, 0.8 mM Na_2HPO_4, 0.1 mM KH_2PO_4, 0.05 mM EDTA) and trypsinized with 0.25% trypsin (1120 BAEE (Nα-benzoyl-L-arginine ethyl ester) units/mg; source: porcine pancreas, Sigma). The cells were allowed to sit at room temperature to allow the monolayer to detach and were then resuspended in the appropriate dilution volume of QM5 maintenance media. Stock QM5 cells were split and passaged twice weekly. Cells used for viral infections were incubated in the above media supplemented with 100 μg/ml penicillin, 100 μg/ml streptomycin sulfate, and 1 μg/ml amphotericin B.

Spodoptera frugiperda Sf9 cells were maintained in serum-free 1x Sf-900 II SFM (Gibco BRL) in a spinner flask kept at 27°C without CO_2. The cells were routinely passaged once cell concentrations reached ~ 1 - 2.5 x 10^6 cells/ml by removal of medium and cells and replenished with fresh medium for a final concentration of 4 x 10^5 cells/ml.

2.2 Avian Reovirus Plaque Assay

10-fold serial dilutions of viral stocks were made in gel/saline (137 mM NaCl, 0.2 mM $CaCl_2$, 0.8 mM $MgCl_2$, 19 mM HBO_3, 0.1 mM $Na_2B_4O_7$, 0.3% (w/v) gelatin). Growth media was removed from sub-confluent QM5 monolayers, diluted virus was added and adsorbed for 1 h at room temperature with occasional rocking every 10 minutes to keep cells moist and allow even distribution of virus over entire area of cell monolayer. The cells were overlaid with 1x Media199 overlay (9.8% fetal calf serum (Gibco BRL), 2 mM L-glutamine, and 0.11% $NaHCO_3$)/1% agar supplemented with 100 μg/mL penicillin, 100 μg/mL streptomycin sulfate, and 1 μg/mL amphotericin B. Dishes were incubated at permissive temperature (33.5°C) and non-permissive temperature(s). The infected monolayers were fed with the same overlay 1x Media199/1% agar supplemented with antibiotics on 3 and 4 days post-infection (d.p.i.) for restrictive and permissive temperatures, respectively. The cells were stained 4 d.p.i. and 6 d.p.i for restrictive and permissive temperatures,

respectively, either with neutral red (0.013% neutral red in a 2 ml overlay of 1% agar/1% PBS) or crystal violet (cells were fixed with 2% formaldehyde before and after removal of agar overlay, then stained with 0.1% crystal violet). Plaques were counted approximately 18 h after neutral red staining or any time after crystal violet staining.

2.3 Efficiency of Plating (EOP) Assay

Serial 1:10 dilutions of ARV138, ARV176, *tsC37, tsC287, tsF206, tsG247,* and reassortants were infected into sub-confluent QM5 monolayers and incubated at 33.5°C (permissive temperature) and non-permissive temperature(s) as described in section 2.2. Viral titers were determined, and the EOP ratios were calculated with the following formula:

$$\text{EOP} = \frac{\text{viral titer at non-permissive temperature}}{\text{viral titer at permissive temperature}} \qquad (1)$$

Three to four separate EOP assays were conducted for all viruses.

2.4 Avian Reovirus Viral Amplification

Maintenance media from sub-confluent QM5 monolayers was removed and the cells were infected with virus at a multiplicity of infection (MOI) less than 1 plaque forming unit (PFU)/cell. After 1 h adsorption at room

temperature, fresh completed 1x Medium199 supplemented with antibiotics was added. The infections were incubated at the appropriate temperature in the presence of 5% CO_2 until 90% cytopathic effect (CPE) was visualized by light microscopy. Wild-type viruses were grown at 37°C and mutant viruses were amplified at 33.5°C. Viral progenies were harvested by cell lysis induced by three cycles of freeze/thawing at -84°C and viruses were stored at 4°C (for immediate use) or -84°C (for long term storage). Viruses were titred prior to use.

2.5 Avian Reovirus Plaque Purification

Samples were infected, overlaid and incubated as described earlier (section 2.2). Plaques were stained with 0.013% neutral red, incubated for 18 h, and picked (P_0). The viral/agar plugs were resuspended in completed 1x Medium199 and stored at 4°C for 24 h to allow viral diffusion into the media. P_0 stocks were amplified twice to give P_1 and P_2, and harvested by freeze/thawing three times as described previously (refer to section 2.4).

2.6 Generation of Reassortants

A 24-well tissue culture dish with sub-confluent QM5 monolayers was co-infected with *tsC37* (derived from ARV138) and unmutagenized ARV176 at MOI ratios of 15:5, 5:5, 5:15 PFU/cell. *tsF206* co-infection with ARV176 occurred at MOI ratios of 2:8, 8:2, 5:5 PFU per cell (assay done by Trina Racine). Infections

were incubated at 33.5°C for 34 hrs. The infections were freeze/thawed thrice and the cell lysates were sterilely sonicated for 15 seconds and serially diluted in gel saline. Aliquots of each dilution (3×10^{-5}, 1×10^{-5}, 4×10^{-6}, $1x\ 10^{-6}$, and $4x\ 10^{-7}$) from each mixed infection were added to P100 tissue culture dishes with sub-confluent QM5 monolayers. After adsorption, the cells were overlaid with 1x Medium199/1% agar and incubated at 33.5°C until 9 d.p.i. The infections were fed 5 d.p.i. with 1x Medium199 overlay/1% agar, and stained 9 d.p.i. with 0.013% neutral red/1% Agar/1% PBS. Individually isolated plaques separated by at least 0.75 cm were picked, and then amplified twice as described earlier.

2.7 Isolation of Viral Double-stranded RNA

The P_2 progeny clones were used to infect P100 dishes of sub-confluent QM5 monolayers, overlaid with 1x Medium199 and incubated at 33.5°C until 60% CPE was visualized under a light microscope. Cells were scraped off the plate and pelleted at 1100 rpm for 10 minutes. To lyse cell membranes, pellets were resuspended in NP40 buffer (140 mM NaCl, 1.5 mM $MgCl_2$, 10 mM Tris-HCl, pH 7.4) with 0.5% NP40 detergent and incubated on ice for 35 minutes; the sample was vortexed every 10 minutes. Cellular nuclei and organelles were pelleted at 1100 rpm for 10 minutes and supernatants were collected in sterile microfuge tubes. Phenol/chloroform extraction of viral dsRNA segments was performed. Each sample was incubated at 42°C for 15 minutes in the following

mixture: 0.5 μM Tris, pH 7.8; 6.5 mM EDTA, pH 8.0; and 0.01% SDS. After 15 minutes, a 1:1 ratio of phenol/chloroform to sample volume was added, along with 0.1 mM NaCl and incubated at 42°C for 30 seconds. The samples were then centrifuged for 5 minutes at 15,000 rpm. The aqueous phase was collected in sterile microfuge tubes. RNA was precipited at -20°C overnight in 0.08 μM sodium acetate (pH 5.3) and 70% ice cold ethanol, then pelleted at 15, 000 rpm for 30 minutes at 4°C. Viral dsRNA pellets were lyophilized (SC100 speed-vac, Savant, Holbrook, NY) for about 1 h and resuspended in 1x Laemmli electrophoresis sample buffer (0.24 mM Tris-HCl pH 6.8, 1.5% dithiothreitol, 1% SDS).

2.8 Electropherotype Profiles

12.5% polyacrylamide slab gels (16 cm x 16 cm x 0.1 cm) were poured and polymerized for 1 h. Viral dsRNA samples were heated to 65°C for 5 minutes prior to loading and electrophoresed for 1.5 h at 18 mAmps/gel, then 66 h at 12 mAmps/gel, then 5 h at 2 mAmps. Viral dsRNA bands were stained with ethidium bromide (2.5 μg/ml) and visualized by ultraviolet irradiation. Photographs were taken with Gel Doc 2000 (BioRad) apparatus and reassortant progeny clones were identified by comparison of progeny gene segment profiles to that of the two parents (ARV138 and ARV176) involved in the infection.

2.9 Sequencing

2.9.1 Viral dsRNA Extraction

Viral dsRNA pooled from 6 P100s was isolated as described under section 2.7. The RNA was precipitated overnight at -20°C in 0.08 μM sodium acetate (pH 5.3) and 70% ice cold ethanol, pelleted at 15, 000 rpm for 30 minutes at 4°C, and washed with 70% ice cold ethanol. Viral dsRNA pellets were lyophilized (SC100 speed-vac, Savant, Holbrook, NY) for about 1 h and resuspended in mixture of 90% DMSO (dimethyl sulfoxide) and 10% 10 mM RNase free Tris-HCl (pH 6.8).

2.9.2 Reverse Transcription and Polymerase Chain Reaction Amplification

2.9.2.1 Reverse Transcription

Purified viral dsRNA (6 μl) was heated at 50°C for 45 minutes and snap-cooled by immediate transferral to ice. To this was added: 63 μl diethylpyrocarbonate-treated sterile double-distilled water (DEPC-ddH_2O), 0.8 μl RNaseOUT™ Recombinant Ribonuclease Inhibitor (40 units/μl) (Invitrogen), 1 μl of each polarity of 10 μM gene-specific primers (refer to Table 3), 5 μl of 10 mM dNTP mix (10 mM each of dCTP, dTTP, dGTP, dATP, in DEPC-H_2O), 20 μl 5x First-Strand buffer (Invitrogen), 1 μl of 10 mg/ml bovine serum albumin (BSA), 1

Table 3. Avian reovirus gene sequencing primers.

Primer Name	Sequence	Orientation	Nucleotide position
A(+) A138 S3 SeqIn[d]	GGAACCCTGCCAGCCGACG	5' → 3'	211-229
A(+) A138 S3 seqIn2[d]	GATGTTGCTGCGACTGGAAAGGC	5' → 3'	661-683
A(+) A138 S3 seqIn4[d]	CTCGGACGGTCTCTGCCAAA	5' → 3'	1021-140
A(-) A138 S3 seqIn[d]	GTAGTAAAGCACACCACAAC	3' → 5'	210-191
A(-) A138 S3 seqIn3[d]	TTTGGCAGAGACCGTCCGAG	3' → 5'	1140-1021
A(-) A138 S3 seqIn2[d]	TATGGTGGTGGTCGTTTGC	3' → 5'	683-661
A(+) A176 S3[c]	CAAGCCGCAATGGAGGTA	5' → 3'	22-39
A(-) A176 S3[c]	CCGTCACATAGGTGGGAGCC	3' → 5'	1179-1160
A(+) A138 S2 SeqMap[b]	TTGAACCTGATGGGAACTA	5' → 3'	617-635
A(+) A138 S4 SeqMap[f]	AAGGCAATGACTTTACCCCG	5' → 3'	481-500
A(+) A176 S2 SeqMap[a]	CCTGTTGAGCCTGATGGAAAT	5' → 3'	613-633
A(+) A176 S4 SeqMap[e]	AAGGTGATGACTTTGCTCCGA	5' → 3'	481-500
RLM probe#2*	GGGGGAAAGGGGCGTAATGGAAAAAGTGGGTTGGGG	5' → 3'	---
RLM ½ probe¥	GGGGGAAAGGGGCGTAATGG	5' → 3'	---
RLM 3' Tail§	CCCCAACCCACTTTTTCCATTACGCCCCTTTCCCCC	5' → 3'	---

Accession #s: AF059716.1 (ARV 176 S2)[a]; AF059717.1 (ARV 138 S2)[b]; AF059720.1 (ARV 176 S3)[c]; AF059721.1 (ARV 138 S3)[d]; AF059724.1 (ARV 176 S4)[e]; AF059725.1 (ARV 138 S4)[f]

§ 5′ phosphorylated and 3′ biotin-blocked

*probe used for RT-PCR specific for ligated 3′ gene end

¥ probe used for sequencing specific for ligated 3′ gene end

μl 100 μM dithiothreitol (DTT), and 0.8 μl Superscript™ II reverse transcriptase (200 U/μl) (Invitrogen). The mixture was incubated at 42°C for 1.5 h.

2.9.2.2 PCR

cDNA produced by reverse transcription (RT) was amplified via polymerase chain reaction using Expand Long Template PCR system (Roche). To an aliquot of cDNA was added (for a 100 μl reaction volume): 67.5 μl ddH_2O, 10 μl 10x Expand Long Buffer 1 (Roche) (17.5 mM $MgCl_2$), 3.5 μl 10 mM dNTP mix (as listed above), 1 μl of each polarity of 100 μM gene-specific primers (refer to Table 3), 1 μl Expand Long Template Enzyme (Roche) (5 U/μl), and 70 μl Mineral Oil (specific for PCR machine used, to prevent evaporation during cycling reaction). PCR amplification cycles were carried out in PTC-100, Programmable Thermocycler (MJ Research Inc., Waltham, MA) with the following reaction specifications: initial denaturation at 96°C for 2 minutes, 35 cycles of: 94°C for 1 minute, anneal at 55°C for 1 minute, primer extension at 68°C for 3 minutes; followed by complete product extension for a further 10 minutes at 68°C, and hold at 4°C after completion of amplification reactions.

PCR product was loaded and run in a 1% agarose gel in 0.5x TBE buffer (4.5 mM Tris, 4.5 mM Boric acid, and 0.9 μM EDTA), stained with ethidium bromide, and observed under UV transillumination. The desired band size was excised from the gel and DNA was extracted using QIAquick™ gel extraction kit

(Qiagen, Germany) according to the manufacturer's instructions. The purified DNA was eluted with sterile ddH_2O.

2.9.3 3′ Ligation for Gene-end Sequencing

A method developed by Lambden *et al.* (1992) was adapted for the sequencing of tsC37 in order to obtain gene-end sequences in both directions. Viral RNA was isolated as described under section 2.9.1. The isolated RNA was resuspended in phosphate buffered saline (PBS) (137 mM NaCl, 0.3 mM KCl, 0.8 mM Na_2HPO_4, 0.1 mM KH_2PO_4). dsRNA genomic segments were resolved in 1% agarose gel, and the desired gene class was extracted and purified by QIAquick™ gel extraction kit (Qiagen, Germany) according to the manufacturer's instructions. The purified RNA was eluted with Qiagen elution buffer. To 8 µl of the gel-purified RNA was added: 1 µl of 10 µM primer (RLM 3′ Tail), 1 µl 10x T4 RNA Ligase Buffer (Roche), 1 µl T4 RNA Ligase (5 U/µl) (Roche). The mixture was allowed to react overnight at 37°C. Next, the mixture was heated to 95°C for 2 minutes to inactivate enzyme, and re-resolved in 1% agarose gel to remove non-incorporated primer, extracted and re-purified using QIAquick™ gel extraction kit (Qiagen, Germany) as described above, but eluted in 2 sequential volumes of elution buffer. The re-purified, 3'end ligated RNA was precipitated overnight at -20°C in 10 µl of 3 M sodium acetate (pH 5.3) and 260 µl ice cold 100% ethanol. The precipitate was washed with 70% ethanol,

lyophilized (SC100 speed-vac, Savant, Holbrook, NY) and resuspended in mixture of 90% DMSO (dimethyl sulfoxide) and 10% 10 mM RNase free Tris-HCl (pH 6.8). Reverse transcription was carried out as described above with "RLM 3'probe#2" and gene-specific internal primer; after which PCR was done as described above. Sequencing of 3'end ligated RNA product was carried out as described above with primers labelled as "RLM½ probe" and gene-specific internal primers. All primer sequences used here are listed in Table 3.

2.9.4 Dideoxynucleotide Cycle Sequencing

Dideoxynucleotide cycle sequencing was carried out to determine the sequences of each cDNAs in both directions, using ABI PRISM® BigDye™ version 3 Terminator Cycle Sequencing Ready Reaction Kit (Perkin Elmer (PE) Applied Biosystems, Foster City, CA). The sequencing reaction mix consisted of an aliquot of PCR-amplified and gel-purified cDNA (described above), 1 µl of 1 µM primer, 2 µl BigDye version 3 mix, and sterile ddH_2O for a final reaction volume of 5 µl. Cycle sequencing was performed in Techne Flexigene Thermal Cycler (Krackeler Scientific, Inc.; Albany, NY) with the following reaction specifications: 96°C for 3 minutes, 60 cycles of 96°C for 1 minute, 53°C for 1 min, 60°C for 4 minutes, and hold at 4°.

The sequencing reaction was precipitated in 0.14 M sodium acetate (pH 5.2) and 70% ice-cold ethanol at room temperature for 3 h in the dark. The

precipitate was pelleted at 15, 000 rpm at 4°C for 30 minutes. The supernatant was aspirated off. The pellet was washed with 70% ice cold ethanol and centrifuged again at 15, 000 rpm at 4°C for 15 minutes. This second supernatant was removed and the pellet was dried at 96°C for 2 minutes. The DNA was resuspended in 20 µl formamide. The resuspended DNA was heated for 1.5 minutes at 96°C and snap-cooled on ice for 1 minute. The samples were transferred to 96-well sequencing plate. The sequence was determined using the ABI PRISM 3100 Genetic Analyzer (PE Applied Biosystems, Foster City, CA). Manual analysis of the sequence was carried out with Chromas version 2.13 (McCarthy 2001). ClustalW (Chenna *et al.* 2003) was used to align sequences for comparison purposes.

2.10 Crystal Structure Manipulations

ARV tsC37 and tsC287 mutations in σB were placed into MRV σ3 (PDB # 1FN9) and the MRV heterohexamer µ1-σ3 crystal structures (PDB # 1JMU) to infer effects. The crystal structures of these MRV outer capsid proteins were manipulated using PyMOL (Delano 2004).

2.11 Direct Particle Counting by Electron Microscopy

A 12-well tissue culture dish with sub-confluent QM5 monolayers were infected with tsC37 and ARV138 at MOI of 5 PFU/cell, incubated at 33.5°C for 30

h or 40°C for 22.5 h, and freeze/thawed three times. Infections were done in quadruplicates for each virus. The infections were harvested and centrifuged at 800 rpm for 5 minutes at 4°C. One set of infections of each virus was pre-cleared by centrifugation at 13,500 rpm for 5 minutes. The samples were fixed in 2% paraformaldehyde-supplemented 1x S-MEM with an addition of 125 μM glycine. 60 μl of each suspension was centrifuged through 100 μl of 30% sodium tartrate cushion (pH 7.2) in Airfuge® A100 rotor (Beckman Instruments, Palo Alto, Ca) at 26 psi for 1 h. The tartrate cushion was removed and the pellet was resuspended in 60 μl 1x S-MEM. A series of 10-fold dilutions (10^{-1} to 10^{-3}) of the suspension was made in 1x S-MEM. 45 μl per dilution of each suspension was airfuged directly onto formvar-coated, carbon-stabilized 400-mesh copper grids for 30 minutes at 26 psi on Airfuge® EM-90 rotor (Beckman Instruments, Palo Alto, Ca). The sample-containing grids were stained with 2.5 mM phosphotungstic acid, pH 7.0, viewed with a Phillips model 201 transmission electron microscope (TEM) at a scanning magnification of 30,000X, and images were recorded at a final machine magnification of 200,000X.

2.12.1 Construction of Gateway® Donor vectors

2.12.1.1 Designing *att*B PCR Primers

Attempted expression of recombinant viral proteins utilizing the Gateway® Technology expression system (Invitrogen). Both forward and

reverse PCR primers were designed with NetPrimer (Premier Biosoft International; Palo Alto, CA) according to the manufacturer's instructions, including Kozak consensus sequence and no stop codon for C-terminal tag (refer to Table 4).

Reverse transcription PCR was carried out as described above. A slight modification to PCR specifications was as followed: initial denature at 96°C for 2 minutes before cycling 35x at 94°C for 1 minute, anneal at 88°C for 1.5 minute, primer extension at 68°C for 3 minutes, and complete product extension for a further 10 minutes at 68°C. PCR product was gel-purified as described above with QIAquick™ gel extraction kit (Qiagen, Germany) according to the manufacturer's instructions. The product was eluted with sterile ddH_2O.

2.12.1.2 Performing BP Recombination Reaction

BaculoDirect™ Baculovirus Expression system (Invitrogen) was used. BP reaction was carried out according to manufacturer's instructions. 50 fmol of gel-purified *att*B PCR product was added to 150 ng of pDONR™ vector (Invitrogen) (150 ng/μl), TE Buffer (pH 8.0) (1 mM EDTA and 10 mM Tris-HCl), and BP Clonase™ enzyme mix (Invitrogen). The reaction was incubated at 25°C overnight. Proteinase K (2 μg/μl) was added to each reaction and incubated at 37°C for 10 minutes. This generated the donor vectors (also known as entry clones).

Table 4. Primers used in the development and sequencing of entry and destination vectors in the Gateway Expression system.

Primer Name	Sequence	Orientation	Nucleotide position
Gate(+)ARV138 S3 attB1[a]	GCAATGGAGGTACGTGTGCCAAAC[d]	5' → 3'	28-51
Gate(-)ARV138 S3 attB2 [a]	ACCAACTACACTCCACAACAGT[e]	3' → 5'	1132-1111
Gate(+)pDONR™201[b]	TCGCGTTAACGCTAGCATGGATCTC	5' → 3'	---
Gate(-)pDONR ™201[b]	GTAACATCAGAGATTTTGAGACAC	3' → 5'	----
Bac –F: polyhedrin forward primer[c]	AAATGATAACCATCTCGC	5' → 3'	---
Bac-R: V5 reverse primer[c]	ACCGAGGAGAGGGTTAGGGAT	3' → 5'	---

[a]Accession # AF059721.1; primers used in development of entry clone
[b]primer sequence from Invitrogen manual "Gateway pDONR™ Vectors," version D –2005
[c]primer sequence from Invitrogen manual "BaculoDirect™ Baculovirus Expression Systems: for cloning and high-level expression of recombinant proteins using Gateway®-adapted Baculovirus DNA," version F - 2004
[d] "Pre-fix" sequence: GGGGACAAGTTTGTACAAAAAAGCAGGCT
[e] "Pre-fix" sequence: GGGGACCACTTTGTACAAGAAAGCTGGGT

2.12.1.3 Transforming One Shot® TOP10 *E. coli*.

Transformation of One Shot® Chemically Competent TOP10 *E. coli* (Invitrogen) was carried out according to manufacturer's instructions. Donor vectors generated from the BP recombination reaction described above were added at 2 µl per vial of TOP10 cells and incubated on ice for 30 minutes, heat-shocked for 42 seconds (instead of the 30 seconds indicated by the manufacturer) at 42°C without shaking, after which they were transferred immediately to ice. Room temperature SOC medium (Invitrogen) was added to the vials and incubated at 37°C for 1 h with shaking at 200 rpm. After incubation, 10-50 µl of each transformation was spread-plated onto pre-made and pre-warmed Luria-Bertani (LB) agar (1 % Tryptone, 0.5 % yeast extract, 1 % NaCl, pH 7, agar (15g/L))(Fisher) selective plates supplemented with kanamycin (50 µg/ml). The plates were incubated upside down at 37°C overnight. Single colonies that were picked for further analysis were streaked onto fresh LB agar plates supplemented with kanamycin (50 µg/ml), incubated upside down at 37°C overnight, parafilmed, and stored at 4°C for immediate use.

2.12.1.4 Preparing Glycerol Stocks of *E. coli* Transformants.

Glycerol stocks of each analyzed transformant were made for long-term storage. 5 ml of Luria-Bertani (LB) media (1 % Tryptone, 0.5 % yeast extract, 1 % NaCl, pH 7)(Fisher) supplemented with kanamycin (50 µg/ml) was inoculated

with single colonies of transformants and incubated at 37°C with shaking (1000-2000 rpm). At 1 h intervals, the optical density (OD) of the culture was determined at 600 nm by taking an aliquot of the inoculant and diluting it 1:10 in LB media. Once an OD_{600} of about 0.5-0.7 was reached (exponential phase), 700 µl of culture was added to 500 µl of sterile glycerol and stored at -84°C.

2.12.1.5 Plasmid Isolation from Transformed *E. coli* cells.

Initial analysis was carried out with crude plasmid isolation via alkaline lysis plasmid miniprep. 5 ml of Luria-Bertani (LB) media (1 % Tryptone, 0.5 % yeast extract, 1 % NaCl, pH 7)(Fisher) supplemented with kanamycin (50 µg/ml) was inoculated with single colonies of transformants and incubated overnight at 37°C with shaking (1000-2000 rpm). The bacteria cells were pelleted at 13,500 rpm for 20 minutes and the supernatant was aspirated off. The pellet was resuspended in ice-cold Solution I (50 mM Glucose, 25 mM Tris-HCl, pH 8, 10 mM EDTA, pH 8) and incubated for 5 minutes at room temperature. To this, Solution II (200 mM NaOH, 1% sodium dodecyl sulfate (SDS)) was added and the mixture was incubated on ice for 5 minutes. Ice-cold Solution III (3 M sodium acetate, 11.5% glacial acetic acid) was added to the mixture, incubated on ice for 10 minutes, centrifuged for 5 minutes at 13 500 rpm at 4°C, and supernatant transferred to sterile tube. Plasmid DNA was precipitated with ~ 65% isopropanol for 5 minutes at room temperature, centrifuged at 13, 500 rpm

for 10 minutes at 4°C, aspirated supernatant off, lyophilized pellet (SC100 speed-vac, Savant, Holbrook, NY), and resuspended plasmid DNA in sterile ddH_2O.

Qiagen Spin Miniprep (Qiagen, Germany) was used to obtain purer samples of isolated plasmid DNA for transfection and sequencing purposes. Plasmid isolation was carried out according to the manufacturer's instructions.

2.12.2 Donor Vector Analysis

2.12.2.1 Determine Position of Insert by Sequencing

The two ends of the insert/vector interfaces were sequenced to determine whether the recombination reaction resulted in an in-frame insert sequence. Sequencing was carried out as described above. Refer to Table 4 for pDONR primer sequences and Table 3 for gene specific internal primer sequences.

2.12.2.2 Enzyme Restriction of Donor Vector

Crude isolated plasmid DNA was linearized with *BstX* I (10 U/μl) (Invitrogen) or Hpa I (5 U/μl) (Invitrogen) at 50°C in 10 μl reaction volume (plasmid DNA, sterile ddH_2O, respective React® buffers (Invitrogen), restriction endonuclease) overnight. These two enzymes have one restriction site each within the vector. The digested product was resolved in 0.5% agarose gel with ethidium bromide and visualized under ultraviolet (UV) light; the transformant with the correct plasmid size was determined.

PART III | RESULTS

3.1 Temperature-sensitivity of Recombination Group C and F Mutants

Replication potentials of *tsC37* and *tsC287* at five different temperatures (33.5°C, 37°C, 39°C, 39.5°C, and 40°C) were analyzed to determine the mutants' degree of temperature-sensitivity (Figure 8). The maximum nonpermissive temperature used was 40°C, since cell viability becomes increasingly compromised beyond that temperature. A rule of thumb generally accepted for reoviruses (both in MRV and ARV) regarding temperature-sensitivity is that wild-type virus EOP values fall within 1.0 ± 1 $\log_{10}$, whereas *ts* mutant EOP values fall below the lower limit of the wild-type EOP value ($1.0 \geq 1$ $\log_{10}$) (reviewed in Coombs 1998). From this, *tsC37* was considered temperature-sensitive at a non-permissive temperature of 40°C, where an EOP value of 0.0096 was obtained (a measure of *ts*); a value well below the lower limit of the wild-type strain. *tsC287* was found to be more temperature-sensitive than *tsC37* beginning at 39°C, with a steep drop to an EOP value of 0.00085 at 40°C, a ten-fold decrease compared to *tsC37* at the same temperature. *tsF206* was also a temperature-sensitive clone at temperatures > 37°C, where the greatest sensitivity is at 40°C with an EOP value of 0.000025. This re-confirmed the previous reports which identifed *tsC37* and *tsF206* as *ts* mutants (Patrick 2001; Patrick *et al.* 2001).

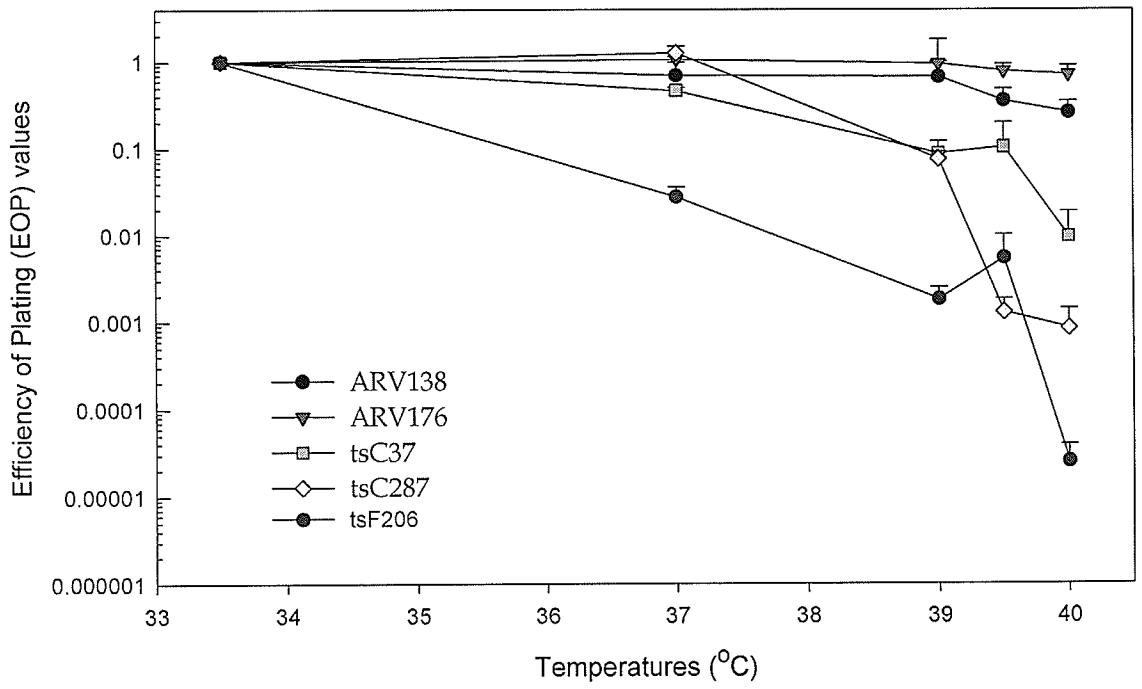

Figure 8. Temperature-sensitivity of ARV138, ARV176, *tsC37*, *tsC287*, and *tsF206* mutants at increasing temperatures from 33.5°C to 40°C. Error bars represent measure of standard deviation from three trials. EOP assay and calculations were carried out as described in Materials and Methods.

3.2 Mapping of *tsC37*

3.2.1 Reassortants Identification

ARV *tsC37* and *tsC287* temperature-sensitve mutants comprise recombination group C. The prototype *tsC37* was crossed with ARV176 to generate progeny clones as described under Materials and Methods. Cross-infection was carried out at three MOI ratios (*ts* to wildtype): 15:5, 5:5, 5:15 PFU per cell. A total of 383 clones were selected and amplified twice in QM5 cells to generate P2 stocks for subsequent analyses. Of these selected clones, 258 were screened for reassortants; the process included further amplification for dsRNA extraction, which were subjected to electrophoresis in 12.5% SDS-PAGE to obtain electropherotypes for each clone. The parental origin of each gene segment was determined by direct comparison of individual gene mobility within the electropherotypes of each clone, ARV176, and *tsC37* (Figure 9). Of the total clones screened, 202 were non-reassortants, meaning their genomic content originated entirely from one parent. Of these non-reassortant clones, 64 derived their genes from parental ARV176 and 137 clones had their genes traced back to the parental *tsC37*. On the other hand, 24 clones were determined to be reassortants, of which 13 were unique and 11 were duplicates. The remaining 32 clones screened represented mixed infections. Overall, this resulted in a reassortment efficiency of 9%.

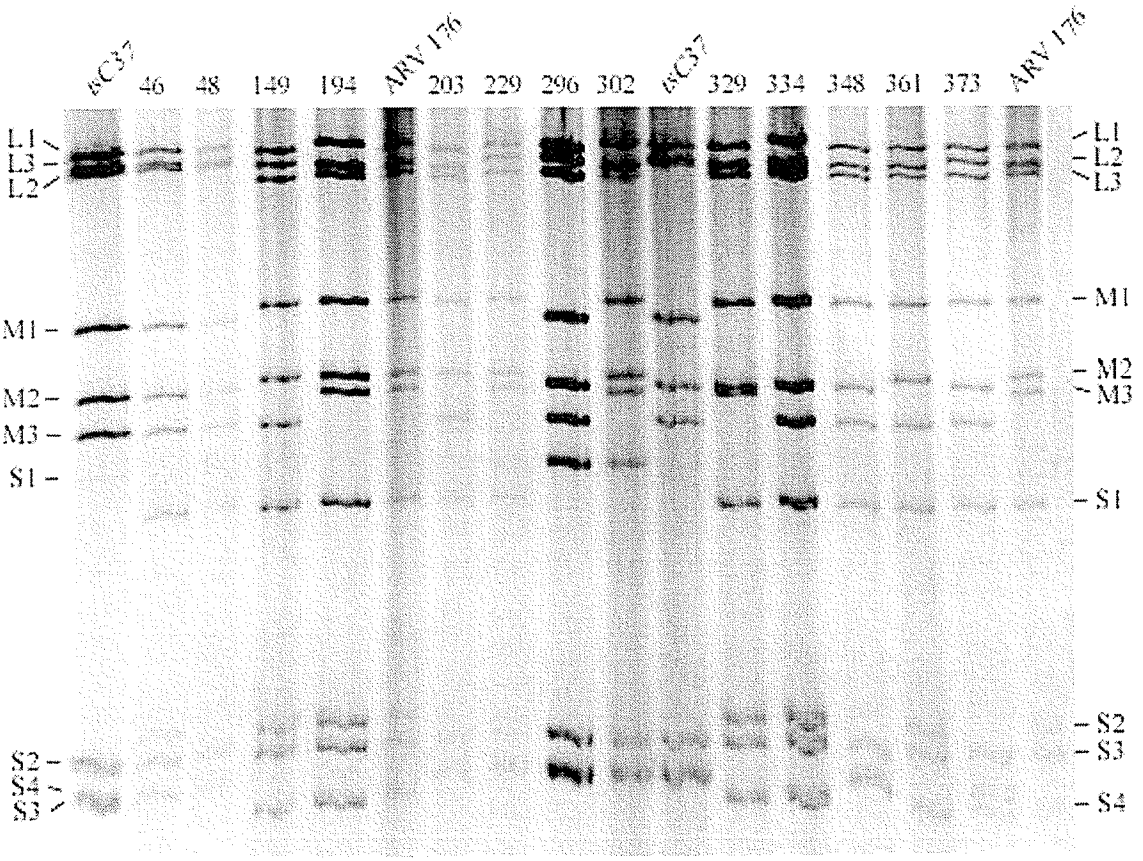

Figure 9. Electropherotypes of reassortant clones derived from ARV176 x *tsC37* cross. Genomic RNAs of wild-type ARV176, *tsC37* mutant, and reassortant clones were isolated, resolved, stained, and photographed as described under Materials and Methods (sections 2.7 and 2.8). Positions and identities of ARV176 and *tsC37* genes are indicated. The parental origin of each genome segment in each reassortant clone was determined by comparison of segment mobility to the parental ARV176 and *tsC37* markers.

In order to generate a table to map the *ts* mutation to a specific gene in *tsC37*, the EOP values and specific parental origin of each gene in every reassortant was ascertained.

3.2.2 *tsC37 lesion mapped to S3*

The efficiency of plating values, which are a measure of temperature-sensitivity, were obtained as described under Materials and Methods. Four separate trials were conducted on different days. Based on the EOP values determined, the reassortants were placed into two categorical groups, *ts* and non-*ts* (Table 5). 7 clones were found to have average EOP values that were at least two-fold lower than the wild-type ARV176 and, hence, are temperature-sensitive. These *ts* clones shared the S3 gene segment that originated from the temperature-sensitive parent (*tsC37*). On the other hand, all non-*ts* reassortants shared the same gene segment from the corresponding wild-type strain ARV176, and exhibited average EOPs that were within one order of magnitude of the wild-type value. The other genes were randomly assorted with regard to temperature-sensitivity.

However, some difficulties were encountered in identifying the origin of the S2 or S4 genes in four specific clones from the electropherotype profiles. Hence, the sequencing of the genes in these four clones were undertaken to decisively confirm their parental origins and complete the mapping.

Table 5. Electropherotypes and EOP values of ARV176 x *tsC37* Reassortants.

	Electropherotypes											
Clone	L1	L2	L3	M1	M2	M3	S1	S2	S3	S4	EOP[c]	SD[d]
229[e]	7[a]	C	7	7	7	7	7	C	C	7	0.00038	0.00028
203[e]	7	7	7	7	7	C	7	7	C	C	0.00048	0.00012
348[f]	7	7	7	7	C	C	7	7	C	7	0.00060	0.00063
296[g]	7	C	7	C	C	C	C	C	C	C	0.0011	0.0012
373[f]	7	C	7	7	C	C	7	C	C	7	0.0019	0.0024
tsC37	C	C	C	C	C	C	C	C	C	C	0.0096	0.0090
48[e]	C	C	C	C	C	C	7	C	C	7	0.010	0.00096
302[g]	C	7	7	7	7	7	C	C	C	C[b]	0.017	0.018
329[f]	7	7	7	C	C	7	7	7	7	7	0.24	0.17
46[e]	C	C	C	C	C	C	7	7	7	C[b]	0.31	0.35
194[e]	C	7	7	7	7	7	7	7	7	7	0.58	0.52
361[f]	7	7	7	7	7	C	7	7	7	C[b]	0.83	0.74
334[f]	C	7	7	7	C	C	7	C[b]	7	7	0.84	0.90
ARV176	7	7	7	7	7	7	7	7	7	7	1.27	0.49
149[e]	7	C	7	7	7	C	7	7	7	7	1.85	1.86
Exceptions	8	5	7	7	6	6	5	3	0	6		

[a] Parental origin of gene: C, *tsC37*; 7, ARV176

[b] Gene origin confirmed by sequencing

[c] Efficiency of plating (titer at 40°C) ÷ (titer at 33.5°C)

[d] Standard deviation based on four experiments

Reassortants derived from MOI ratios 5:15[e], 5:5[f], 15:5[g]

3.2.3 Parental Origin determined via Sequencing

There were some difficulties in determining the origin of the S2 and S4 genes in some clones from the electropherotype profiles; therefore, the parental origin of the S2 gene of clone 334 and S4 genes of clones 302, 361, and 46 were further confirmed by sequence analysis as described under Materials and Methods. A BLAST nucleotide-nucleotide sequence alignment of S2 and S4 genes revealed a relatively high sequence homology between the two wild-type strains ARV138 and ARV176. S2 and S4 have 94% and 82% identity, respectively. Recall that *tsC37* was derived from ARV138 via chemical mutagenesis. Therefore, only the region(s) that shows relatively high nucleotide differences sufficient to facilitate the identification of the parental origin in these clonal genes were sequenced and analysed. As seen in figures 10-13, the S2 gene from clone 334 was identified to have originated from the *tsC37* parent. Moreover, the S4 gene from clones 302, 46, and 361 also were confirmed to have originated from the *tsC37* parent.

3.2.4 Sequence analysis of *tsC37* S3 gene

Reassortant mapping of *tsC37* pinpointed the S3 gene segment, which encodes the major outer capsid protein σB, as the carrier of the *ts* mutation. Sequencing of the S3 genes of both *tsC37* and *tsC287* revealed a single nucleotide mutation from cytosine-to-adenine at nucleotide position 871 and cytosine-to-

```
ARV176_S2      660 TTAGTTTGTGGCTTCTTTCATACATTGGGGTGGTCAATCAGACCAACACCATCAGCGGCT
ARV138_S2          .............C.................A.....C........T.............
R334               .............C.................A.....C........T.............

ARV176_S2      719 TCTACTTCTCCTCGAAGACTCGGGGTCAAGCGTTGGACAGTTGGACTTTATTCTACACTA
ARV138_S2          ..............................................C........T....
R334               ..............................................C........T....

ARV176_S2      779 CAAACACTAATCGTGTTCAAATTACGCAGAGGCATTTCGCTTACGTGTGTGCTCGGTCTC
ARV138_S2          .......C..C.....C........C.....A...................A.......
R334               .......C..C.....C........C.....A...................A.......

ARV176_S2      839 CCGACTGGAACGTGGATAAATCATGGATCGCTGCAGCGAACTTAACCGCTATCGTCATGG
ARV138_S2          ....T.............G.............G.....................
R334               ....T.............G.............G.....................

ARV176_S2      899 CTTGCCGTCAACCGCCGGTGTTCGCCAATCAAGGCGTTATTAACCAAGCGCAGAACCGAC
ARV138_S2          ................A....T.....................G..A.........
R334               ................A....T.....................G..A.........

ARV176_S2      959 CTGGCTTTTCCATGAATGGGGGGACGCCCGTCCATGAGCTCAACTTACTGACTACCGCGC
ARV138_S2          ..............................................A.........
R334               ..............................................A.........

ARV176_S2     1019 AGGAATGTATTCGGCAGTGGGTGATGGCCGGTTTGGTGTCAGCAGCGAAGGGGCAAGCCT
ARV138_S2          .......C..C...........G.A..T..G.....................A.
R334               .......C..C...........G.A..T..G.................N.....A.

ARV176_S2     1079 TAACGCAGGAGGCTAATGACTTCTCAAACCTCATCCAGGCGGATCTAGGACAAATCAAAG
ARV138_S2          ..................T..G............A..........G.....G.
R334               ..................T..G............A..........G.....G.

ARV176_S2     1139 CGCGGGATGACGCTCTGTACAACCAGCAGCCAGGGTACGCGAGGAGAATAAAACCCTTCG
ARV138_S2          ...A................T..........A.....A..A.............
R334               ...A................T..........A.....A..A.............

ARV176_S2     1199 TTAACGGTGACTGGACACCAGGTATGACCGCGCAAGCTCTGGCCGTTCTAGCCACTTTTA
ARV138_S2          ....................................T.....................
R334               ....................................T.....................
```

Figure 10. Parental origin of reassortant 334 S2 gene determined via sequence comparison with ARV176 and ARV138 S2 genes. The lower two sequences are compared to the sequence listed at the top, where only the nucleotide differences to ARV176 sequence are shown. Non-differences are indicated as a dot (.) Only regions of greatest differences between the parental sequences are indicated for clarity. ARV176 and ARV138 S2 accession nos. AF059716.1 and AF059717.1, respectively. Sequences were aligned with ClustalW (Chenna *et al.* 2003).

```
ARV176_S4      541 ATAAGTTTGTGCTCCCTTACATGCTTGACATGGTAGATGGTCGTCCTCAGATTGTCCTGC
ARV138_S4          .C........A..T..........G.....A..G..C..A.....G........T..T.
R302               .C........A..T..........G.....A..G..C..A.....G........T..T.

ARV176_S4      601 CGTCTCATACCGTAGAAGAAATGTTGACCAACACCAGCTTGCTGAACTCGATTGATGCTT
ARV138_S4          .T..A..C.....T..G..G...C..........G........T..T..A..........
R302               .T..A..C.....T..G..G...C..........G........T..T..A..........

ARV176_S4      661 CATTTGGTATCGAAGCGCGCAGTGATCAAAGGATGACTCGTGATGCTGCTGAGATGAGTT
ARV138_S4          ..........T...T.TA.G..C......C.T.....C........G.....A.....C.
R302               ..........T...T.TA.G..C......C.T.....C........G.....A.....C.

ARV176_S4      721 CTCGCTCCCTCAATGAACTTGAGGATCATGATCAGAGAGGTCGTATGCCTTGGAAGATCA
ARV138_S4          ....T..G..T.....G...........C..G.....G..C..............A....
R302               ....T..G..T.....G...........C..G.....G..C..............A....

ARV176_S4      781 TGCTAGCGATGATGGCGGCCCAATTGAAGGTTGAGTTGGACGCGCTGGCGGACGAGCGTA
ARV138_S4          ..ACG......T.C..A..T...C.......G........T..C..A..T.........G
R302               ..ACG......T.C..A..T...C.......G........T..C..A..T.........G

ARV176_S4      841 CGGAGTCACAAGTTAATGCTCACGTTACATCCTTCGGATCCCGTTTATTTAATCAGATGT
ARV138_S4          TC.....T..G.C...C........G..G..T.....G.....GC....C..C.......
R302               TC.....T..G.C...C........G..G..T.....G.....GC....C..C.......

ARV176_S4      901 CGGCGTTCGTTACTATTGATCGTGAACTGATGGAACTGGCCCTTCTCATCAAGGAACAGG
ARV138_S4          .T..C..T...C.A........C..GT.......G.....T..AA....T........A.
R302               .T..C..T...C.A........C..GT.......G.....T..AA....T........A.

ARV176_S4      961 GCTTCGCCATGAATCCGGGTCAGATTGCATCTAAGTGGTCGCTGATACGTCGTTCCGGTC
ARV138_S4          .T..T..G........A..G..AG.C........A......T.......A..A..T....
R302               .T..T..G........A..G..AG.C........A......T.......A..A..T....

ARV176_S4     1021 CTACTCGTCCACTTTCAGGTGCCCGTCTTGAAATCAGGAATGGTAATTGGATGATCCGTG
ARV138_S4          .CG.C..C.....GG.T..C..A..C..C..G.....A.....C..C........T..C.
R302               .CG.C..C.....GG.T..C..A..C..C..G.....A.....C..C........T..C.
```

Figure 11. Parental origin of reassortant 302 S4 gene determined via sequence comparison with ARV176 and ARV138 S4 genes. The lower two sequences are compared to the sequence listed at the top, where only the nucleotide differences to ARV176 sequence are shown. Non-differences are indicated as a dot (.) Only regions of greatest differences between the parental sequences are indicated for clarity. ARV176 and ARV138 S4 accession nos. AF059724.1 and AF059725.1, respectively. Sequences were aligned with ClustalW (Chenna *et al.* 2003).

```
ARV176_S4       601 CGTCTCATACCGTAGAAGAAATGTTGACCAACACCAGCTTGCTGAACTCGATTGATGCTT
ARV138_S4           .T..A..C.....T..G..G...C..........G........T..T..A..........
R46                 ---------------------------------.G........T..T..A..........

ARV176_S4       661 CATTTGGTATCGAAGCGCGCAGTGATCAAAGGATGACTCGTGATGCTGCTGAGATGAGTT
ARV138_S4           ..........T...T.TA.G..C......C.T.....C........G.....A.....C.
R46                 ..........T...T.TA.G..C......C.T.....C........G.....A.....C.

ARV176_S4       721 CTCGCTCCCTCAATGAACTTGAGGATCATGATCAGAGAGGTCGTATGCCTTGGAAGATCA
ARV138_S4           ....T..G..T.....G...........C..G.....G..C..............A....
R46                 ....T..G..T.....G...........C..G.....G..C..............A....

ARV176_S4       781 TGCTAGCGATGATGGCGGCCCAATTGAAGGTTGAGTTGGACGCGCTGGCGGACGAGCGTA
ARV138_S4           ..ACG......T.C..A..T...C.......G........T..C..A..T.........G
R46                 ..ACG......T.C..A..T...C.......G........T..C..A..T.....N...G

ARV176_S4       841 CGGAGTCACAAGTTAATGCTCACGTTACATCCTTCGGATCCCGTTTATTTAATCAGATGT
ARV138_S4           TC.....T..G.C...C........G..G..T.....G.....GC....C..C.......
R46                 TC.....T..G.C...C........G..G..T.....G.....GC....C..C.......

ARV176_S4       901 CGGCGTTCGTTACTATTGATCGTGAACTGATGGAACTGGCCCTTCTCATCAAGGAACAGG
ARV138_S4           .T..C..T...C.A........C..GT.......G.....T..AA....T........A.
R46                 .T..C..T...C.A........C..GT.......G.....T..AA....T........A.

ARV176_S4       961 GCTTCGCCATGAATCCGGGTCAGATTGCATCTAAGTGGTCGCTGATACGTCGTTCCGGTC
ARV138_S4           .T..T..G........A..G..AG.C........A......T.......A..A..T....
R46                 .T..T..G........A..G..AG.C........A......T.......A..A..T....

ARV176_S4      1021 CTACTCGTCCACTTTCAGGTGCCCGTCTTGAAATCAGGAATGGTAATTGGATGATCCGTG
ARV138_S4           .CG.C..C.....GG.T..C..A..C..C..G.....A.....C..C........T..C.
R46                 .CG.C..C.-------------------------------------------------
```

Figure 12. Parental origin of reassortant (R) 46 S4 gene determined via sequence comparison with ARV176 and ARV138 S4 genes. The lower two sequences are compared to the sequence listed at the top, where only the nucleotide differences to ARV176 sequence are shown. Non-differences are indicated as a dot (.) Only regions of greatest differences between the parental sequences are indicated for clarity. ARV176 and ARV138 S4 accession nos. AF059724.1 and AF059725.1, respectively. Sequences were aligned with ClustalW (Chenna *et al.* 2003).

```
ARV176_S4      121 CAGCTGATGGCCGTAATGCAACGAAGGCGGTACAATCCCACTTTCCATTCCTTTCACGTG
ARV138_S4          .........T..C........A..A.....G.....T.............C..T....
R361               .........T..C........A..A.....G.....T.............C..T....

ARV176_S4      181 CTGTGCGATGCCTATCGCCTCTTGCCGCTCACTGTGCTGATAGAACCCTTCGCCGTGACA
ARV138_S4          ....C.....TT....T.....A..T.....T..C........G.....A..T.......
R361               ....C.....TT....T.....A..T.....T..C........G.....A..T.......

ARV176_S4      241 ACGTGAAACAGATTCTTACTCGTGAACTGCCATTTTCCTCGGATTTAATCAACTATGCAC
ARV138_S4          ....A..G...........G.....GT....C...C.A......C....T..T..C..G.
R361               ....A..G...........G.....GT....C...C.A......C....T..T..C..G.

ARV176_S4      301 ACCATGTCAATTCATCATCCCTTACTACCTCTCAAGGCGTCGAAGCGGCTCGTTTGGTAG
ARV138_S4          .T.....A........C..T..C..C..T.....G..T..T........A...C.A..G.
R361               .T.....A........C..T..C..C..T.....G..T..T........A...C.A..G.

ARV176_S4      361 CTCAAGTTTATGGGGAACAAGTACCGTTCGATCACATTTATCCTACTGGTTCAGCGACAT
ARV138_S4          ...............G...C.GT....T......G.C.....C........T..A....
R361               ...............G...C.GT....T......G.C.....C........T..A....

ARV176_S4      421 ACTGTCCTGGTGCAATCGCAAATGCTATTTCTCGCATTATGGCTGGCTTTGTACCTCGTG
ARV138_S4          ....C.....A..G.....G.....G.....C.....C........T..C.....C.A..
R361               ....C.....A..G.....G.....G.....C.....C........T..C.....C.A..

ARV176_S4      481 AAGGTGATGACTTTGCTCCGAGTGGCCCTATTGACTACCTCGCTGCTGACCTGATCGCGT
ARV138_S4          ....CA........A.C...GAC..TG.C...........T..G..G..T...G......
R361               ....CA........A.C...GAC..TG.C...........T..G..G..T...G......

ARV176_S4      541 ATAAGTTTGTGCTCCCTTACATGCTTGACATGGTAGATGGTCGTCCTCAGATTGTCCTGC
ARV138_S4          .C........A..T...........G.....A..G..C..A.....G........T..T.
R361               .C........A..T...........G.....A..G..C..A.....G........T..T.

ARV176_S4      601 CGTCTCATACCGTAGAAGAAATGTTGACCAACACCAGCTTGCTGAACTCGATTGATGCTT
ARV138_S4          .T..A..C.....T..G..G...C..........G........T..T..A..........
R361               .T..A..C.....T..G..G...C..........G........T..T..A..........

ARV176_S4      661 CATTTGGTATCGAAGCGCGCAGTGATCAAAGGATGACTCGTGATGCTGCTGAGATGAGTT
ARV138_S4          ..........T...T.TA.G..C......C.T.....C........G.....A.....C.
R361               ..........T...T.TA.G..C......C.T.....C........G.....A.....C.

ARV176_S4      721 CTCGCTCCCTCAATGAACTTGAGGATCATGATCAGAGAGGTCGTATGCCTTGGAAGATCA
ARV138_S4          ....T..G..T.....G...........C..G.....G..C..............A....
R361               ....T..G..T.....G...........C..G.....G..C..............A....

ARV176_S4      781 TGCTAGCGATGATGGCGGCCCAATTGAAGGTTGAGTTGGACGCGCTGGCGGACGAGCGTA
ARV138_S4          ..ACG......T.C..A..T...C.......G........T..C..A..T.........G
R361               ..ACG......T.C..A..T...C.......G........T..C..A..T.........G

ARV176_S4      841 CGGAGTCACAAGTTAATGCTCACGTTACATCCTTCGGATCCCGTTTATTTAATCAGATGT
ARV138_S4          TC.....T..G.C...C........G..G..T.....G.....GC....C..C.......
R361               TC.....T..G.C...C........G..G..T.....G.....GC....C..C.......

ARV176_S4      901 CGGCGTTCGTTACTATTGATCGTGAACTGATGGAACTGGCCCTTCTCATCAAGGAACAGG
ARV138_S4          .T..C..T...C.A........C..GT.......G.....T..AA....T........A.
R361               .T..C..T...C.A........C..GT.......G.....T..AA....T........A.

ARV176_S4      961 GCTTCGCCATGAATCCGGGTCAGATTGCATCTAAGTGGTCGCTGATACGTCGTTCCGGTC
ARV138_S4          .T..T..G........A..G..AG.C........A......T.......A..A..T....
R361               .T..T..G........A..G..AG.C........A......T.......A..A..T....

ARV176_S4     1021 CTACTCGTCCACTTTCAGGTGCCCGTCTTGAAATCAGGAATGGTAATTGGATGATCCGTG
ARV138_S4          .CG.C..C.....GG.T..C..A..C..C..G.....A.....C..C........T..C.
R361               .CG.C..C.....GG.T..C..A..C..C..G.....A.....C..C........T..C.
```

Figure 13. Parental origin of reassortant (R) 361 S4 gene determined via sequence comparison with ARV176 and ARV138 S4 genes. The lower two sequences are compared to the sequence listed at the top, where only the nucleotide differences to ARV176 sequence are shown. Non-differences are indicated as a dot (.) Only regions of greatest differences between the parental sequences are indicated for clarity. ARV176 and ARV138 S4 accession nos. AF059724.1 and AF059725.1, respectively. Sequences were aligned with ClustalW (Chenna *et al.* 2003).

thymidine at position 872, respectively (Figure 14, A). These nucleotide alterations led to the same amino acid substitution at position 281, from a proline-to-threonine for *tsC37* and proline-to-leucine for *tsC287* (Figure 14, B). Alignments of amino acid sequences of corresponding orthoreovirus and orbivirus major outer capsid proteins revealed this Pro_{281} to be highly conserved, suggesting the amino acid at this position may be critical for the proper folding of σB (Figure 15).

Little is known about ARV σB major outer capsid protein. Currently, most information regarding this structural protein is extrapolated from its homolog MRV σ3, which has been determined to play roles in dsRNA binding, inhibition of PKR signalling, and critical association with MRV μ1 structural protein. However, preliminary work with *tsC37* reported here revealed that ARV σB shares similar functions with its MRV homolog. It should be noted at this point that most of the above results have been published in *Virology* (refer to Xu *et al.* 2005).

3.3 Core-like Structures produced by *tsC37* at Restrictive Temperature

QM5 monolayers were infected with *tsC37* and ARV138 at MOI of 5 PFU/cell, incubated at 33.5°C for 30 h and 40°C for 22.5 h. The samples were fixed in 2% paraformaldehyde. A series of 10-fold dilutions (10^{-1} to 10^{-3}) of the suspension was made; each was airfuged directly onto formvar-coated, carbon-

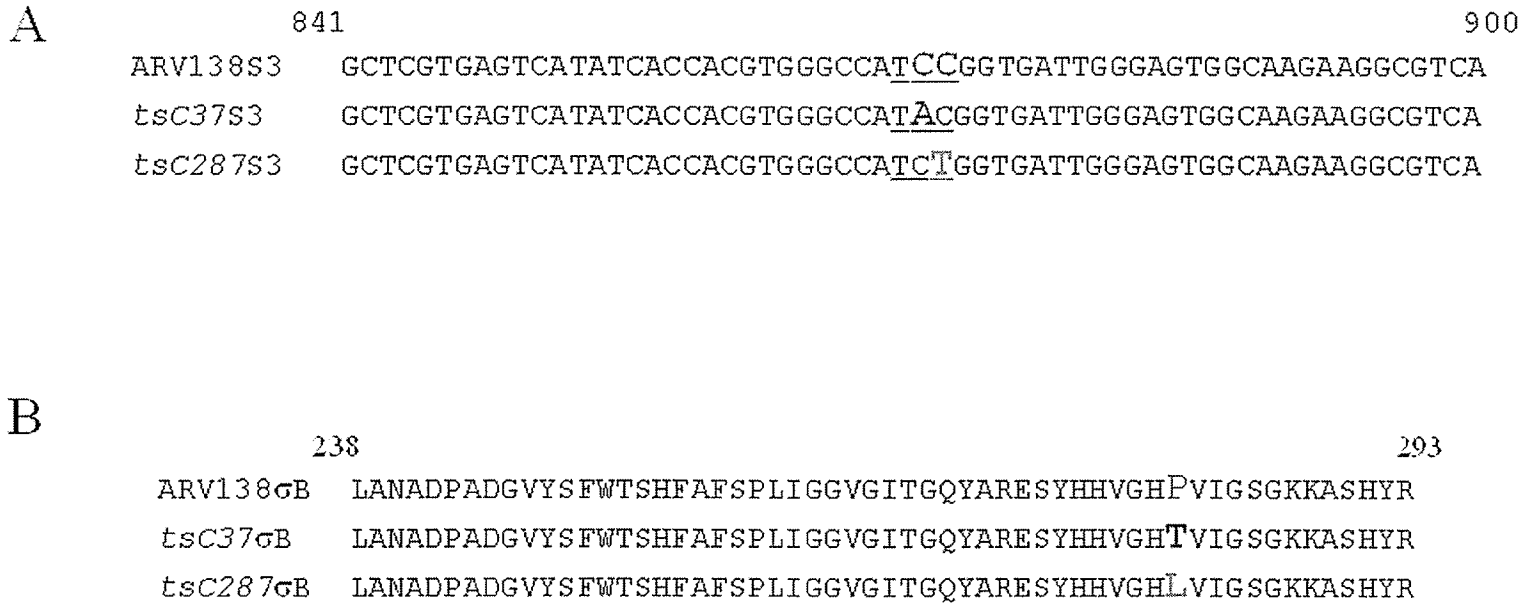

Figure 14. Position of nucleotide and amino acid mutations in avian reovirus recombination group C mutants. Only the regions that contain the mutations are shown. (A) Nucleotide mutation in *tsC37* indicated in blue and *tsC287* in green. Corresponding wild-type nucleotide indicated in red. The codon is underlined. (B) Amino acid substitution in *tsC37* indicated in blue and *tsC287* in green. Corresponding wild-type amino acid indicated in red. Sequencing was done in both directions as described in Materials and Methods (section 2.9). ARV138 σB GeneBank accession no. AAC18126. ARV138 S3 accession no. AF059721.1.

ARV176σB 238 LAN--ADPAEGVYSFWTSHF--AFSPLIGGVGITGQYARESYHHVGHPVIGSGKKASHYR
ARV138σB 238 LAN--ADPADGVYSFWTSHF--AFSPLIGGVGITGQYARESYHHVGHPVIGSGKKASHYR
NBVσ2 231 LQPHVTKEVAAAALLKPEHV--IITPDMAGLPVLAR-SHQSSLFVGMPLVESAQKASLYR
MRVT3Dσ3 238 YRKELVTPARDFGHFGLSHYSRATTPILGKMPAVFSGMLTGNCKM-YPFIKGTAKLKTVR
MRVT1Lσ3 238 YRKELVTPARDFGHFGLSHYSRATTPILGKMPAVFSGMLTGNCKM-YPFIKGTAKLKTVR
NDEVσ2 238 YRKELVTPARDFGHFGLSHYSRATTPILGKMPAVFSGMLTGNCKM-YPFIKGTAKLKTVR
MRVT2Jσ3 238 YRNEVVTPARDFGHFGLSHYSRATTPILGKMPAVFSGMLTGNCKM-YPFIKGTAKLRTVK
BRVσ2 259 NDTFFSEHHGDIKKTLLGTD-LIVAPLAGNVPLIIGPLDDRYSFP-MPYVRPETQKALCN
BTVVP5 301 TSVLNKKTAVADNCNELAHIKQEILPKFKQIMNEEKELEGIEDKVIHPRWMMRFKIPRTQ
tsC37σB 238 LAN--ADPADGVYSFWTSHF--AFSPLIGGVGITGQYARESYHHVGHTVIGSGKKASHYR
tsC287σB 238 LAN--ADPADGVYSFWTSHF--AFSPLIGGVGITGQYARESYHHVGHLVIGSGKKASHYR

Figure 15. Alignment of amino acid sequences of corresponding orthoreovirus and orbivirus outer capsid proteins. Only the region that contains the amino acid substitution in the *tsC37* mutant is shown. Amino acid residues shaded in black are identical in at least six of the sequences. Gray background shading indicates conservative amino acid substitutions in at least six of the sequences. The viral proteins used for comparison are: ARV strains 138 σB (GeneBank accession no. AAC18126); 176 σB (GeneBank accession no. AAC18125); MRV strains Lang (T1L) σ3 (GeneBank accession no. P07939), Jones (T2J) σ3 (GeneBank accession no. P30211), and Dearing (T3D) σ3 (GeneBank accession no. P03527); baboon reovirus (BRV) σ2 (GeneBank accession no. AAC18128); Nelson Bay virus (NBV) σ2 (GeneBank accession no. AAC18127); Ndelle virus (NDEV) σ2 (GeneBank accession no. AAL36031); bluetongue virus (BTV) VP5 (GeneBank accession no. P33475). Amino acid substitution at position 281 is indicated in large, coloured fonts. Sequences were aligned with ClustalW (Chenna *et al.* 2003).

stabilized 400-mesh copper grids; and stained with phosphotungstic acid. The samples were visualized under EM, where the proportions of particle-types (cores, complete virion, top components, and outer shell) were determined (Figure 16).

At permissive temperature (33.5°C), the proportions of different particles produced by *tsC37* were similar to the wild-type ARV138, where the greatest proportion of particles produced was complete virion at 46.1% (Table 6). However, at non-permissive temperature (40°C), *tsC37* infection resulted in 68.6% of the particles produced that are core-like in structure and lacked genomic content, compared to only 5.3% (actual cores) observed in ARV138 (approximately a thirteen-fold difference). Similarly, top components produced by the wild-type were more than two-fold greater than *tsC37*; 44.8% compared to only 20.7%. At this restrictive temperature, only 9.3% of the particles produced by the mutant were actual complete virions, more than five-fold less than the wild-type (46.1%). Furthermore, only 1.4% outer shell structures were observed in the mutant samples (Table 6), twice as much was seen in the wild-type. Additionally, the majority of the particles produced (the core-like structures) were observed to lack genomic content (refer to Figure 22 under section 4.3 for EM image).

Additionally, infectivity was correlated with total complete virion concentration to obtain the relative infectivity of each sample expressed as a particle-to-PFU ratio. Infectivity at nonpermissive temperature for the mutant

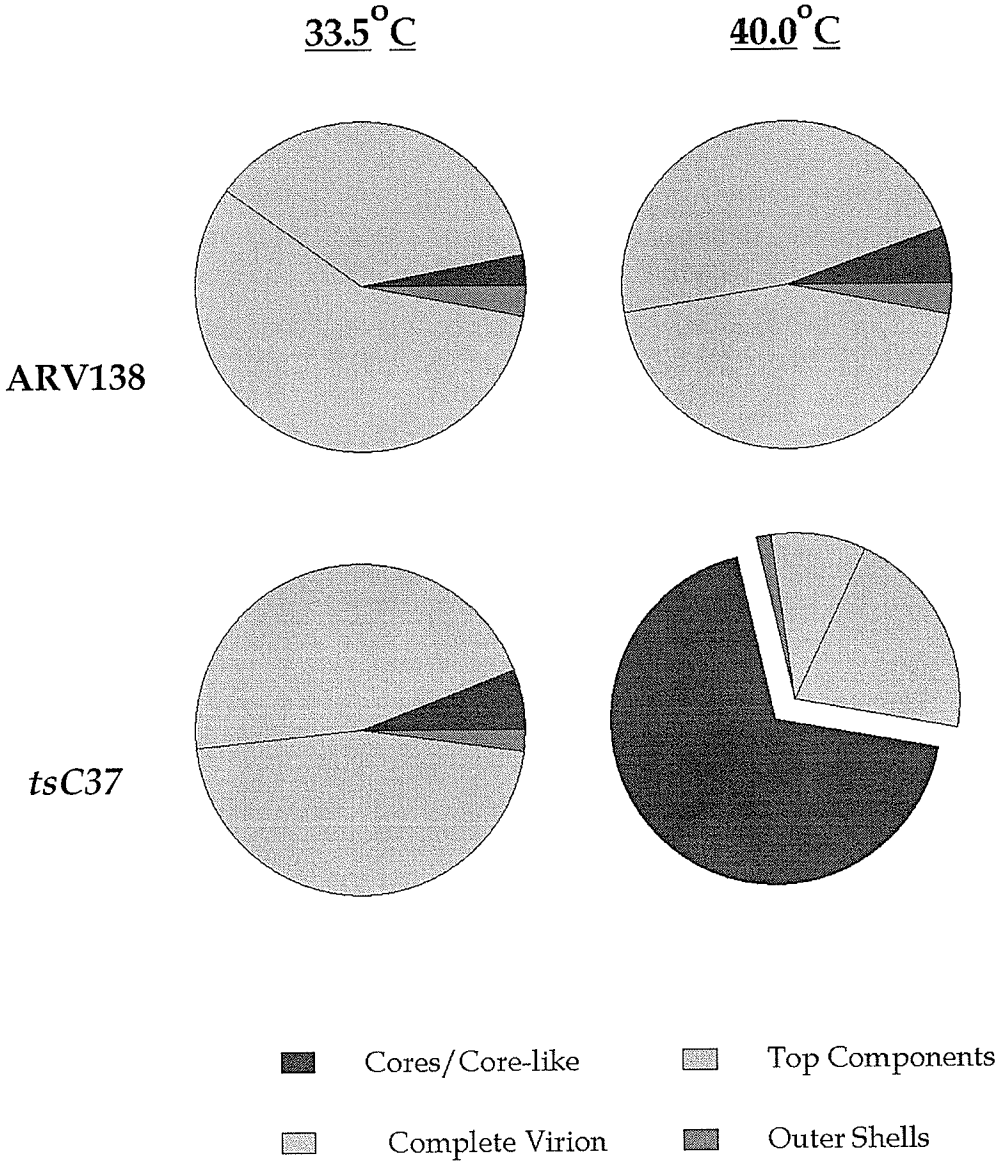

Figure 16. Proportions of particle types produced during ARV138 and *tsC37* infection. "Core-like" refers to core-type particles produced by *tsC37* at 40°C. Samples were prepared as described in Materials and Methods (section 2.11), viewed with TEM at magnification of 30,000X and images recorded at magnification of 70,000X. Proportions of particle-types produced by ARV138 at 33.5°C obtained from Patrick 2001.

Table 6. Proportion of particle-types produced by ARV138 and *tsC37* at nonpermissive and permissive temperatures[a].

Clones	Temperatures (°C)	Total No. of particles/ml[b]	Particle/ PFU ratio	Proportion of particles (%[SEM])[c]			
				Complete virion	Top Component	Outer Shell	Core/ core-like[e]
ARV138	33.5[d]	$6.1x10^7$	---[d]	57.0	37.0	3.0	3.0
	40	$3.06x10^7$	6:1	42.1 [1.5]	44.8 [6.2]	2.9 [2.8]	5.3 [3.7]
tsC37	33.5	$1.51x10^9$	68:1	46.1 [9.5]	45.9 [8.3]	2.2 [1.92]	5.8 [4.8]
	40	$3.94x10^7$	627:1	9.3 [7.9]	20.7 [9.9]	1.4 [1.6]	68.6 [23]

[a] values represent 3 trials

[b] Total particles/ml calculated as: particles/ml = (average number of particles)$(1.79x10^5)$(dilution factor) (Hammond *et al.* 1981)

[c] percentage of total particles represents average of 5 sample grids, standard error of the mean (SEM) shown in square brackets []

[d] values for 33.5°C were obtained from Patrick 2001; PFU and SEM were not determined

[e] core-like term refers to core-type particles produced by *tsC37* at 40°C (refer to sections 3.3 and 4.3 for details)

tsC37 is quite low compared to the wild-type (particle-to-PFU ratio of 627:1 to 6:1, respectively) (Table 6). This indicates that infectious virion production at the restrictive temperature is greatly hindered in *tsC37* by the mutation on σB. Therefore, the mutation in *tsC37* affects not only the assembly of complete virions but also affects the degree of infectivity of the virus population as a whole. Further, the infectivity of the mutant at the permissive temperature is observably better than at the restrictive temperature (68:1 compared to 627:1, respectively) but still much lower than the 40°C wild-type 6:1 ratio. This would suggest that although the percentage of complete virion production is similar to the wild-type (46.1% for the mutant to 42.1% wild-type), infectivity is reduced due to the mutation in σB even at permissive temperature. It may be possible that the protein's conformation is affected to a certain extent even at 33.5°C, such that the heterohexameric complex it forms in association with μB is less stable than its wild-type counterpart. Infectivity for ARV138 at 33.5°C was not determined (Patrick 2001).

3.4 Mapping of *tsF206*

Avian reovirus recombination group F mutant has only one member, *tsF206*. Mapping of this mutant was initiated by a former undergraduate Honours student, Trina Racine, who conducted the cross-infection of *tsF206* x ARV176, selection, and amplification of progeny clones to the P_2 stage. At that

point, the project was then integrated into this study where the completion of *tsF206* map involved determining the EOP for each clone and re-confirming the parental origin identification of each gene. The cross-infection of *tsF206* x ARV176, selection, and amplification of progeny clones were carried out as described under Materials and Methods. Co-infection was carried out at MOI ratios of 2:8, 8:2, and 5:5 PFU per cell of *tsF206* to ARV176. The clones were selected and amplified twice in QM5 cells to generate P2 stocks for subsequent analyses. The selected clones were screened for reassortants, a process that included further amplification for dsRNA extraction, which were subjugated to electrophoresis in 12.5% SDS-PAGE to obtain electropherotypes for each clone (carried out by Trina Racine). The parental origin of each gene segment was determined and re-confirmed by direct comparison of individual gene mobility within the electropherotypes of each clone, ARV176, and *tsF206* (Figure 17). In order to facilitate the mapping of *tsF206*, the electropherotypes of 5 additional clones were determined and parental origin of each gene was assigned.

Further, the temperature-sensitivity (EOP values) of each clone, ARV176, and *tsF206* were obtained as described under Materials and Methods. Two categories of reassortants (*ts* and non-*ts*) were created based on their EOP values (Table 7). 12 clones (not including the *ts* parent) were found to have average EOP values that were one- to two-folds lower than the wild-type ARV176 and, hence, are temperature-sensitive. These *ts* clones shared the S4 gene segment that originated from the temperature-sensitive parent (*tsF206*); all non-*ts*

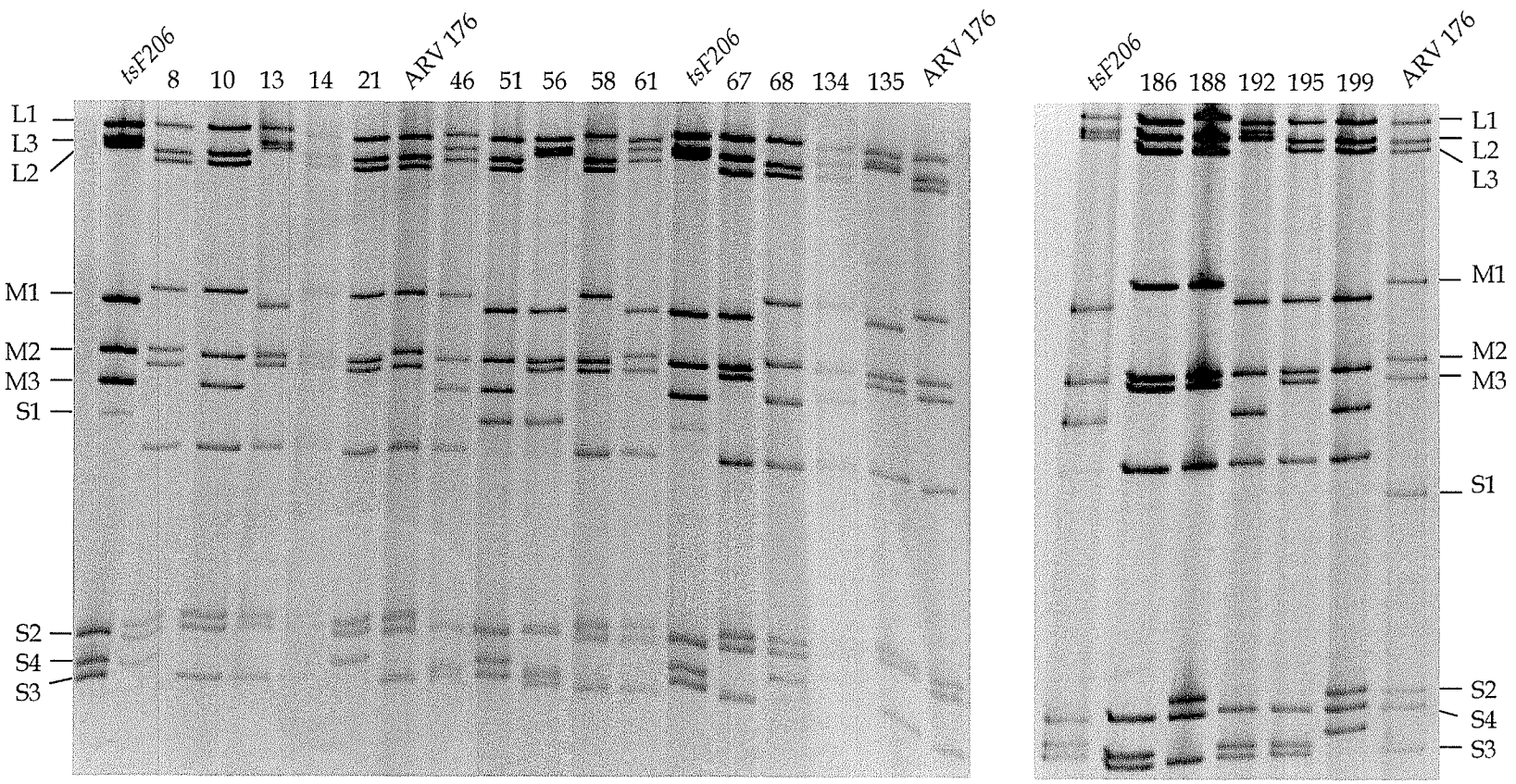
tsF206
8
10
13
14
21
ARV 176
46
51
56
58
61
tsF206
67
68
134
135
ARV 176
L1
L3
L2
M1
M2
M3
S1
S2
S4
S3
tsF206
186
188
192
195
199
ARV 176
L1
L2
L3
M1
M2
M3
S1
S2
S4
S3

Figure 17. Electropherotypes of reassortant clones derived from ARV176 x *tsF206* cross. Genomic RNAs of wild-type ARV176, *tsF206* mutant, and reassortant clones were resolved, stained, and photographed as described under Materials and Methods. Positions and identities of ARV176 and *tsF206* genes are indicated. The parental origin of each genome segment in each reassortant clone was determined by comparison of segment mobility to the parental ARV176 and *tsF206* markers.

Table 7. Electropherotypes and EOP values of ARV176 x *tsF206* Reassortants.

Clone	Electropherotypes										EOP[b]	SD[c]
	L1	L2	L3	M1	M2	M3	S1	S2	S3	S4		
tsF206	F[a]	F	F	F	F	F	F	F	F	F	0.000067	0.000072
51	7	7	7	F	F	F	F	F	F	F	0.00041	0.00047
199	F	7	7	F	F	F	F	7	7	F	0.0018	0.0028
134	7	F	7	7	F	F	7	7	7	F	0.0050	0.0031
21	7	7	7	7	F	7	7	7	7	F	0.0056	0.0029
56	7	F	F	F	F	7	F	F	F	F	0.010	0.0081
68	F	7	7	7	7	F	7	7	7	F	0.016	0.013
8	F	7	7	7	7	7	7	7	7	F	0.017	0.0045
195	7	7	7	F	F	7	F	F	F	F	0.018	0.023
188	F	F	7	7	F	7	F	7	7	7	0.024	0.018
192	7	F	F	F	F	F	F	F	F	F	0.026	0.020
186	7	F	7	7	F	7	F	F	F	F	0.062	0.043
46	F	F	F	7	F	F	7	F	F	F	0.078	0.0066
58	F	7	7	7	F	7	7	7	7	7	0.28	0.14
14	F	F	F	F	F	7	7	7	7	7	0.29	0.22
61	F	7	F	F	7	7	7	7	7	7	0.39	0.30
135	7	F	F	F	F	7	7	7	7	7	0.41	0.074
A176	7	7	7	7	7	7	7	7	7	7	0.59	0.60
10	7	7	7	7	F	F	7	7	7	7	0.65	0.63
13	F	F	F	F	F	7	7	7	7	7	1.85	1.88
67	F	F	7	F	F	7	7	7	7	7	2.60	1.62
Exceptions	12	10	13	12	8	7	5	6	6	1		

[a] Parental origin of gene: F, *tsF206*; 7, ARV176

[b] Efficiency of plating (titer at 40°C) ÷ (titer at 33.5°C)

[c] Standard deviation based on three experiments

reassortants shared the same gene segment from the corresponding wild-type strain ARV176, and exhibited average EOPs that were within one order of magnitude of the wild-type value. The other genes were randomly assorted with regard to temperature-sensitivity. Similar to *tsG247* discussed in the next section, *tsF206* map also has one exception in clone 188, which has its S4 gene orgininating from the wild-type parent. However, its EOP value indicates that it is a temperature-sensitive clone. Two possible explanations would be the presence of a mutation within the S4 gene that occurred during the generation of these reassortants (which would not be unexpected since this is an RNA virus), which would give rise to the *ts* phenotype observed, or the specific gene constellation is less than optimum so as to give the low EOP value.

The ARV S4 gene encodes for the non-structural protein σNS, one of the proteins produced early in viral infection. Similar to the homologous MRV protein σNS (encoded by the MRV S3 gene), ARV non-structural protein (σNS) binds single-stranded (ss) RNA in a sequence independent manner (Touris-Otero *et al.* 2005), but unlike MRV, its role in RNA assortment remains to be determined. Interestingly, it was found that *tsF209* mutant could not synthesize genomic dsRNA (RNA^-). This implies that σNS may play an important role in genomic dsRNA recruitment and/or packaging.

3.5 Mapping of *tsG247*

Similar to avian reovirus recombination group F, ARV recombination group G also has only one member, *tsG247*. Mapping of this mutant was initiated by a former undergraduate Honours student, Alex Selaghi, who conducted the cross-infection of *tsG247* x ARV176, selection, and amplification of progeny clones to the P_2 stage. At that point, the project was then integrated into this study where the completion of *tsG247* map involved determining the EOP for each clone and re-confirming the parental origin identification of each gene. The cross-infection of *tsG247* x ARV176, selection, and amplification of progeny clones were carried out as described under Materials and Methods. Cross-infection was carried out at MOI ratios (*ts* to wildtype): 10:10, 5:10, and 10:5 PFU per cell. The clones were selected and amplified twice in QM5 cells to generate P2 stocks for subsequent analyses. The selected clones were screened for reassortants, a process that included further amplification for dsRNA extraction, which were subjugated to electrophoresis in 12.5% SDS-PAGE to obtain electropherotypes for each clone (carried out by Alex Selaghi). The parental origin of each gene segment was determined and re-confirmed by direct comparison of individual gene mobility within the electropherotypes of each clone, ARV176, and *tsG247* (Figure 18). The electropherotype and EOP value was determined for an additional clone to facilitate completion of the map.

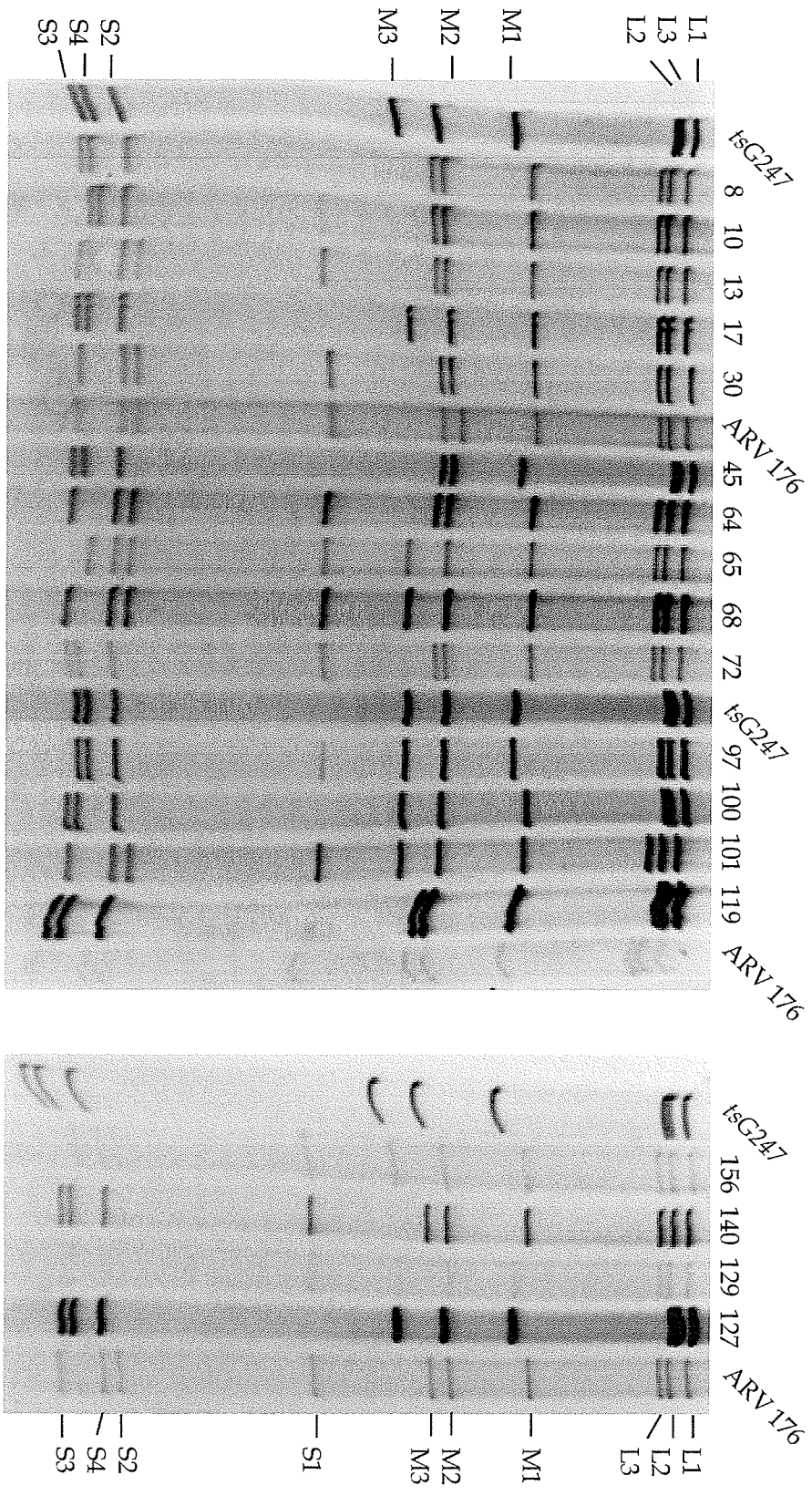
tsG247
8
10
13
17
30
ARV176
45
64
65
68
72
tsG247
97
100
101
119
ARV176
L1
L3
L2
M1
M2
M3
S2
S4
S3
tsG247
156
140
129
127
ARV176
L1
L2
L3
M1
M2
M3
S1
S2
S4
S3

Figure 18. Electropherotypes of reassortant clones derived from ARV176 x *tsG247* cross. Genomic RNAs of wild-type ARV176, *tsG247* mutant, and reassortant clones were resolved, stained, and photographed as described under Materials and Methods. Positions and identities of ARV176 and *tsG247* genes are indicated. The parental origin of each genome segment in each reassortant clone was determined by comparison of segment mobility to the parental ARV176 and *tsG247* markers.

The EOP values were determined for each clone, ARV176, and *tsG247* as described under Materials and Methods. Three separate trials were conducted on different days. Reassortants were divided into two categories, *ts* and non-*ts* based on their EOP values (Table 8). 6 clones (not including the *ts* parent) were found to have average EOP values that were one- to two-folds lower than the wild-type ARV176 and, hence, are temperature-sensitive. These *ts* clones shared the L3 gene segment that originated from the temperature-sensitive parent (*tsG247*). Conversely, all non-*ts* reassortants shared the same gene segment from the corresponding wild-type strain ARV176, and exhibited average EOPs that were within one order of magnitude to the wild-type value. The other genes were randomly assorted with regard to temperature-sensitivity. However, clone 101 has its L3 gene derived from the wild-type parent but its EOP value indicates that it is a temperature-sensitive clone. Two possible explanations would be the presence of a mutation within its L3 gene that occurred during the generation of these reassortants which would give rise to the *ts* phenotype observed, or the specific gene constellation is less than optimum such that gave rise to the low EOP value. Further, clone 101's EOP value is at the borderline between *ts* and non-*ts*.

The ARV L3 gene encodes for the core spike protein λC, which exhibits guanylyltransferase (Hsiao *et al.* 2002) and methyltransferase activities (Spandidos and Graham 1976; Martínez-Costas *et al.* 1995) involved in mRNA cap methylation (Martínez-Costas *et al.* 1995). Interestingly, Patrick (2001)

Table 8. Electropherotypes and EOP values of ARV176 x *tsG247* Reassortants.

Clone	Electropherotypes										EOP[b]	SD[c]
	L1	L2	L3	M1	M2	M3	S1	S2	S3	S4		
119	G[a]	G	G	7	G	7	---[d]	G	G	7	0.000021	0.0000064
127	G	G	G	G	7	G	---	G	G	G	0.00015	0.00016
45	G	G	G	G	G	7	---	G	G	7	0.00031	0.00026
100	G	G	G	7	G	G	---	G	G	7	0.00046	0.00026
tsG247	G	G	G	G	G	G	---	G	G	G	0.0010	0.0018
97	G	7	G	G	G	G	---	G	G	G	0.0066	0.011
101	7	G	7	7	G	G	7	7	7	7	0.070	0.059
129	7	7	7	G	7	G	7	G	G	7	0.17	0.17
68	7	7	7	7	G	G	7	7	7	7	0.39	0.35
72	7	7	7	7	G	7	7	G	G	7	0.48	0.39
13	7	7	7	7	G	7	7	7	7	7	0.49	0.38
156	G	7	7	7	7	G	7	7	7	G	0.49	0.51
64	7	G	7	7	G	7	7	7	7	7	0.50	0.35
10	7	7	7	7	G	7	---	G	G	G	0.55	0.51
ARV176	7	7	7	7	7	7	7	7	7	7	0.75	0.13
30	G	7	7	7	G	7	7	7	7	7	0.79	0.89
65	7	7	7	7	G	G	7	7	7	G	0.85	0.56
8	7	7	7	7	G	7	---	G	G	7	0.92	1.31
77	7	7	7	7	G	G	---	G	G	7	1.02	1.27
140	7	G	7	7	7	7	7	G	G	7	1.28	1.28
Exceptions	3	3	1	4	10	7	4	7	7	7		

[a] Parental origin of gene: G, *tsG247*; 7, ARV176

[b] Efficiency of plating (titer at 39.5°C) ÷ (titer at 33.5°C)

[c] Standard deviation based on three experiments

[d] S1 gene was not detected in the electropherotype

determined *tsG247* mutant to be RNA^{--}, which denotes its inability to synthesize genomic dsRNA. This implies that λC may play an important role in genome production.

3.6 S1 Gene absent in some viral progenies

The absence of S1 gene segment has been observed in several non-reassortant clones isolated from the cross-infection of *tsC37* x ARV176 (data not shown) and in the mutant *tsG247* (Figure 18). It is uncertain, in the case of *tsC37* and *tsG247*, whether this particular segment is completely absent or truncated. *tsC37* itself appeared to contain a subpopulation that either lacked the S1 gene or contains a truncated version of the S1 gene, as evident by the faintness of the S1 band in the mutant's electropherotype (Figure 9). Moreover, of the 258 clones screened, 30 were found to lack the S1 gene (either truncation or complete absence) (frequency = 11.6%): 15 S1 mutants were generated with cross-infections at MOI ratio 5:15 (frequency = 11.5%), 10 were generated at the MOI ratio 15:5 (frequency = 20%), and 5 were generated at MOI ratio 5:5 (frequency = 11.1%)— where ratios are *tsC37* to ARV176. χ^2 analysis indicated there is no significant statistical association between the MOI ratios and the frequency at which these S1 mutant viral progenies are generated ($p > 0.1$).

3.7 Recombinant Protein Expression in Baculovirus

Recall that *tsC37* results indicate that ARV σB plays a role very similar to MRV σ3; that it associates with ARV μB to form a heterohexamer complex, which is critical for the maturation of progeny virions. The mutation in *tsC37* occurred at a significant position in the protein sequence, which led to the inhibition of proper protein function; hence, mainly core-like structures were produced with very little production of mature virions. Additionally, EM visualization of these particles revealed empty structures that lacked genomic content, which may suggest possible involvement of this structural protein with genome packaging. Recall that MRV σ3 is believed to be involved in gene assortment. Logically, further analysis of the σB protein function and structure necessitates the isolation of the viral structural protein (ARV σB), possibly at high concentrations. Hence, the initiative to develop an expression system for recombinant protein in Baculoviruses.

3.7.1 Entry Clone Analysis

ARV138 and *tsC37* S3 open reading frames with the *attB* recombination sites on each end were generated by PCR. Using BP Clonase™ enzyme mix, an overnight recombination reaction was carried out according to the manufacturer's instructions with the PCR insert and pDONR™ vector to generate the entry clone; the initial step toward viral recombinant protein

expression in Sf9 cells. The entry clones were used to transform TOP10 chemically competent *E. coli*, which were grown on LB agar selective medium. Kanamycin was used as a negative selection against non-transformed cells. Five transformed, kanamycin resistant, colonies were picked, cultured, and the plasmids isolated and linearized with *BstX* I at 50°C. The linearized plasmids were resolved in 1% agarose gel.

The expected plasmid size for pDONR + S3 ORF is approximately 3.4 kb. From figure 19A, all the clones appeared to harbour the correct plasmid size. As shown in figure 19B, GEC3S3c5 appears to be of the correct size. Therefore, plasmids from clones (GEA3S3c5 and GEt3S3c1) were isolated and the entire ORF was sequenced to genetically determine whether the insert is correctly oriented in the plasmid after recombination.

Sequence analysis confirmed that indeed the entire S3 ORF from both clones were recombined correctly into the pDONR™ vector. Additionally, sequencing also confirmed that the mutation in *tsC37* S3 ORF at nucleotide position 871 was retained (data not shown).

3.7.2 Western Blot Detection of Recombinant Protein σB

Using plasmids isolated from GBA3S3c5 and GBt3S3c1, the LR reaction was carried out according to the manufacturer's instructions to generate the destination clone used to transfect Sf9 cells.

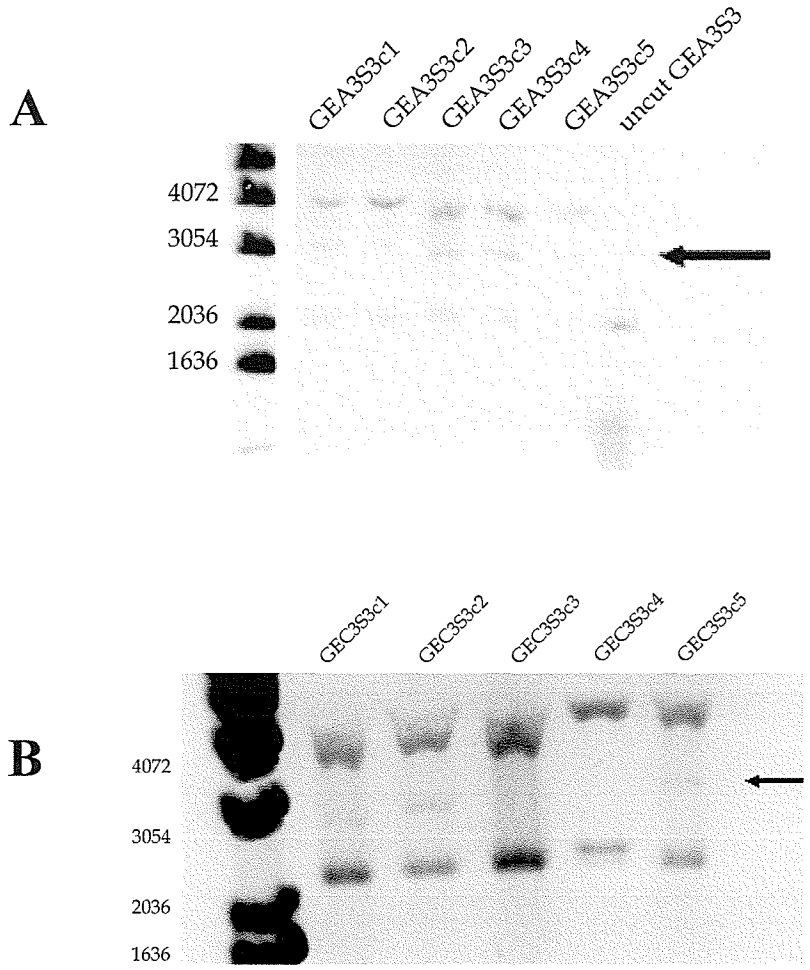

Figure 19. Entry clones resolved in 1% agarose gel. Entry clone plasmids containing: (A) ARV138 S3 insert and (B) *tsC37* S3 insert. In both (A) and (B): top most bands represent nicked, circular plasmid (refer to Mickel *et al.* 1977 for details); middle bands indicated by the black arrow represent linearized plasmid; bottom most bands represent supercoiled plasmid. The generation, isolation, and restriction of entry clone plasmids were carried out as described in Materials and Methods (sections 2.12.1 and 2.12.2). Entry clones are named as follow (acronyms are underlined): gateway entry ARV138/*tsC37* S3 clone #.

Following manufacturer's instructions, Sf9 cells were transfected using Cellfectin® or Lipofectamine™2000. The transfected cells were incubated until CPE was visible. However, it was extremely difficult to observe CPE development, so the incubation was allowed to run for approximately 9 days. After amplification to a P2 stage, what hoped to be infected cells were harvested and resuspended in electrophoresis buffer for detection of recombinant protein production via Western blot with anti-His, anti-Reo, and anti-V5 antibodies. The recombinant protein should have 6xHis and V5 tags on the C-terminus that the respective antibodies would bind. The protein-bound antibodies were then detected by horseradish peroxidase (HRP) chemical reaction. The methods described above can be referred to in the appendix.

Two sets of Western blot analysis were carried out: whole cell and cytoplasmic and nuclear lysates. Initial detection with anti-His antibodies on whole cell samples showed a distinct band at approximately 60 kDa for ARV138 S3 and *tsC37* S3 expressing Baculoviruses as well as for the negative control (which were untransfected Sf9 cells); strangely, there was no visible band for the positive control vector which accompanied the expression kit, pENTR/CAT (Invitrogen) (data not shown). This vector should express the LacZ gene. Besides observing the same band size in the negative control lane, the molecular weight of the bands was much larger than the expected 44 kDa size (the C-terminal tag would add approximately 4 kDa to the 40 kDa protein, σB).

Detection by anti-V5 antibodies was completely negative for all lanes including both controls.

For isolated cytoplasmic and nuclear samples, detection by anti-avian reovirus polyclonal antibodies revealed poor specificity, too much cross-reactivity. Nevertheless, a band approximately 44 kDa was observed in lane "Bac-ARV138 S3 nuc", nuclear lysate, which was not observed in either the positive (pENTR/CAT LacZ expressing vector) or negative controls (Figure 20). This suggests that the band observed in lane "Bac-ARV138 S3 nuc" might be the recombinant proteins. However, similar size bands were not observed in both lanes (cytoplasmic and nuclear lysates) transfected with vectors harbouring *tsC37* S3, indicating that recombinant protein expression did not occur for *tsC37* transfection. Moreover, mouse anti-His and anti-V5 antibodies treated blots did not detect any presence of recombinant proteins, suggesting that the band observed in Figure 20 may possibly be cellular protein of similar molecular weight. Lipofectamine transfected cells showed similar results that clearly indicated no expression of recombinant proteins were produced; therefore, the data of that experiment was not shown here. In summary, Western blot analysis indicated that recombinant protein production did not occur, irrespective of whether Lipofectamine or Cellfectin transfection agents were used.

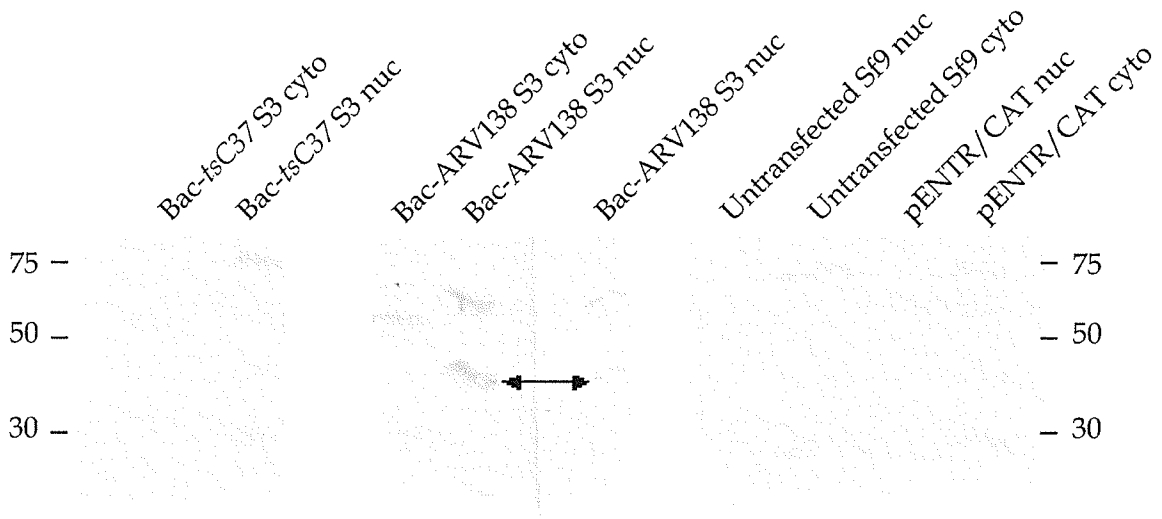

Figure 20. Anti-ARV138 polyclonal antibody treated Western blot of nuclear (nuc) and cytoplasmic (cyto) lysates of Sf9 transfected cells. The double-headed arrow indicates a band of approximately 44 kDa. The standard molecular weights are indicated. The samples were loaded onto 10% SDS-PAGE and ran for approximately 1 h. Sample and Western blot preparation were carried out as described in the Appendix (section IV).

3.7.3 Determination of Baculovirus Production

A plaque assay was carried out to see whether viral production could be observed. The plaque assay was done as indicated by the manufacturer. 6-well plates were seeded with Sf9 cells at 8 x 10^5 cells per well, infected with 100 µl of P2 Baculovirus stock, overlaid with Sf-900 II/agar mix, and incubated at 27°C in a sealed moist bag for 10 days. No plaque formation was visible even on day 10. This suggests that viral production was inhibited. Further analysis of potential problems will be discussed in the next section.

PART IV | DISCUSSION

4.1 Temperature-sensitivity of *tsC37*, *tsC287*, and *tsF206* mutants

Replication potentials of *tsC37* and *tsC287* at five different temperatures (33.5°C, 37°C, 39°C, 39.5°C, and 40°C) were analyzed to determine the mutants' degree of temperature-sensitivity. From this, *tsC37* was considered temperature-sensitive at a non-permissive temperature of 40°C, where an EOP value of 0.0096 was obtained (a measure of *ts*), a value well below the lower limit of the wild-type strains (Figure 8). This re-confirmed a previous report which identifed *tsC37* as a *ts* mutant (Patrick 2001; Patrick *et al.* 2001). *tsC287* was found to be more temperature-sensitive than *tsC37* beginning at 39°C, with a steep decline to an EOP value of 0.00085 at 40°C, an almost ten-fold drop compared to *tsC37* at the same temperature. The difference in temperature-sensitivity between these two mutants (*tsC37* and *tsC287*) may be due to the type or position of the amino acid substituted within the respective mutant. A possible explanation is discussed in the next section. *tsF206* also is a temperature-sensitive clone at temperatures > 37°C, where the greatest sensitivity is at 40°C with an EOP value of 0.000025, more than a thousand-fold decrease relative to the wild-types. This re-confirmed the previous reports that identified *tsC37* and *tsF206* as *ts* mutants (Patrick 2001; Patrick *et al.* 2001)

4.2 Assignment of *ts* Lesion in Recombination group C mutants

The prototype of recombination group C (*tsC37*) was crossed with ARV176 at three different MOI ratios to generate progeny clones that were screened for reassortants. The EOP values were determined that gave rise to two categorical groups, *ts* and non-*ts* clones (Table 5). The parental origin of each gene segment was ascertained by direct comparisons of individual genes within the electropherotypes of the clones, ARV176 and *tsC37*. *ts* clones shared the S3 gene segment that originated from the temperature-sensitive parent (*tsC37*), while all non-ts clones shared the same gene segment from the corresponding wild-type strain ARV176. The other genes were randomly assorted with regard to temperature- sensitivity. The map indicates that the S3 gene, which encodes the major outer capsid protein σB, harboured the lesion. This gene was sequenced to reveal a nucleotide change from cytosine-to-adenine at nucleotide position 871. This nucleotide alteration led to a proline-to-threonine substitution at amino acid position 281 (Figure 15). Recombination studies carried out by Patrick (2001) suggested that all recombination group C mutants have their mutations on the same gene. Therefore, sequencing of the S3 gene of *tsC287* (the other mutant in this group) was also carried out. Indeed, a single nucleotide change was uncovered on the S3 gene of *tsC287* at position 872, adjacent to that found in *tsC37*. The cytosine-to-thymidine mutation gave rise to a proline-to-leucine substitution at the same amino acid position, 281 (Figure 15).

Considering the recombination analysis carried out by Megan Patrick (refer to Patrick 2001), there is a good degree of certainty that the mutation giving rise to the temperature-sensitive phenotype observed in both mutants of recombination group C is located on the S3 gene, which is confirmed by the mapping of *tsC37* and the sequencing of the gene in both mutants. In mammalian reovirus *ts* group G, the mutation of prototypic member *tsG453* was assigned to the S4 gene, known to encode the homologous σ3 viral protein (Mustoe *et al.* 1978), where it has been established to contain at least 3 missenses; Asn_{16} → Lys, Met_{141} → Ile; and Glu_{229} → Asp (Danis *et al.* 1992; Shing and Coombs 1996). This group of MRV mutants makes up the second-largest group of MRV *ts* mutants, where at present only *tsG453* (derived from reovirus serotype 3 Dearing (T3D)) has been examined in detail (Fields *et a*l. 1971; Cross and Fields 1972; Mustoe *et al.* 1978; Danis *et al.* 1992; Shing and Coombs 1996; reviewed in Coombs 1998). Both prototype mutants in ARV group C (Patrick 2001; Patrick *et al.* 2001) and MRV group G are able to produce genomic dsRNA designated being RNA^+ (Fields and Joklik 1969; Cross and Fields 1972).

It is of interest to note that, although the mutation in both *tsC37* and *tsC287* occurred at the same amino acid position, the difference in type of amino acid substituted there led to a significant difference in temperature-sensitivity observed in these two mutants (Figure 8). σB in wild-type ARVs contains a proline at position 281, as mentioned above, which is a non-polar, hydrophobic amino acid. Proline has a distinctive cyclic structure with the secondary amino

(imino) group held in a rigid conformation that reduces the structural flexibility of polypeptide region within the protein. Given this characteristic, prolines are known as helix-breaking residues, because they are unlikely to be found in alpha-helical regions of proteins. In σB, Pro_{281} is located within a junction connecting a region of helices in the small lobe to the β-sheets in the large lobe. In *tsC37*, Pro_{281} is substituted with threonine; from a non-polar, hydrophobic residue to a polar, hydrophilic residue, its almost complete opposite in terms of generic biochemical characteristics. On the other hand, *tsC287* has leucine substituted for Pro_{281}, which happens to also be a non-polar, hydrophobic amino acid that belongs in the same family of amino acids as proline. One might expect *tsC287* to be less temperature-sensitive than *tsC37*, since leucine falls within the same generic group as proline. However, the opposite is true; *tsC287* is more temperature-sensitive than *tsC37*, suggesting that perhaps the presence of a hydrophilic residue at position 281 would provide greater stability to the protein's overall structure.

Sequence alignment of homologous major outer capsid proteins in orthoreoviruses and orbivirus indicated that proline at position 281 (ARV), 284 (MRV and Ndelle virus), 275 (Nelson Bay virus), 304 (baboon reovirus), and 348 (bluetongue virus) are highly conserved, suggesting underlying structural importance (Figure 15). Furthermore, sequence alignment revealed that ARV σB shares only 15% identity (61% of conserved residues within the small lobe) with MRV σ3. The low values of homology between the outer capsid proteins of these

two species comes as no surprise, since the location of these major outer capsid proteins and their relative substructures (small and large lobes) are located on the external surface of the virion, thus involved in significant roles in virus infection specificity.

Since crystal structures of ARV proteins are currently unavailable, speculations on probable molecular effects due to the mutations determined in ARV recombination group C mutants are inferred from analysis of homologous MRV μ1/σ3 heterohexameric (Figure 21, A) and σ3-σ3 dimeric crystal structures.

As previously mentioned, MRV σ3 can be subdivided into two sections: the small lobe (with residues 1-90 and 287-336, and a CCHC zinc-binding motif) and the large lobe (residues 91-286 and 337-365). The large lobe contains several extended loops, which may provide the sites for the proteolytic cleavages that start the disassembly process during reovirus entry (Olland 2001). The large lobe faces the virion surface; the small lobe mediates most contacts to μ1.

4.3 Particle Distributions in *tsC37* infection via EM quantification

The missense mutation is located in the large lobe of σB, but also rather centrally in the overall structure of the protein (Figure 21, C). The mutation is believed to cause a change or disruption in the structural composition of the protein that inhibits the proper function of σB, hypothesized to affect the later assembly process of viral replication. Preliminary EM results, looking at the

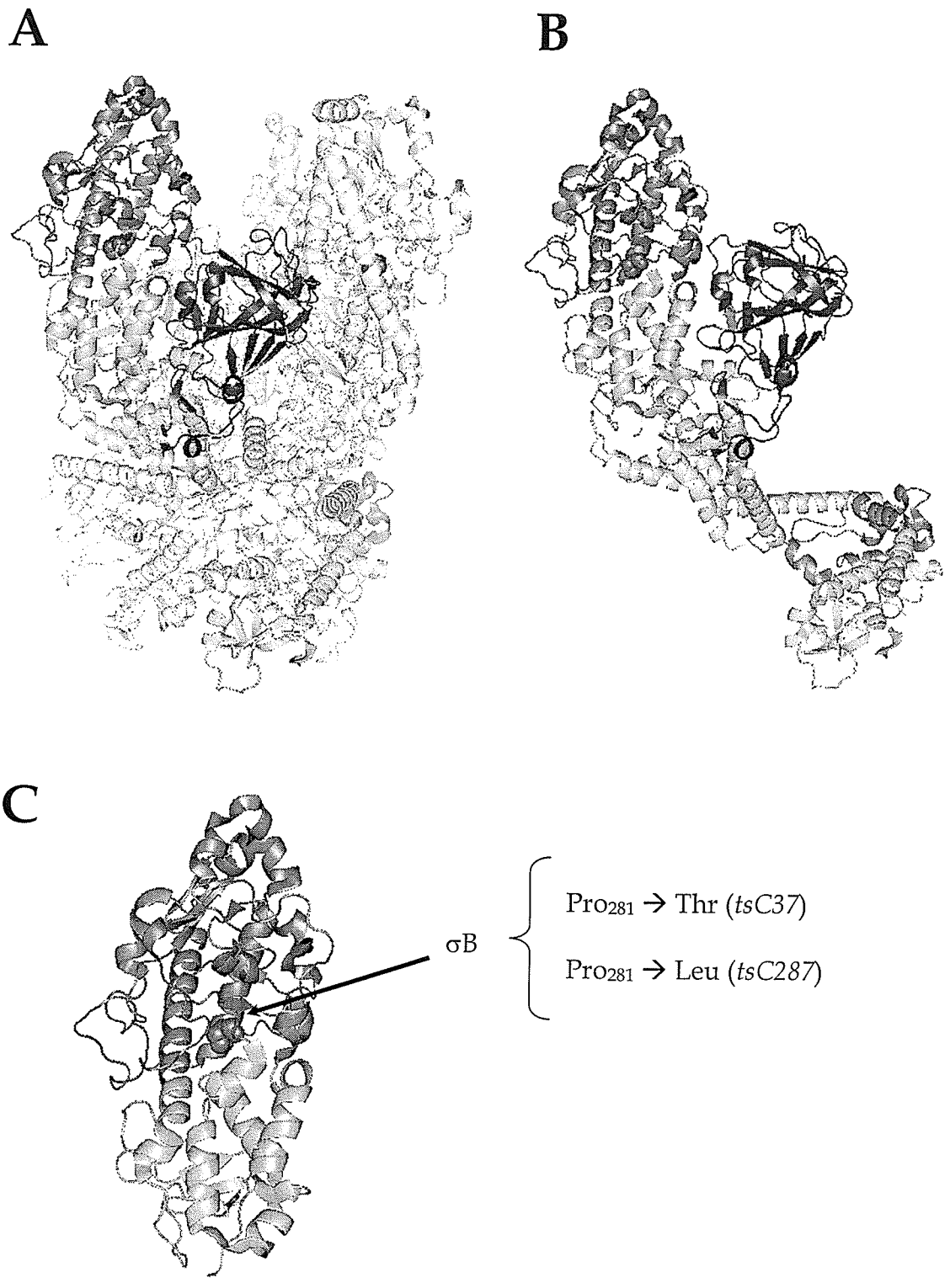
A
B
C
σB
Pro281 → Thr (tsC37)
Pro281 → Leu (tsC287)

Figure 21. Locations of *tsC37* σB mutations in MRV μ1-σ3 heterohexameric crystal structure (PDB # 1JMU). The mutation is indicated as a red sphere in all three panels. (A) Side view of a $\mu1_3\sigma3_3$ complex in cartoon format. The μ1 trimers are shown in white with one subunit coloured by domain (domain I, yellow; domain II, purple; domain III, light blue; domain IV, ruby). The σ3 subunits are shown in wheat with one subunit coloured as: large lobe, blue; small lobe, green. *tsC37* Pro_{281} → Thr and *tsC287* Pro_{281} → Leu amino acid mutation shown in red spheres. (B) A single μ1-σ3 subunit as seen in A. (C) "Exploded" view of one σ3 subunit as seen in B with indicated mutation. Images created with PyMOL (DeLano 2004).

proportions of particle-type produced and general structural composition of the particles at non-permissive temperatures by *tsC37*, supports this hypothesis (Figure 16). QM5 monolayers were infected with *tsC37* and ARV138 at MOI of 5 PFU/cell and incubated at permissive and nonpermissive temperatures, fixed in 2% paraformaldehyde, airfuged directly onto formvar-coated, carbon-stabilized 400-mesh copper grids; and stained with phosphotungstic acid and visualized under EM.

tsC37 was found to produce mainly core-like structures at non-permissive temperature (Figure 22, B), suggesting the inability of σB to interact with μB to form the μB-σB heterohexameric complex essential for assembly of outer capsids around nascent cores. Moreover, these preliminary EM data implicate the necessity for σB association to the correct conformation of μB (something also observed in MRV studies), thereby allowing the formation of the outer capsid onto nascent cores. Furthermore, it can be extrapolated that the association of μB and σB to cores are in the form of a heterohexameric complex and not as independent proteins, which supports a recent report made by studies from Benavente's laboratory (Tourís-Otero *et al.* 2004a) and that observed in MRV where the co-expression of σ3 is required for μ1 folding and trimerization (Chandran *et al.* 1999). Additionally, the majority of particles produced at the restrictive temperatures by *tsC37* were observed to lack genomic content. Studies with MRV have associated σ3 to having a possible role in viral genome

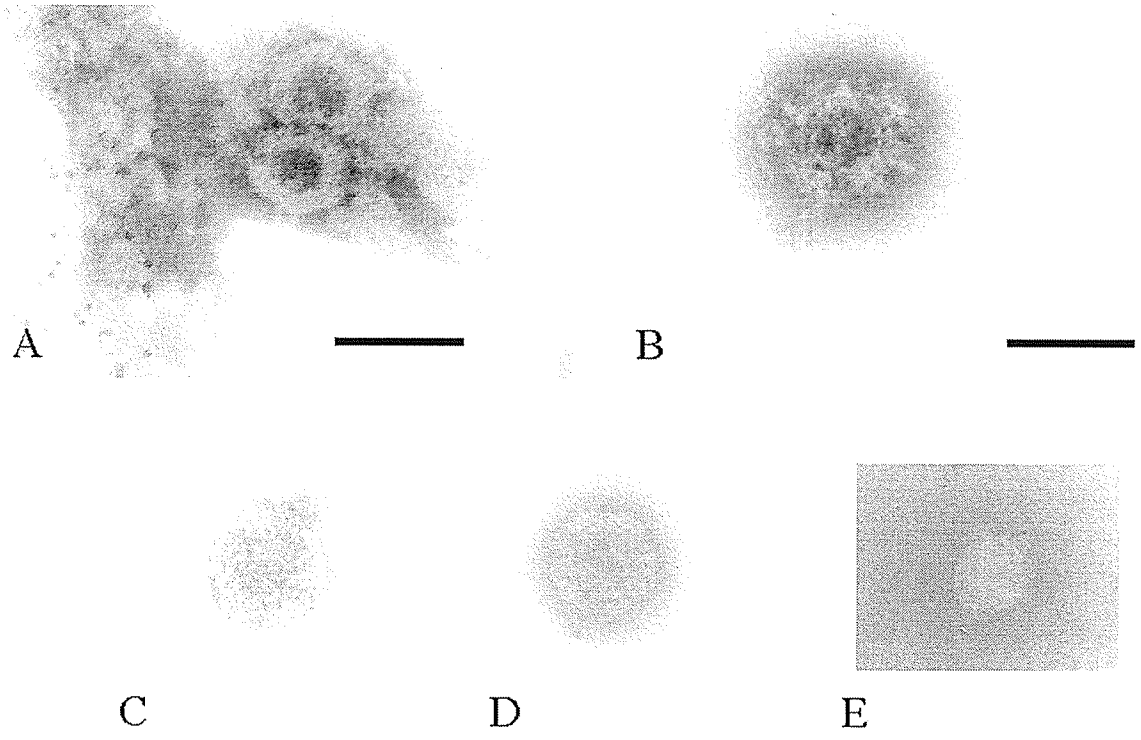

Figure 22. Electron micrograph of major particles produced during *tsC37* and ARV138 infections. (A) *tsC37* top component, defective particle with double protein shell that lacks genomic RNA, produced at permissive temperature (33.5°C), (B) *tsC37* core-like particle produced at restrictive temperature (40°C)., (C) ARV138 Outer shell, (D) ARV138 whole virion, (E) ARV138 core. Black bar represents 100 nm. Samples were fixed with paraformaldehyde, airfuged directly onto formvar-coated, carbon-stabilized 400-mesh copper grids, stained with phosphotungstic acid, viewed with TEM at a scanning magnification of 30,000X and images recorded at a magnification of 200,000X.

assortment (Antczak and Joklik 1992). Thus, the preliminary EM results suggest ARV σB may play a significant role in genome packaging.

Not surprisingly, infectivity, expressed as particle/PFU ratio, declines from permissive (68:1) to nonpermissive (627:1) for *tsC37* (Table 6). This indicates that infectious virion production at the restrictive temperature is greatly hindered in *tsC37* by the mutation on σB, and also affects the degree of infectivity of the virus population as a whole.

Likewise, MRV *tsG453* also produced mainly core-like particles at non-permissive temperature (Fields *et al.* 1971; Morgan and Zweerink 1974; Danis *et al.* 1992) because of the inability for the mutant σ3 protein to interact with μ1 to form the heterohexameric complex (Shing and Coombs 1996). The mutation at amino acid position 16 in MRV *tsG453* alone was found to be sufficient to prevent σ3-μ1 interaction (Bergeron *et al.* 1998), thus it was not surprising to uncover that the lone mutation in ARV *tsC37* could disrupt the σB-μB heterohexamer. Moreover, it was reported that MRV *tsG453* had approximately a 20% reduction in protein synthesis (Fields *et al.* 1972; Danis *et al.* 1992; Shing and Coombs 1996) and RNA (Cross and Fields 1972) at the nonpermissive temperature. Similarly, preliminary data on protein production in ARV ts mutants in recombination group C (*tsC37* and *tsC287*) suggested a reduction in protein production relative to ARV138 wild-type (Patrick and Coombs unpublished data, Figure 23).

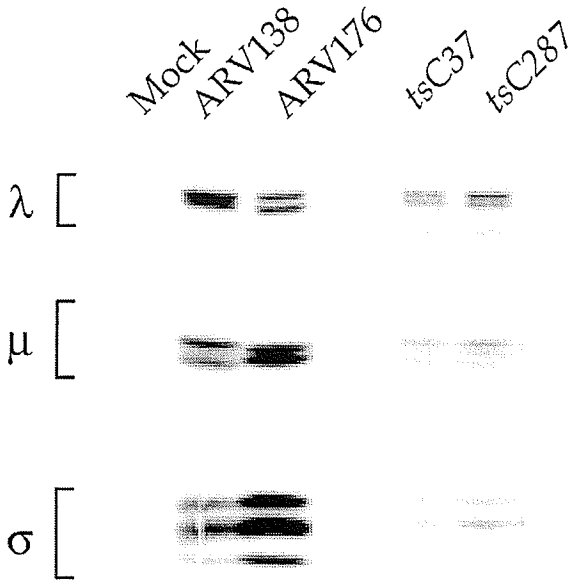

Figure 23. Total protein production of ARV138, ARV176, *tsC37*, and *tsC287* at nonpermissive temperature (39.5°C) (Megan Patrick and Kevin Coombs unpublished data). Positions and identities of genomic and protein classes (λ, μ, σ) are labelled.

Each σ3 contacts two μ1 subunits within each trimer (Liemann *et al.* 2002). Assuming that ARV σB and MRV σ3 proteins are folded similarly, amino acids at the following positions on 2 μB proteins are located in the closest proximity to ARV Pro_{281}/Thr_{340} in one adjacent μB and Ser_{475}/Ala_{476} in the other adjacent μB (Figure 24). All three amino acids are positioned in Domain IV of μB. Thr_{340} is located on a loop at the tip of the long β-hairpins, which are believed to interact with the large and small lobes of two different σB proteins. Hence, a mutation at Pro_{281} could disrupt possible interactions with 2 μB proteins, thereby preventing proper association of σB with μB to form the important heterohexameric complex (Figure 25).

Additionally, aside from its associating role with μ1, σ3 has a regulatory function during infection that involves its ability to bind dsRNA (Huismans and Joklik 1976; Schiff *et al.* 1988; Liemann *et al.* 2002), thereby preventing activation of the interferon-induced inhibitory protein kinase (PKR) (Liemann *et al.* 2002). PKR is considered as one of the main antiviral mechanisms induced by interferon and is believed to be the main intracellular factor interfering with reovirus multiplication (Wiebe and Joklik 1975; Miyamoto and Samuel 1980; Gupta *et al.* 1982; DeBenedetti *et al.* 1985). The dimer appears to be the prevalent form in solution, and is proposed to be the significant species that binds dsRNA (Olland *et al.* 2001; Liemann *et al.* 2002). There is significant overlap of the σ3 residues that contact μ1 in the complex with those that stabilize the σ3 dimer (Olland *et al.* 2001; Liemann *et al.* 2002). Therefore, the disruption of the heterhexamer

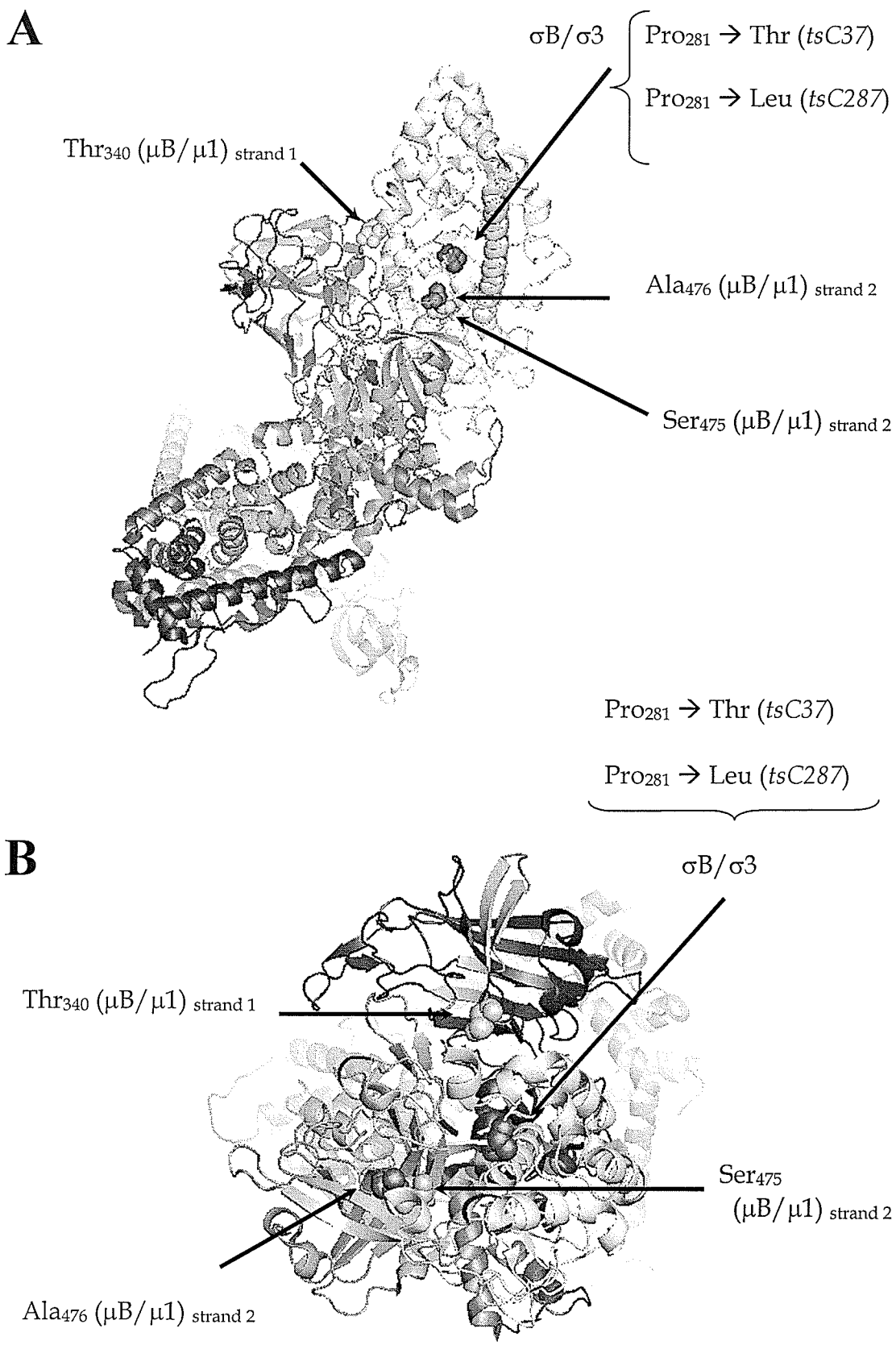
A
σB/σ3
Pro281 → Thr (tsC37)
Pro281 → Leu (tsC287)
Thr340 (μB/μ1) strand 1
Ala476 (μB/μ1) strand 2
Ser475 (μB/μ1) strand 2
Pro281 → Thr (tsC37)
Pro281 → Leu (tsC287)
B
σB/σ3
Thr340 (μB/μ1) strand 1
Ser475
(μB/μ1) strand 2
Ala476 (μB/μ1) strand 2

Figure 24. Location of residues in two ARV μB that are hypothesized to interact with proline at position 281 in one σB subunits in MRV μ1-σ3 heterohexameric crystal structure (PDB # 1JMU). (A) Hypothesized interacting residues are shown in spheres with position and location indicated. Pink helices and blue sheet in Domain III and green sheet in Domain IV represent regions in μ1 subunit believed to be responsible for interaction with σ3 in MRV μ1-σ3 heterohexameric (Liemann 2002). (B) Top view of same structure shown in (A), with much of large lobe removed to allow better view of the indicated residues. Thr_{340} in $\mu B_{Strand\ 1}$ and Ala_{476} and Ser_{475} in Strand 2 are situated closest to the mutation at position 281 in σB. Images created with PyMOL (DeLano 2004).

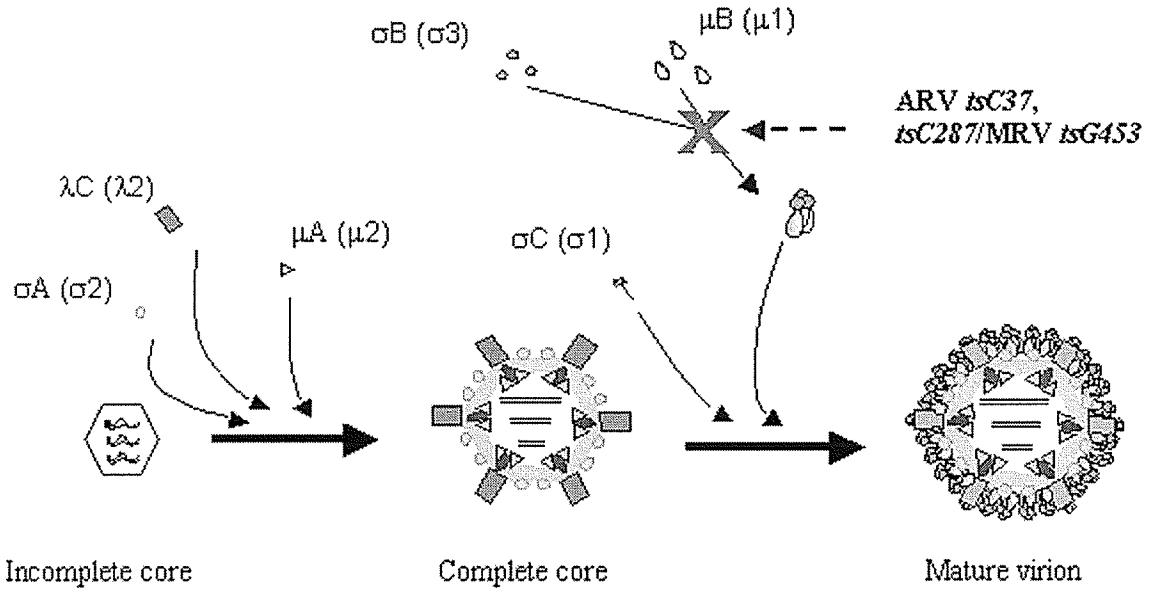

Figure 25. Proposed avian reovirus assembly step blocked by ARV *tsC37*, *tsC287*, and MRV *tsG453* mutation. X represents the step of blockage. MRV equivalent proteins are indicated in parentheses. At restrictive temperature, ARV *tsC37*, *tsC287*, and MRV *tsG453* are unable to form the μB-σB/μ1-σ3 heterohexameric complex, thereby preventing formation of outer capsid protein shell on nascent core.

complex due to the mutation in *tsC37* σB may in turn affect its ability to form dimers as well. Normally, the formation of a $\mu1_3\sigma3_3$ complex competes with σ3 dimerization (Tillotson and Shatkin 1992; Liemann *et al.* 2002), and σ3 dimers may be disrupted at a sufficient μ1 concentration in favor of the heterohexamer (Olland *et al.* 2001; Liemann *et al.* 2002). This competition may be part of the mechanism whereby μ1 counteracts the effects of σ3 on PKR activation and translation (Tillotson and Shatkin 1992; Liemann *et al.* 2002). Studies found the MRV *tsG453* mutant to be resistant to the effect of interferon at restrictive temperature, providing further evidence for the importance of σ3 (ARV σB) in PKR regulation.

It is possible to conjecture that the conformational change due to the mutation at ARV amino acid position 281 in σB may affect the ability of this protein (positively or negatively) to either dimerize or bind dsRNA as observed in MRV *tsG453*. Studies found the MRV *tsG453* mutant to be resistant to the effect of interferon at restrictive temperature, providing further evidence for the importance of σ3 (ARV σB) in PKR regulation. Paradoxically, *tsG453* mutant MRV σ3 protein exhibited an increased dsRNA binding and an altered subcellular distribution (Bergeron *et al.* 1998). The synthesis of viral proteins in MRV *tsG453*-infected cells was found to be resistant to interferon when compared to the sensitivity in cells infected with the wild-type virus. This further supports the idea that the dsRNA binding activity of σ3 can act as a major determinant in reovirus resistance to interferon. The difference in

interferon sensitivity between wild-type and MRV *tsG453* virus was also found to be mostly abolished when infections were carried out with infectious subviral particles (Bergeron *et al.* 1998). The fact that ISVPs have a reduced interferon resistance suggests that viral proteins from infecting virions can play a key role in translational regulation at early stages of viral infection (Bergeron *et al.* 1998). Since infection by ISVPs, lacking σ3, is believed to be the main route of natural reovirus infection at mucosal surfaces (Amerongen *et al.* 1994), studies have raised the possibility that interferon can play a greater role in the control of reovirus infection in this context.

Various works have demonstrated the correlation between dsRNA binding and the ability of σ3 to stimulate translation via PKR inhibition. It appears that a conformational change exerted by amino acid substitutions within the zinc finger or surrounding this motif of the protein is responsible for the stimulatory effect on dsRNA binding activity (Bergeron *et al.* 1998). Whether the mutation found in ARV *tsC37* or *tsC287* σB protein has a similar affect on dsRNA binding or dimerization remains to be determined. However, assuming that ARV and MRV σ proteins are folded similarly, ARV Pro_{281} (MRV Pro_{284}) is situated relatively near residue ARV His_{276} (MRV Asn_{279}), one of many residues deemed important in σB dimerization (Figure 26). Hence, slight conformational change may inhibit proper association of this residue with the other σB protein, thereby weakening dimer formation—leading to disruption of dsRNA binding ability of this protein. However, there is a question whether disruption of only a

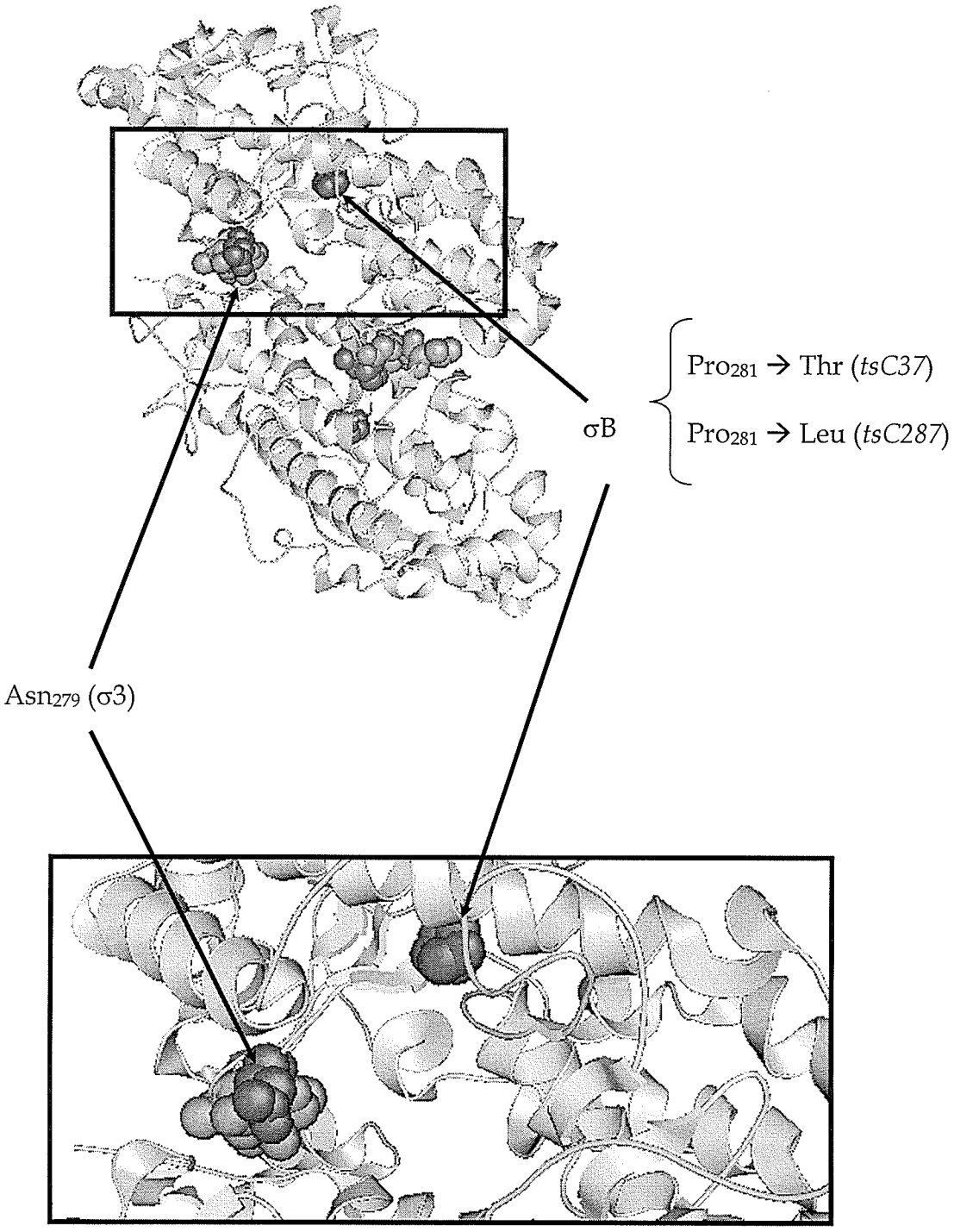
σB
Pro281 → Thr (tsC37)
Pro281 → Leu (tsC287)
Asn279 (σ3)

Figure 26. Position of *tsC37* and *tsC287* mutation in ARV σB dimer as seen in MRV σ3-σ3 dimer crystal structure (PDB # 1FN9). UPPER panel: spheres represent recombination group C mutation in σB and one amino acid region (276-279) believed involved in stabilizing the dimer structure (Olland 2001). Pink sphere represents Asn_{279}, which is situated closest to the mutation represented in red sphere. LOWER panel shows enlarged view of boxed residues shown in upper panel. Images created with PyMOL (DeLano 2004).

small patch of residues responsible for dimerization will lead to actual inhibition of dimer formation/dsRNA-binding or, in the case of MRV *tsG453*, enhance dsRNA binding. Hence, further investigation into this property of σB is necessary to fully understand the significance of the mutational effects on the multifunctionality of σB in avian reovirus replication and pathogenesis.

4.4 Assignment of *ts* Lesion in *tsF206* mutants

tsF206 cross-infection with ARV176, selection and amplification of progeny clones to the P_2 stage, and electropherotype profile resolution were carried out by Trina Racine (a former undergraduate Honours student). The cross-infection was done at MOI ratios of 2:8, 8:2, and 5:5 PFU per cell of *tsF206* to ARV176. After inclusion of *tsF206* into this study, EOP determination was carried out for each clone, ARV176, and *tsF206*, from which the reassortants were divided into two groups, *ts* or non-*ts*. The parental origin of the reassortant electropherotype profiles were re-confirmed or changed accordingly. Five additional clones were screened from which the electropherotypes and EOP values were determined to facilitate the mapping of *tsF206*.

tsF206 was mapped to the S4 gene, which encodes for the nonstructural protein σNS. Similarly, MRV *tsE320* was mapped to the S3 gene, which in MRV encodes for σNS (Ramig *et al.* 1978; Becker *et al.* 2001), from which information could be extrapolated for *tsF206*. MRV S3 of *tsE320* was sequenced to discover

an amino acid substitution Met_{260} → Thr (Wiener and Joklik 1987), which led to reduce production of ssRNA and protein (Cross and Fields 1972), low levels of dsRNA synthesis (Cross and Fields 1972), and few viral inclusions were formed (Cross and Fields 1972; Becker *et al.* 2001) at the restrictive temperature. Recall that MRV σNS (like ARV σNS) associates with μNS during viral inclusion formation. It is yet uncertain whether the defect observed in ARV *tsF206* will lead to a similar disruption of protein function as seen in MRV *tsE320*; however, something quite similar is expected to be observed since σNS in both MRV and ARV play very similar, if not the same, functions in reovirus pathogenesis.

4.5 Assignment of *ts* Lesion in *tsG247* mutants

A cross-infection of *tsG247* x ARV176, selection and amplification of progeny clones to the P_2 stage, and electropherotype profile resolution were carried out by Alex Selaghi (a former undergraduate Honours student). After inclusion of *tsG247* into this study, EOP determination was carried out for each clone, ARV176, and *tsG247*, which permitted the division of the reassortants to *ts* or non-*ts* categories. The electropherotype and EOP of an additional clone was obtained to facilitate the completion of *tsG247* map. The parental origin of the reassortant electropherotype profiles were re-confirmed or changed accordingly.

tsG247 temperature-sensitive lesion was mapped to the L3 gene, which encodes for the core spike protein λC. Presently, only the S-genes of ARV138

have been fully sequenced; therefore, the specific nucleotide and amino acid change for *tsG247* could not be determined via sequencing at the present time. However, extrapolations can be made from studies carried out on MRV *tsB352*, which was mapped to the λ2 homolog (Mustoe *et al.* 1978). Similar to ARV *tsC37* and MRV tsG453, MRV *tsB352* produces mainly core-like particles, which suggests that the defect in MRV λ2 prevents association of the outer capsid proteins onto nascent cores. It remains to be seen whether the defect in ARV *tsG247* exhibits a similar disruption in the viral protein's functional role in avian reovirus pathogenesis.

4.6 S1 Gene Phenomena

The absence of S1 gene segment has been observed in several non-reassortant clones isolated from the cross-infection of *tsC37* x ARV176 (data not shown) and in the mutant *tsG247* (Figure 18). It is uncertain, in the case of *tsC37* and *tsG247*, whether this particular segment is completely absent or truncated (also known as subgenomic segment), similar to what had been previously reported by Ni (1994) and Xu (2004). It is equally uncertain why this occurs. Absence of the S1 gene does not appear to affect the virus' ability to infect and replicate (Xu 2004). However, it had been suggested that the presence of the subgenomic segments is MOI-dependent. Infectivity assays, conducted with serially diluted progeny from a cross-infection of strain 883 x 81-5, revealed the

infectious titers increased in parallel to the increase of the dilution factor (Ni 1994), which further supported the proposal that these subgenomic segments are defective interfering RNAs directly responsible for competing or interfering with the S1 genome segment during replication and/or packaging (Ni 1994).

However, Xu's studies reported that cross-infection with *tsB31* and ARV176 generated a subset of progenies that were S1 deletion mutant (Xu 2004) -these S1 deletion mutants were found to be either nonreassortant or reassortant—while the parental strains were observed to contain the full 10 genomic segments. In contrast, *tsC37* itself appeared to contain a subpopulation that either lacked the S1 gene or contains a truncated version of the S1 gene, as evident by the faintness of the S1 band in the mutant's electropherotype (Figure 9). Moreover, of the 258 clones screened, 30 were found to lack the S1 gene (either truncation or complete absence) (frequency = 11.6%): 15 S1 mutants were generated with cross-infections at MOI ratio 5:15 (frequency = 11.5%), 10 were generated at the MOI ratio 15:5 (frequency = 20%), and 5 were generated at MOI ratio 5:5 (frequency = 11.1%)—where ratios are *tsC37* to ARV176. An initial consideration may be the association between the MOI ratios and frequencies at which these S1 mutants are generated. However, a quick χ^2 calculation indicated that there is no statistical association between these two factors ($p > 0.1$). This would suggest that the generation of these S1 mutants in the co-infection is independent of the mutant-to-wild-type MOI ratio. Furthermore, these S1 mutants were all non-reassortants, with an electropherotype representative of its

tsC37 parent, unlike the observations reported for the *tsB31* S1 deletion mutants. The S1 deletion mutants observed in *tsB31* x ARV176 infections appeared to be generated or amplified during infection—since the original parentals contained all 10 dsRNA genomic segments. Previous studies proposed that these subgenomic segments are replicated and not generated *de novo* (Ni 1994). It remains to be determined whether these S1 mutants from *tsC37* cross-infections are deletion mutants similar to those isolated from the *tsB31* studies, where it was reported that sequences encoding the p17 protein was completely deleted and partial deletions in the ORFs encoding p10 and σC (Xu 2004).

4.7 Recombinant Protein Expression in Baculovirus

There have been recurring problems with the development of an expression system for viral recombinant proteins with regards to this study. The initial development of an entry clone using Invitrogen's Gateway technology was obtainable; however, once the entry clone was recombined with BaculoDirect™ Linear destination vector and transfected into Sf9 cells, no indication of expression and recombinant protein production was seen via Western blot analysis. The recombinant protein is expected to have a molecular weight of approximately 44 kDa (40 kDa protein + 4 kDa tag). The recombinant protein was designed to contain a 6xHis/V5 fusion tag. The V5 tag is a 14 amino acid

epitope derived from the P and V proteins of the paramyxovirus, SV5 (Southern *et al.* 1991).

As expected, there were high levels of cross-reactivity when polyclonal rabbit anti-ARV138 antibodies were used for detection of recombinant protein in cytoplasmic and nuclear lysates. Nevertheless, a band approximately 44 kDa was observed in lane "Bac-ARV138 S3 nuc", nuclear lysate, which was not observed in either the positive or negative controls (Figure 20). This suggests that these two bands observed in lanes "Bac-ARV138 S3 nuc" might be the recombinant proteins. However, similar size bands were not observed in both lanes (cytoplasmic and nuclear lysates) transfected with vectors harbouring *tsC37* S3, indicating that recombinant protein expression did not occur for *tsC37* transfection. Moreover, mouse anti-His and anti-V5 antibodies treated blots did not detect any presence of recombinant proteins, suggesting that the band observed in figure 20 may possibly be cellular protein of similar molecular weight that is cross-reactive.

Nevertheless, it would not be unexpected to detect recombinant protein σB concentrations in the nucleus. Other studies have reported to detect expressed MRV σ3 in the nucleus of *Spodoptera frugiperda* clone 21 (Sf21) insect cells (Jané-Valbuena *et al.* 1999) and HeLa cells (Yue and Shatkin 1996). The nuclear presence of σ3 appears rather surprising considering that reovirus multiplication does not appear to involve the nucleus (Follet *et al.* 1975; Zarbl and Millward 1983), despite some studies having indicated morphological alterations

of the nucleus in infected cells (Chaly *et al.* 1980). The dsRNA-binding activity of the protein was held responsible for this subcellular distribution (Yue and Shatkin 1996). It should be mentioned that other dsRNA-binding proteins, such as the cellular PKR (RNA-dependent protein kinase) or the E3L protein of vaccinia virus (a DNA virus replicating in the cytoplasm of infected cells), were also shown to be partly localized to the nucleus (Yuwen *et al.* 1993; Jeffrey *et al.* 1995).

PART V | FUTURE STUDIES

Despite recent increase in molecular interest and work in avian orthoreoviruses (Hsiao *et al.* 2002; Gonziález-López *et al.* 2003; Shmulevitz *et al.* 2004; Tourís-Otero *et al.* 2004; Xu *et al.* 2004; Costas *et al.* 2005; Liu *et al.* 2005; Tourís-Otero *et al.* 2005; Xu *et al.* 2005; Zhang *et al.* 2005), much remains to be understood about this species. Further analysis of these novel ARV *ts* mutants would certainly facilitate progress toward understanding this virus group.

As part of the progression in the characterization of *tsG247*, the sequence for the wild-type ARV138 L3 gene should be determined, which would then allow for the sequencing of the mutant L3 gene. The determination of the specific nucleotide and amino acid substitution, and its location, could help answer questions such as how the mutation affects the protein conformation and whether the mutation is located at a site significant for association with the outer capsid proteins.

In addition to sequencing the S4 gene in *tsF206* to determine the exact mutational substitution, thin-section analysis of infected cells via electron microscopy would be a logical next step to determine whether viral inclusion body formation is affected by the mutation in σNS. Recall that ARV σNS plays a significant role in facilitating viral inclusion formations via its association with ARV μNS.

Despite sharing a mutation at the same amino acid position, *tsC37* and *tsC287* exhibit different degrees of temperature-sensitivity as mentioned above, which suggests that the different amino acids substituted at Pro_{281} result in different effects. Therefore, it would be a logical step to determine the proportions of particle-types produced by *tsC287* at restrictive temperature and compare that to the prototype *tsC37*. It would not be surprising, however, if the majority of the particles produced turned out to be core-like structures similar to *tsC37*, since the mutation does occur at the same amino acid position. Although it would be most interesting if the particle distribution for *tsC287* turned out to be different to that observed in *tsC37*, especially regarding the presence or absence of genome content. Recall that *tsC37* produced core-like structures, which lacked genome.

Further confirmation of the maps attained for these *ts* mutants would require expression of complement wild-type viral proteins that would compensate for the mutations exhibited by each *ts* mutants at non-permissive temperatures. One would expect a *ts* mutant infection of cell lines expressing wild-type viral proteins compensatory to the mutation would rescue the growth of these mutants to wild-type levels. This would confirm the accuracy of the mapping results. Quail fibrosarcoma cells (QM5) are currently used for virus infections. Therefore, expression of viral proteins in this cell line would be a necessary future step in order to conduct the aforementioned complementation assays.

Protease sensitivity of MRV σ3 has been associated with specific conformation of the large lobe (Olland 2001). In ARV recombination group C (prototypic member *tsC37*), the mutation lies within the large lobe. This raises the question of whether the conformational alteration of the protein due to the mutation would lead to a change in protease sensitivity of ARV σB or perhaps a change in protease cleavage sites. Determination of specific protease cleavage in MRV σ3 has been undertaken (Mendez *et al.* 2003; Hadzisejdić 2005). A similar approach can be carried out to determine specific sites of protease cleavage in wild-type ARV σB, which can then be extended to its mutant counterpart isolated from *tsC37*. A comparison of such analyses would allow for the understanding of how, if any, affects the conformational change in the mutant protein may have on cleavage sites and protease sensitivity.

Both avian and mammalian reoviruses assemble progeny virion in dense structures known as inclusion bodies observed in the cytoplasm of infected cells. σ3 in MRV is known to associate with the non-structural proteins μNS and σNS in these inclusion bodies (Becker *et al.* 2003). Thus, it would be of interest to carry out thin section EM analysis of *tsC37* infected cells to determine whether inclusion body formation is affected by the mutation, which would lead to suggest that σB plays a significant role in the formation of inclusion bodies along with the nonstructural proteins. On the other hand, another possible angle of attack here would be to examine whether the as yet unknown signal required for the recruitment of this major outer capsid protein to inclusion bodies rely solely

on specific amino acid sequences or does this involve conformational aspects as well, to which the mutant protein may be useful in this case.

Recall that MRV σ3 plays a significant role in inhibiting PKR function during early stages of viral replication due to its ability to bind dsRNA, whose presence activates the PKR signalling pathway—and ARV σB is speculated to play a similar role. Presently, it remains to be determined with certainty whether the increased dsRNA binding or lack of interaction with μ1 is responsible for this increased interferon resistance of MRV *tsG453* virus. However, a better affinity of σ3 for dsRNA could certainly increase its ability to inhibit PKR, especially considering that a previous report has established this affinity to be at least 50-fold lower than that of PKR (Yue and Shatkin 1997). Therefore, it would be of interest to determine whether the mutation in recombination group C mutants (*tsC37* and *tsC287*) would enhance or inhibit this protein's ability to bind dsRNA and inhibit the PKR signalling pathway—assuming its functional characteristic is similar to its MRV counterpart. A possible approach would be to co-precipitate the mutant protein with dsRNA. If the two molecular structures do co-precipitate then this would indicate that the mutation has no effect on the protein's ability to bind dsRNA.

The ability for σB to bind dsRNA relates to its ability to form dimers in solution. It is in this dimer conformation that permits the structural protein to bind to dsRNA, whereby the disruption of the dimer (either by mutation or association with μB) would lead to loss in dsRNA binding. In relation to its

ability to affect the PKR signalling pathway, it also would be interesting to prove whether *tsC37* or *tsC287* σB protein maintains its ability to form dimers despite the presence of the mutation. Since residues associated with dsRNA-binding have been speculated to be scattered along the side of the protein and overlap with regions important in μ1 (ARV μB) association (Olland 2001; Liemann *et al.* 2002), the determination whether conformational change due to the mutation in *tsC37* would affect the protein's ability to dimerize would emphasize the importance of conformation in this protein's functional abilities. The yeast two-hybrid system can be used here to observe whether the mutation in σ3 has any affect on the protein's ability to interact with each other in forming dimers.

The abovementioned studies could be achieved once an expressing cell line is developed. A Baculovirus expression system that expresses a recombinant mutant protein (using that encoded by the S3 from *tsC37* as template) would allow for the dimerization studies and dsRNA-binding assays, which would relate structure to function. Additionally, the expression of wild-type complement protein, which should be done prior to the mutation studies, would confirm or negate the speculations that ARV σB proteins do indeed bind dsRNA and form dimers, as have been seen in MRV. More importantly, co-expression of μB and σB wild-types could answer the question whether the association of these two proteins would inhibit σB's ability to bind dsRNA – something that has only been indirectly conjectured from MRV studies.

Crystallographic structural analysis of the mutant protein would provide insight into the actual conformational change due to the mutation. This may provide further observation to specific residues involved in dimerization and dsRNA binding, and how the spatial alteration inhibits interacting residues or create new ones. Additionally, a crystal structure of the avian reovirus μB-σB heterohexamer would be insightful to the understanding of how these two proteins interact in context of the avian reovirus system. So far, a lot of what is known about avian reoviruses is indirect references from MRV studies. However, as avian reovirus research progresses, significant differences are being uncovered between MRV and ARV, both in virus structure (Zhang *et al.* 2005) and in biological aspects. However, if the crystal structure of the mutant protein is to be attained, then a different expression system to the ones already mentioned must be developed. Baculovirus expression cannot be used in this case, since the *ts* phenotype is exhibited at 40°C and baculovirus host cells (Sf9) are capable of growing only around 27°C. A possible system to use would be a bacterial one such as *E. coli*, which are capable of growing at the restrictive temperature. Additionally, high expression of the recombinant proteins can often be obtained in bacterial expression systems.

Moreover, purified recombinant proteins from a Baculovirus expression system would be useful for the generation of monoclonal antibodies in animal models such as mice. Currently, only polyclonal avian reovirus antibodies are available in the laboratory, which proved to have a high degree of cross-

reactivity when used in Western blot analysis. As a result, studies which involved immunoprecipitation or others requiring Ab-binding specificity would entail the development of monoclonal Abs. Additionally, this would allow for epitope mapping of Ab-binding sites on individual viral proteins if such areas were of interest.

More importantly, recombinant outer capsid structural proteins (σB and μB) could allow for re-coating experiments to be carried out on avian reoviruses, similar to that undertaken for MRV. Another very interesting aspect that arises from such re-coating experiments is the idea of carrying out various combinations of MRV and ARV outer capsid structural proteins (MRV μ1 + ARV σB or MRV σ3 + μB) on either mammalian reovirus cores or avian reovirus cores. Several questions arise from this: (1) how well do MRV and ARV structural proteins associate with each other, if at all, (2) would there be a difference in virion morphology; (3) how does this affect the chimera virus' ability to infect L929 cells (common cell line used for MRV infection) or QM5 (cell line used in ARV infections); and (4) how does this affect the generation of ISVPs from a chimera virus? Recall that the cleavage of σB/σ3 is necessary for the early stages of viral infection. Thus, it is questionable whether the association of an ARV σB with MRV μ1 (and vice versa) would lead to a different state of conformation that may affect or alter protease sensitivity of σB, or change the site of cleavage. Additionally, the MRV and ARV outer capsid protein combinations can be

carried out with yeast two-hybrid system to analyse whether proteins from these two species of orthoreoviruses can at all interact.

Furthermore, determination of specific residues involved in dsRNA-binding, μB association, dimer formation, and proteolytic cleavage can be studied using site-directed mutagenesis.

Therefore, immediate work to develop an *in vitro* expression system for recombinant viral proteins is necessary towards further understanding the functional properties of individual ARV proteins and its role in specific steps in the viral replication cycle. Current effort to develop such an expression system, in this case a Baculovirus system, has not been very promising. As previously mentioned, Western blot analysis suggested there is failure in expression from the promoter in the destination vectors, which have been transfected into Sf9 insect cells; no recombinant protein production was detected. Additionally, attempts to detect viral production via plaque assays also turned up negative (i.e. no plaques were observable).

Thus, the logical next step would be to determine where and at what stage the problem of expression arises. Several immediate questions should be addressed: (1) did recombination occur to generate a destination vector, (2) did the recombination process disrupt some crucial area in the vector or insert necessary for expression of the protein (although the recombination reaction should be specific to *att*L and *att*R recombination sites, it would be of interest to

confirm this at this stage), (3) are there problems regarding the virus' ability to infect the Sf9 cells currently being used in this study.

To answer question (1), PCR will be carried out directly on the LR recombination reaction samples, followed by sequencing to uncover whether recombination did occur. This also will provide an explanation to question (2) on whether the recombination process may have disrupted significant areas in the vector or insert necessary for expression. With regards to (3), wild-type baculovirus stocks will be titered using Sf9 cells. This will resolve whether the lack of visual plaques is due to the virus' inability to infect or replicate in the Sf9 stocks currently employed.

Currently, only six of the seven recombination groups have been mapped (Figure 27). The complete characterization of the available panel of ARV ts mutants (which covers 7 of the 10 genomic segments) would greatly facilitate the understanding of avian reovirus assembly and replication mechanisms. Moreover, *ts* mutants can be used to shed light into functional-structural relations of the respective proteins. Studies on MRV certainly provide insight into possible comparable mechanisms in ARV and are a good starting point for investigation. However, as ongoing work begins to unravel the mysteries of ARV pathogenesis, it will be more than likely that possible novel mechanisms shall be unraveled that has not been seen in MRV—the ability to promote syncytia is only the beginning to decipher the differences between two species that are so similar yet vastly different.

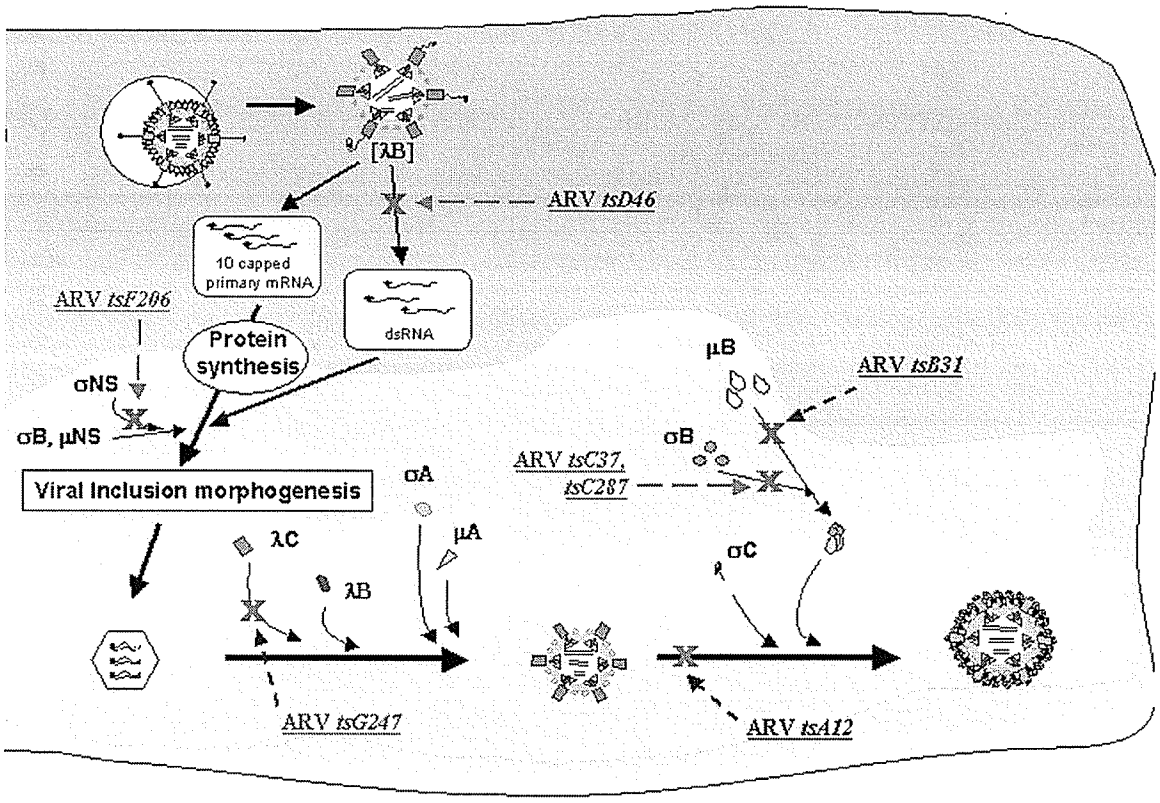

Figure 27. Proposed steps in avian reovirus assembly blocked by mutations in ARV *tsA12, tsB31, tsC37, tsC287, tsD46* (Patrick *et al.* 2001; Xu *et al.* 2004; Xu *et al.* 2005), *tsF206,* and *tsG247* mutants. X represents the step of blockage. The salmon coloured background represents cellular cytoplasmic space. The lower pink background represents viral inclusion where assembly is believed to occur. The ARV replication mechanism has been simplified to clearly highlight the specific steps affected by the mutations.

Past and present work with *ts* mutants stress the importance of these agents for the study of viral proteins in *Reoviridae*. In the absence of an adequate reverse-genetics system, the *ts* mutants currently represent the best tool to delineate mechanistic stages of the viral replication and assembly cycle.

APPENDIX

I. Construction of Gateway® Destination vectors

I-i. Performing LR Recombination Reaction

LR reaction was carried out according to manufacturer's instructions. 50 ng of isolated donor vector was added to 150 ng of BaculoDirect™ Linear DNA (Invitrogen) (150 ng/reaction), TE Buffer (pH 8.0) (1 mM EDTA and 10 mM Tris-HCl), and LR Clonase™ enzyme mix (Invitrogen). The reaction was incubated at 25°C overnight. Proteinase K was added to each reaction and incubated at 37°C for 10 minutes. This generated the destination vectors.

I-ii. Transfection of Destination Vectors into Sf9 Cells

Initially, transfection was carried out according to the manufacturer's instructions, but some modifications were later made when initial transfections did not give results. In a 6-well plate, 8 x 10^5 cells of Sf9 were seeded per well and allowed to adhere for 1 h at 27°C. Two transfection mixtures were prepared: Mixture A contained 5 µl of LR recombination reaction product and 100 µl of unsupplemented Grace's Insect Medium (Invitrogen), Mixture B contained 6 µl of Cellfectin® Reagent (Invitrogen) and 100 µl of unsupplemented Grace's Insect Medium. Mixture A and B were combined and incubated at room temperature for 45 minutes. Next, 800 µl of unsupplemented Grace's Insect Medium was

added to the transfection mix. Maintenance medium from the cells was removed, and the cells were washed with fresh unsupplemented Grace's Insect Medium. This washed medium was removed. The entire transfection mix was added and the cells were incubated at 27°C for 5 h (during second attempt, modified to 24 h); after which the transfection mixture was removed and 2 ml of SF-900 II SFM (Invitrogen) was added with 100 μg/ml ganciclovir. The plates were placed in a sealed plastic bag with moist paper towels and incubated for more than 96 h at 27°C, until CPE was observed.

Lipofectamine™ 2000 (Invitrogen) was also tested in-place of cellfectin. The transfection procedure was followed as instructed by the manufacturer. 2 μg of LR recombination reaction and Lipofectamine™ 2000 was diluted in 50 μl each of unsupplemented Grace's Insect Medium, incubated for 5 minutes at room temperature, combined together, incubated mixture at room temperature for 20 minutes, added mixture to cells containing 2 ml of Sf-900 II SFM medium, and incubated in a sealed plastic bag with moist paper towels at 27°C for more than 96 h, until CPE was observed.

II. Baculovirus Stock and Amplification

Sf9 cells were seeded at 8.5 x 10^5 cells per well in 6-well plates and incubated at 27°C for 1 h to allow cell attachment. Maintenance media was removed, viral P1 stock was added at MOI 5, and adsorbed for 1 h at 27°C with

10 minute rocking intervals. After adsorption, fresh 1X SF-900 II SFM (Gibco BRL) supplemented with antibiotics, as mentioned above, and 100 μg/ml Ganciclovir. Ganciclovir was added only for the generation of P1 and P2 stocks. The infection was incubated for 96 h until CPE was observed, after which the medium was transferred to sterile snap-cap tubes, centrifuged for 3400 rpm for 5 minutes, and the virus-containing supernatant, supplemented with 2% FCS, was stored in the dark at 4°C (for immediate use) or -84°C (for long term).

III. Baculovirus Plaque Assay

Sf9 cells were seeded at 8.5 x 10^5 cells per well in 6- well plates and incubated at 27°C for 1 h to allow cell attachment. 10-fold serial dilutions of viral stock were made in 1x Sf-900 II SFM media (Gibco BLR). After incubation, growth media was removed, diluted virus was added, and adsorbed for 1 h at 27°C with 10 minute rocking intervals. Cells were overlaid with 4% agar and 1.3X Sf 900 Medium in a 1:3 ratio (Gibco BRL) supplemented with 100 μg/mL penicillin, 100 μg/mL streptomycin sulfate, 1 μg/mL amphotericin B, and 150 μg/ml X-Gal. Plates were incubated at 27°C in a sealed plastic bag containing moist paper towel for 4 d.p.i.

IV. Analysis for Recombinant Protein Expression

IV-i. SDS-PAGE Protein Mini-gel

Infect Sf9 cells as described under 'Baculovirus stock and amplification'. Growth medium was discarded, and cells were pelleted in 1 ml of 1X PBS at 13, 500 rpm for 10 minutes. The supernatant was removed and pellet was resuspended in approximately 100 µl of 5X SDS-PAGE sample buffer (0.3 M Tris, pH 6.8; 50% Glycerol; 0.3 M SDS; 5 mM DTT; 10 mM Bromophenol blue). 10% SDS-PAGE (8.3 cm x 6.2 cm x 0.075 cm) were poured and polymerized for 1 h. Samples were heated to 95°C for 5 minutes prior to loading and electrophoresed for ~ 1 h at 180 V in Mini-Protean® II (BioRad).

IV-ii. Coomassie Stain

Protein gels were stained using MAPS (microwave assisted protein staining) method (Nesatyy *et al.* 2002). This method involves the following steps: gel was fixed in 100 ml solution of 30% Isopropanol and 10% Acetic acid, then stained with 100 ml of Coomassie brilliant blue (Coomassie Brilliant Blue R-250, 2.5 mg/ml) (Fisher), and finally destained in solution of 10% Methanol and 10% Acetic acid. The gel was incubated in each solution at each step by heating for 1 minute in the microwave at 700 W (or High power). At certain times, gels were allowed to destain overnight rather than microwaving - conventional method.

Protein bands were visualized by Gel Doc 2000 (Bio Rad) and some were subsequently gels were dried between layers of cellophane for preservation.

V-iii. Western Blot

After electrophoresis, as described above, the protein bands were transferred onto Immobilon-P membrane (Millipore, Billerica, MA) in transblot buffer (39 mM glycine, 48 mM Tris, 0.037% SDS, 20% methanol) for 15 minutes at 50 V. Western blots were carried out in conical tubes. The membrane was blocked with blocking buffer (5% Skim milk, 0.04% sodium azide, 0.05% Tween 20, 20 mM Tris base, 0.1 M NaCl) for 3 h. Primary antibodies were applied to the membrane(s) for 1.5 h, with the following dilutions made in blocking buffer: mouse anti-His monoclonal Ab 1:1 dilution (courtesy of John Wilkin's Lab), rabbit anti-avian reovirus polyclonal Ab 1:3000 dilution, mouse anti-V5-HRP monoclonal Ab 1:5000 dilution (Invitrogen). The membrane(s) was washed in TBST, pH 7.5 (0.05% Tween 20, 20 mM Tris base, 0.1 M NaCl) then treated with 0.1% bovine serum albumin in TBST for 10 minutes. HorseRadish Peroxidase conjugated goat anti-rabbit or goat anti-mouse secondary antibodies in 1:3000 dilution in 0.1 bovine serum albumin/TBST was applied to the membrane for 1.5 h, then washed with TBST. The antibody-bound proteins were detected with a developing solution of DiAminoBenzoate, 1X PBS, 0.02% $CoCl_2$, and 0.006% H_2O_2.

REFERENCES

Ahmed, R., P.R. Chakraborty, and B.N. Fields. 1980. Genetic variation during lytic reovirus infection: high-passage stocks of wild-type reovirus contain temperature-sensitive mutants. J. Virol. **34:**285-287.

Amerongen, H.M., G.R. Wilson, B.N. Fields, and M.R. Neutra. 1994. Proteolytic processing of reovirus is required for adherence to intestinal M cells. J. Virol. **68:**8428-8432.

Antczak, J.B., R. Chmelo, D.J. Pickup, and W.K. Joklik. 1982. Sequences at both termini of the 10 genes of reovirus serotype 3 (strain Dearing). Virology **121:**307-319.

Antczak, J.B., and W.K. Joklik. 1992. Reovirus genome segment assortment into progeny genomes studied by the use of monoclonal antibodies directed against reovirus proteins. Virology **187:**760-776.

Attoui, H., F. Mohd Jaafar, M. Belhouchet, P. Biagini, J.F. Cantaloube, P. de Micco, and X. de Lamballerie. 2005. Expansion of family Reoviridae to include nine-segmented dsRNA viruses: Isolation and characterization of a new virus designated aedes pseudoscutellaris reovirus assigned to a proposed genus (Dinovernavirus). Virology **343:**212-223.

Barton, E.S., J.D. Chappell, J.L. Connolly, J.C. Forrest, and T.S Dermody. 2001. Reovirus receptors and apoptosis. Virology **290:**173-180.

Barton, E.S., J.C. Forrest, J.L. Connolly, J.D. Chappell, Y. Liu, F.J. Schnell, A. Nusrat, C.A. Parkos and T.S. Dermody. 2001a. Junction adhesion molecule is a receptor for reovirus. Cell **104:**441-451.

Beattie, E., K. Denzler, J. Tartaglia, M. Perkus, E. Paoletti, and B.L. Jacobs. 1995. Reversal of the interferon-sensitive phenotype of a vaccinia virus lacking E3L by expression of the reovirus S4 gene. J Virology **69:**499-505.

Becker, M.M., M.I. Goral, P.R. Hazelton, G.S Baer, S.E. Rodgers, E.G. Brown, K.M. Coombs, and T.S Dermody. 2001. Reovirus sigmaNS protein is required for nucleation of viral assembly complexes and formation of viral inclusions. J. Virol. **75:**1459-1475.

Becker, M.M., T.R. Peters, and T.S. Dermody. 2003. Reovirus sigma NS and mu NS proteins form cytoplasmic inclusion structures in the absence of viral infection. J. Virol. **77:**5948-5963.

Bergeron, J., T. Mabrouk, S. Garzon, and G. Lemay. 1998. Characterization of the thermosensitive *ts453* reovirus mutant: increased dsRNA binding of σ3 protein correlates with interferon resistance. Virology **246:**199-210.

Bodelón, G., L. Labrada, J. Martínez-Costas, and J. Benavente. 2001. The avian reovirus genome segment S1 is a functionally tricistronic gene that expresses one structural and two nonstructural proteins in infected cells. Virology **290:**181-191.

Borsa, J., and A.F. Graham. 1968. Reovirus: RNA polymerase activity in purified virions. Biochem. Biophys. Res. Commun. **33:**895-901.

Broering, T.J., M.M Arnold, C.L. Miller, J.A. Hurt, P.L. Joyce, and M.L. Nibert. 2005. Carboxyl-proximal regions of reovirus nonstructural protein muNS necessary and sufficient for forming factory-like inclusions. J. Virol. **79:**6194-6206.

Broering, T.J., J.S. Parker, P.L. Joyce, J. Kim, and M.L. Nibert. 2002. Mammalian reovirus nonstructural protein microns forms large inclusions and colocalizes with reovirus microtubule-associated protein micro2 in transfected cells. J. Virol. **76:**8285-8297.

Calnek, B.W., J.H. Barnes, C.W. Beard, L.R. McDougald, and Y.M. Saif, eds. 1997. Diseases of Poultry. 10th ed. Iowa State University Press, Ames, Iowa.

Chaly, N., M. Johnstone, and R. Hand. 1980. Alterations in nuclear structure and function in reovirus-infected cells. Clin. Invest. Med. **2:**141-152.

Chandran, K., S.B. Walker, Y. Chen, C.M. Contreras, L.A. Schiff, T.S. Baker, and M.L. Nibert. 1999. *In vitro* recoating of reovirus cores with baculovirus-expressed outer-capsid proteins μ1 and σ3. J. Virol. **73:**3941-3950.

Chang, C.T., and H.J. Zweerink. 1971. Fate of parental reovirus in infected cell. Virology **46:**544-555.

Chappell, J.D., A.E. Prota, T.S. Dermody, and T. Stehle. 2002. Crystal structure of reovirus attachment protein σ1 reveals evolutionary relationship to adenovirus fiber. EMBO J. **21:**1-11.

Chappell, J.D., R. Duncan, P.P.C. Mertens, and T.S. Dermody. 2005. Genus *Orthoreovirus*. *In:* Virus Taxonomy Eighth Report of the International Committee on Taxonomy of Viruses. 8th ed. Eds. Fauquet, C.M., M.A. Mayo, J. Maniloff, U. Desselberger, and L.A. Ball. Elsevier Inc., San Diego, CA, pp. 455-465.

Chenna, R., H. Sugawara, T. Koike, R. Lopez, T.J. Gibson, D.G. Higgins, and J.D. Thompson. 2003. Multiple sequence alignment with the Clustal series of programs. Nucleic Acids Res. **31:**3497-3500.
(http://www.ebi.ac.uk/clustalw/).

Clemens, M.J. 1996. Protein kinases that phosphorylate eIF2 and eIF2B and their role in eukaryotic cell translational control. *In*: Translational Control. Eds. Hershey J., M. Mathews, and N. Sonenberg. Cold Spring Harbor Laboratory Press, Cold Spring Harbor, NY, pp. 139-172.

Coombs, K.M. 1998. Temperature-sensitive mutants of reovirus. Curr. Top. Microbiol. Immunol. **233:**69-107.

Coombs, K.M., S.-C. Mak, and L.D. Petrycky-Cox. 1994. Studies of the major reovirus core protein σ2: reversion of the assembly-defective mutant *tsC447* is an intragenic process and involves back mutation of Asp-383 to Asn. J. Virol. **68:**177-186.

Costas, C., J. Martínez-Costas, G. Bodeló, and J. Benavente. 2005. The second open reading frame of the avian reovirus S1 gene encodes a transcription-dependent and CRM1-Independent nucleocytoplasmic shuttling protein. J. Virol. **79:**2141-2150.

Cross, R.K., and B.N. Fields. 1972. Temperature-sensitive mutants of reovirus type 3: studies on the synthesis of viral RNA. Virology **50:**799-809.

Danis, C., S. Garzon, G. Lemay. 1992. Further characterization of the ts453 mutant of mammalian orthoreovirus serotype 3 and nucleotide sequence of the mutated S4 gene. Virology **190:**494-498.

De Beneditti, A., G.J. Williams, and C. Baglioni. 1985. Inhibition of binding to initiation complexes of nascent reovirus mRNA by double-stranded RNA-dependent protein kinase. J. Virol. **54:**408-413.

DeLano, W.L. 2004. The PyMOL molecular graphics system. (http://www.pymol.org)

Dichter, M.A., and H.L. Weiner. 1984. Infection of neuronal cell cultures with reovirus mimics in vitro patterns of neurotropism. Ann. Neurol. **16:**603–10.

Dryden, K.A., D.L. Farsetta, G. Wang, J.M. Keegan, B.N. Fields, T.S. Baker, and M. Nibert. 1998. Internal structures containing transcriptase-related proteins in top component particles of mammalian orthoreovirus. Virology **245:**33-46.

Dryden, K.A., G. Wang, M. Yeager, M.L. Nibert, K.M. Coombs, D.B. Furlong, B.N. Fields, and T.S. Baker. 1993. Early steps in reovirus infection are associated with dramatic changes in supramolecular structure and protein conformation: analysis of virions and subviral particles by cryoelectron microscopy and image reconstruction. J. Cell. Biol. **122:**1023-1041.

Duncan, R. 1999. Extensive sequence divergence and phylogenetic relationships between the fusogenic and nonfusogenic Orthoreoviruses: a species proposal. Virology **260:**316-328.

Duncan, R. 1996. The low pH-dependent entry of avian reovirus is accompanied by two specific cleavages of the major outer capsid protein μ2C. Virology **219:**179-189.

Duncan, R., D. Home, L.W. Cashdollar, W.L. Joklik, and P.W.K. Lee. 1990. Identification of conserved domains in the cell attachment proteins of the three serotypes of reovirus. Virology **174:**399-409.

Duncan, R., and K. Sullivan. 1998. Characterization of two avian reoviruses that exhibit strain-specific quantitative differences in their syncytium-inducing and pathogenic capabilities. Virology **250:**263-272.

Enebak, S.A. 1992. Characterization of dsRNA-containing strains of Cryphonectria parasitica recovered from the central Appalachian. Ph.D. thesis. West Virginia University, Morgantown.

Ernst, H., and A.J. Shatkin. 1985. Reovirus hemagglutinin mRNA codes for two polypeptides in overlapping reading frames. Proc. Natl. Acad. Sci. USA. **82:**48-52.

Estes, M.K. 2001. Rotaviruses and their replication. *In:* Fields Virology. 4th ed. Eds. Knipe, D.V. and P.M. Howley. Lippincott Williams and Wilkins, Philadelphia, PA, pp. 1835-1869.

Fields, B.N. 1971. Temperature-sensitive mutants of reovirus type 3: features of genetic recombination. Virology **46:**142-148.

Fields, B.N. 1973. Genetic reassortment with reovirus mutants. *In:* Virus research. Proceedings of 2nd ICN-UCLA Symposium on Molecular Biology. Eds. Fox, C.F., and W. S. Robinson. Academic Press, New York, pp. 461-479.

Fields, B.N. 1996. Reoviridae. *In*: Fields Virology. Eds. Fields, B.N., D.M. Knipe, and P.M. Howley. 3rd ed. Lippincott-Raven, Philadelphia, PA, pp. 1553-1555.

Fields, B.N., and W.K. Joklik. 1969. Isolation and preliminary genetic and biochemical characterization of temperature-sensitive mutants of reovirus. Virology **37:**335-342.

Fields, B.N., C.S. Raine, S.G. Baum. 1971. Temperature-sensitive mutants of reovirus type 3: Defects in viral maturation as studied by immunofluorescence and electron microscopy. Virology **43:**569-578.

Follet, E.A., C.R. Pringle, and T.H. Pennington. 1975. Virus development in enucleated cells: echovirus, poliovirus, pseudorabies virus, reovirus, respiratory syncytial virus and Semliki forest virus. J. Gen. Virol. **26:**183-196.

Furuichi, Y., M. Morgan, S. Muthukrishnan, and A.J. Shatkin. 1975. Reovirus messenger RNA contains a methylated, blocked 5′-terminal structure: m7G(5′)ppp(5′)G-MpCp-. Proc. Natl. Acad. Sci. USA. **72:**362-366.

Furuichi, Y., S. Muthukrishnan, J. Tomasz, and A.J. Shatkin. 1976. Mechanism of formation of reovirus mRNA 5′-terminal blocked and methylated sequence, ^{m7}GpppG^{m}pC. J. Biol. Chem. **251:**5043-5053.

Gershowitz, A., and R.W. Wooley. 1973. Characterization of two reoviruses isolated from turkeys with infectious enteritis. Avian Dis. **17:**406-414.

Giantini, M., L.S. Seliger, Y. Furuichi, and A.J. Shatkin. 1984. Reovirus type 3 genome segment S4: nucleotide sequence of the gene encoding a major virion surface protein. J. Virol. **52:**984-987.

Glass, S.E., S.A. Nagi, C.F. Hall, and K.M. Kerr. 1973. Isolation and characterization of a virus associated with arthritis of chickens. Avian Dis. **17:**415-424.

Gonziález-López, C., J. Martínez-Costas, M. Esteban, and J. Benavente. 2003. Evidence that avian reovirus σA protein is an inhibitor of the double-stranded RNA-dependent protein kinase. J. Gen. Virol. **84:**1629-1639.

Gouvea, V., and T.J. Schnitzer. 1982. Polymorphism of the genomic RNAs among avian reoviruses. J. Gen. Virol. **61:**87-91.

Gupta, S.L., S.L. Holmes, and L.L. Mehra. 1982. Interferon action against reovirus: activation of interferon-induced protein kinase in mouse L929 cells upon reovirus infection. Virology **120:**495-499.

Hadzisejdić, I. 2005. Mammalian reovirus: characterization of outer capsid protein changes along virus to ISVP transition pathway. M.Sc. Thesis. University of Manitoba, Winnipeg.

Hammond, G.W., P.R. Hazelton, I. Cheung, and B. Klisko. 1981. Improved detection of viruses by electron microscopy after direct ultracentrifuge preparation of specimens. J. Clin. Microbiol. **14:**210-221.

Harrison, S.C. 2001. Virus structure. *In:* Fields Virology. 4th ed. Eds. Knipe, D.M., and P.M. Howley. Lippincott Williams and Wilkins, Philadelphia, PA, pp. 53-85.

Hazelton, P.R., and K.M. Coombs. 1999. The reovirus mutant *tsA279* L2 gene is associated with generation of a spikeless core particle: implications for capsid assembly. J. Virol. **73:**2298-2308.

Hazelton, P.R., and K.M. Coombs. 1995. The reovirus mutant *tsA279* has temperature-sensitive lesions in the M2 and L2 genes: the M2 gene is associated with decreased viral protein production and blockade in transmembrane transport. Virology **207:**46-58.

Heironymus, D.R., K.P. Villegas, and S.H. Kleven. 1983. Identification and serological differentiation of several reovirus strains isolated from chickens with suspected malabsorption syndrome. Avian Dis. **27:**246-254.

Hermann, L.L. 2005. Characterization of a novel reovirus and antiviral activity against mammalian reovirus. Ph.D. Thesis. University of Manitoba, Winnipeg.

Hillman, B.I., S. Supyani, H. Kondo, N. Suzuki. 2004. A reovirus of the fungus Cryphonectria parasitica that is infectious as particles and related to the coltivirus genus of animal pathogens. J. Virol. **78**:892-898.

Hovanessian, A.G. 1991. Interferon-induced and dsRNA activated enzymes: a specific protein kinase and 2'5'-oligodenylate synthetases. J. Interferon. Res. **11:**199-205.

Hsiao, J., J. Martínez-Costas, J. Benavente, and V.N. Vakharia. 2002. Cloning, expression, and characterization of avian reovirus guanylyltransferase. Virology **296:**288-299.

Huismans, H., and W.K. Joklik. 1976. Reovirus-coded polypeptides in infected cells: isolation of two naïve monomeric polypeptides with affinity for single-stranded and double-stranded RNA, respectively. Virology **70:**411-424.

Ikegami, N., and P.J. Gomatos. 1968. Temperature-sensitive conditional-lethal mutants of reovirus 3: isolation and characterization. Virology **36:**447-458.

Jacobs, B.L., and C.E. Samuel. 1985. The reovirus S1 mRNA encodes two primary translation products. Virology **143:**63-74.

Jané-Valbuena, J., L.A. Breun, L.A. Schiff, and M.L. Nibert. 2002. Sites and determinants of early cleavages in the proteolytic processing pathway of reovirus surface protein sigma 3. J. Virol. **76:**5184-5197.

Jané-Valbuena, J., M.L. Nibert, S.M. Spencer, S.B. Walker, T.S. Baker, Y. Chen, V.E. Centonze, and L.A. Schiff. 1999. Reovirus virion-like particles obtained by recoating infectious subvirion particles with baculovirus-expressed σ3 protein: an approach for analyzing σ3 functions during virus entry. J. Virol. **73:** 2963-2973.

Jeffrey, I.W., S. Kadereit, E.F. Meurs, T. Metzger, M. Bachmann, M. Schwemmle, A.G. Hovanessian, and M.J. Clemens. 1995. Nuclear localization of the interferon-inducible protein kinase PKR in human cells and transfected mouse cells. Exp. Cell. Res. **218:**17-27.

Johansson, P.J., T. Sveger, K. Ahlfors, J. Ekstrand, L. Svensson. 1996. Reovirus type 1 associated with meningitis. Scand. J. Infect. Dis. **28:**117–20.

Joklik, W.K. 1998. Assembly of the reovirus genome. Curr. Top. Microbiol. Immunol. **233:**57-68.

Joklik, W.K. 1972. Studies on the effect of chymotrypsin on reoviruses. Virology **49:**700-715.

Joklik, W.K., and M.R. Roner. 1995. What reassorts when reovirus genome segments reassort? J. Biol. Chem. **270:**4181-4184.

Jordan, F.T.W., and M. Pattison, eds. 1996. Reoviridae: *In*: Poultry Diseases. 4th ed. W.B. Saunders Company, London, pp 218-225.

Joske, R.A., D.D Keall, P.J. Leak, N.F. Stanley, and M.N. Walters. 1964. Hepatitis encephalitis in humans with reovirus infections. Arch. Intern. Med. **113:**811–816.

Kapikian, A., Y. Hoshino, and R. Chanock. Rotaviruses. 2001. *In:* Fields Virology. 4th ed. Eds. Knipe, D.M., and P.M. Howley. Lippincott-Raven, Philadelphia, PA, pp. 1787–1833.

Kapuler, A.M., N. Mendelsohn, H. Klett, and G. Acs. 1970. Four base-specific nucleoside 5′-triphosphatases in the subviral core of reovirus. Nature **225:**1209-1213.

Keirstead, N.D., and K.M. Coombs. 1998. Absence of superinfection exclusion during asynchronous reovirus infections of mouse, monkey, and human cell lines. Virus Res. **54:**225-235.

Kharrat, A., M.J. Macias, T.J. Gibson, M. Nilges, and A. Pastore. 1995. Structure of the dsRNA binding domain of *E. coli* RNase III. EMBO J. **14:**3572-3584.

Klasco, R. 2002. Colorado tick fever. Med. Clin. North Am. **86:**435–440.

Kouwenhoven, B., M. Vertommen, and J.H. van Eck. 1978. Runting and leg weakness in broilers: involvement of infectious factors. Vet. Sci. Comm. **2:** 253-259.

Kozak, M., and A.J. Shatkin. 1978. Identification of features in 5′ terminal fragments from reovirus mRNA which are important for ribosome binding. Cell **13:** 201-212.

Krainer, L., and B.E. Aronson. 1959. Disseminated encephalomyelitis in humans with recovery of hepatoencephalitis virus. J. Neuropathol. Exp. Neurol. **18:**339–42.

Lambden, P.R., S.J. Cooke, E.O. Caul, and I.N. Clarke. 1992. Cloning of noncultivatable human rotavirus by single primer amplification. J. Virol. **66:**1817-1822.

Lee, P.W., E.C. Hayes, and W.K. Joklik. 1981. Protein σ1 is the reovirus cell attachment protein. Virology **108:**156–63.

Lemay, G. and C. Danis. 1994. Reovirus lambda 1 protein: affinity for double-stranded nucleic acids by a small amino-terminal region of the protein independent from the zinc finger motif. J. Gen. Virol. **75:**3261-3266.

Liemann, S., K. Chandran, T.S. Baker, M.L. Nibert, and S.C. Harrison. 2002. Structure of the reovirus membrane-penetration protein, μ1, in a complex with its protector protein, σ3. Cell **108:**283-295.

Liu, H.-J., P.-Y. Lin, , J.-W. Lee, H.-Y. Hsu, and W.-L. Shih. 2005. Retardation of cell growth by avian reovirus p17 through the activation of p53 pathway. Biochem. Biophys. Res. Commun. **336:**709-715.

Liu, Y., A. Nusrat, F.J. Schnell, T.A. Reaves, S. Walsh, M. Pochet, and C.A. Parkos. 2000. Human junction adhesion molecule regulates tight junction resealing in epithelia. J. Cell Sci. **113:**2363–2374.

Lloyd, R.M., and A.J. Shatkin. 1992. Translational stimulation by reovirus polypeptide σ3: substitution for VAI RNA and inhibition of phosphorylation of the α subunit of eukaryotic initiation factor 2. J. Virol. **66:**6878-6884.

Lynch, M., B. Lee, P. Azimi, J. Gentsch, C. Glaser, S. Gilliam, H.G. Chang, R. Ward, and R.I. Glass. 2001 Rotavirus and central nervous system symptoms: cause or contaminant? Case reports and review. Clin. Infect. Dis. **33:**932–938.

Mabrouk, T., and G. Lemay. 1994. Mutations in a CCHC zinc-binding motif of the reovirus sigma 3 protein decrease its intracellular stability. J. Virol. **68:**5287-5290.

Mabrouk, T., C. Danis, and G. Lemay. 1995. Two basic motifs of reovirus σ3 protein are involved in double-stranded RNA binding. Biochem. Cell. Biol. **73:**137-145.

Martin-Padura, I., S. Lostaglio, M. Schneemann, L. Williams, M. Romano, P. Fruscella, C. Panzeri, A. Stoppacciaro, L. Ruco, A. Villa, D. Simmons, and E. Dejana. 1998. Junctional adhesion molecule, a novel member of the immunoglobulin superfamily that distributes at intercellular junctions and modulates monocyte transmigration. J. Cell. Biol. **142:**117–127.

Martínez-Costas, J., A. Grande, R. Varela, C. García-Martínez, and J. Benavente. 1997. Protein architecture of avian reovirus S1133 and identification of the cell attachment protein. J. Virol. **71:** 59-64.

Martínez-Costas, J., R. Varlea, and J. Benavente. 1995. Endogenous enzymatic activities of the avian reovirus S1133: identification of the viral capping enzyme. Virology **206:**1017-1026.

Mathews, M.B. 1996. Interactions between viruses and the cellular machinery for protein synthesis. *In:* Translational Control. Eds. Hershey, J.W.B., M.B. Mathews, and N. Sonenberg. Cold Spring Harbor Laboratory Press, Cold Spring Harbor, NY, pp 505-548.

McCarthy, C. 2001. Chromas© version 2.13. School of Health Science, Griffith University, Gold Coast Campus, Southport, Queensland, Australia.

Mendez, I.I., Y.-M. She, W. Ens, and K.M. Coombs. 2003. Digestion pattern of reovirus outer capsid protein σ3 determined by mass spectrometry. Virology **311:**289-304.

Mickel, S., V. Arena Jr., and W. Bauer. 1977. Physical properties and gel electrophoresis behavior of R12-derived plasmid DNAs. Nucleic Acids. Res. **4:**1465-1482.

Mikulasova, A., E. Vareckova, and E. Fodor. 2000. Transcription and replication of the influenza a virus genome. Acta. Virol. **44**:273-282.

Miyamoto, N.G., and C.E. Samuel. 1980. Mechanism of interferon action: interferon-mediated inhibition of reovirus mRNA translation in the absence of detectable mRNA degradation but in the presence of protein phosphorylation. Virology **107:**461-475.

Morrison, L.A., R.L. Sidman, and B.N. Fields. 1991. Direct spread of reovirus from the intestinal lumen to the central nervous system through vagal autonomic nerve fibers. Proc. Natl. Acad. Sci. USA. **88:**3852–6.

Mustoe, T.A., R.F. Ramig, A.H. Sharpe, and B.N. Fields. 1978. A genetic map of reovirus III. Assignment of the double-stranded RNA-positive mutant groups A, B, and G to genome segments. Virology **85:**545-556.

Nanduri, S., B.W. Carpick, Y. Yang, B.R.G. Williams, and J. Qin. 1998. Structure of the double-stranded RNA-binding domain of the protein kinase PKR reveals the molecular basis of its dsRNA-mediated activation. EMBO J. **17:**5458-5465.

Neelima, S., G.C. Ram, J.M. Kataria, and T.K. Goswami. 2003. Avian reovirus induces an inhibitory effect on lymphoproliferation in chickens. Vet. Res. Commun. **27:**73-85.

Nesatyy, V.J., A. Dacanay, J.F. Kelly, and N.W. Ross. 2002. Microwave-assisted protein staining: mass spectrometry compatible methods for rapid protein visualisation. Rapid Commun. Mass Spectrom. **16:**272-280.

Ni, Y., and M.C. Kemp. 1994. Subgenomic S1 segments are packaged by avian reovirus defective interfering particles having an S1 segment deletion. Virus Res. **32**:329-342.

Ni, Y., and R. Ramig. 1993. Characterization of avian reovirus-induced cell fusion: the role of viral structural proteins. Virology **194:**705-714.

Ni, Y., R.F. Ramig, and M.C. Kemp. 1993. Identification of proteins encoded by avian reoviruses and evidence for post-translational modification. Virology **193:**466-469.

Nibert, M.L., and B.N. Fields. 1992. A carboxy-terminal fragment of protein μ1/μ1C is present in infectious subvirion particles of mammalian reoviruses and is proposed to have a role in penetratin. J. Virol. **66:**6408-6418.

Nibert, M.L., R.L. Margraf, and K.M. Coombs. 1996. Nonrandom segregation of parental alleles in reovirus reassortants. J. Virol. **70:**7295-7300.

Nibert, M.L. and L.A. Schiff. 2001. Reoviruses and their replication. *In:* Fields Virology. 4th ed. Eds. Knipe, D.V. and P.M. Howley. Lippincott Williams and Wilkins, Philadelphia, PA, pp.793-842.

Nibert, M.L., T.S. Dermody, and B.N. Fields. 1990. Structure of the reovirus cell-attachment protein: a model for the domain organization of σ1. J. Virol. **64:** 2976-2989.

Noad, L. 2004. Characterization of orthoreovirus core proteins by sequencing and proteomic analysis of avian reovirus mu proteins and development of anti-mammalian reovirus core protein monoclonal antibodies. M.Sc. Thesis. University of Manitoba, Winnipeg.

Noble, S., and M.L. Nibert. 1997. Characterization of an ATPase activity in reovirus cores and its genetic association with core-shell protein λ1. J. Virol. **71:**2182-2191.

O'Hara, D., M. Patrick, D. Cepica, K.M. Coombs, and R. Duncan. 2001. Avian reovirus major mu-class outer capsid protein influences efficiency of productive macrophage infection in a virus strain-specific manner. J. Virol. **75:**5027-5035.

Olland, A.M., J. Jane-Valbuena, L.A. Schiff, M.L. Nibert, S.C. Harrison. 2001. Structure of the reovirus outer capsid and dsRNA-binding protein s3 at 1.8 Å resolution. EMBO J. **20:**979-989.

Olson, N.O. 1959. Transmissible synovitis of poultry. Lab. Invest. **8:** 1384-1393.

Olson, N.O. 1978. Reovirus infections. *In:* Diseases of poultry. Ed. Hofstad, M.S. Iowa State University Press, Ames, Iowa, pp. 641-647.

Olson, N.O., and D.P. Solomon. 1968. A natural outbreak of synovitis caused by the viral arthritis agent. Avian Dis. **12:** 311-316.

Osaki, H., C.Z. Wei, M. Arakawa, T. Iwanami, K. Nomura, N. Matsumoto, and Y. Ohtsu. 2002. Nucleotide sequences of double-stranded RNA segments from a hypovirulent strain of the white root rot fungus Rosellinia necatrix: possibility of the first member of the Reoviridae from fungus. Virus Genes **25:**101-107.

Patrick, M.K, R. Duncan, and K.M. Coombs. 2001. Generation and genetic characterization of avian reovirus temperature-sensitive mutants. Virology **284:** 113-122.

Patrick, M.K. 2001. The generation and characterization of avian reovirus temperature sensitive mutants. M.Sc. Thesis. University of Manitoba, Winnipeg.

Patton, J.T., and E. Spencer. 2000. Genome replication and packaging of segmented double-stranded RNA viruses. Virology **277:**217-225.

Poranen, M.M., and R. Tuma. 2004. Self-assembly of double-stranded RNA bacteriophages. Virus Res. **101:**93-100.

Prota, A.E., J.A. Campbell, P. Schelling, J.C. Forrest, M.J. Watson, T.R. Peters, M. Aurrand-Lions, B.A. Imhof, T.S. Dermody, and T. Stehle. 2003. Crystal structure of human junctional adhesion molecule 1: implications for reovirus binding. Proc. Natl. Acad. Sci. USA. **100:**5366-5371.

Ramig, R.F. and R.L. Ward. 1991. Genomic segment reassortment in rotavirus and other *Reoviridae*. Adv. Virus Res. **39:**164-207.

Ramig, R.F., T.A. Mustoe, A.H. Sharpe, and B.N. Fields. 1978. A genetic map of reovirus. II. Assigment of the double-stranded RNA-negative mutant groups C, D, and E to genome segments. Virology **85:**531-534.

Rankin, J.T., Jr., S.B. Eppes, J.B. Antczak, and W.K. Joklik. 1989. Studies on the mechanisms of the antiviral activity of ribavirin against reovirus. Virology **168:**147-158.

Reinisch, K.M., M.L. Nibert, and S.C. Harrison. 2000. Structure of the reovirus core at 3.6 Å resolution. Nature **404:**960-967.

Rescigno, M., G. Rotta, B. Valzasina, and P. Ricciardi-Castagnoli. 2001. Dendritic cells shuttle microbes across gut epithelial monolayers. Immunobiology **204:**572–581.

Roner, M.R., K. Bassett, and J. Roehr. 2004. Identification of the 5′ sequences required for incorporation of an engineered ssRNA into the Reovirus genome. Virology **329:**348-360.

Roner, M.R., and W.K. Joklik. 2001. Reovirus reverse genetics: incorporation of the *CAT* gene into the reovirus genome. Proc. Natl. Acad. Sci. USA. **98:**8036-8041.

Roner, M.R., I. Nepliouev, B. Sherry, W.K. Joklik. 1997. Construction and characterization of a reovirus double temperature-sensitive mutant. Proc. Natl. Acad. Sci. USA. **94:**6826-6830.

Rosenberger, J.K., and N.O. Olson. 1991. Reovirus infections. *In:* Diseases of Poultry. Eds. Calnek, B.W., M.J. Burnes, C.W. Beard, W.M. Reid and H.W. Yoder. Iowa State University Press, Ames, Iowa.

Rosenberger, J.K., F.J. Sterner, S. Botts, K.P. Lee, and A. Margolin. 1989a. *In vitro* and *in vivo* characterization of avian reoviruses. Pathogenicity and antigenic relatedness of several avian reovirus isolates. Avian Dis. **33:**535-544.

Rosenberger, J.K., F.J. Sterner, S. Botts, K.P. Lee, and A. Margolin. 1989. *In vitro* and *in vivo* characterization of avian reoviruses. I. Pathogenicity and antigenic relatedness of several avian reovirus isolates. Avian Dis. **29:**465-478.

Roy, P. 2001. Orbiviruses. *In:* Fields Virology. 4th ed. Eds. Knipe, D.V. and P.M. Howley. Lippincott Williams and Wilkins, Philadelphia, PA, pp. 1835-1869.

Ryter, J.M., and S.C. Schultz. 1998. Molecular basis of double-stranded RNA-protein interactions: structure of a dsRNA-binding domain complexed with dsRNA. EMBO J. **17:**7505-7513.

Sabin, A.B. 1959. Reoviruses: a new group of respiratory and enteric viruses formerly classified as ECHO type 10 is described. Science **130:**1387–9.

Schiff, L.A., M.L. Nibert, M.S. Co, E.G. Brown, and B.N. Fields. 1988. Distinct binding sites for zinc and double-stranded RNA in the reovirus outer capsid protein sigma 3. Mol. Cell. Biol. **8:**273-283.

Schmechel, S., M. Chute, P. Skinner, R. Anderson, and L. Schiff. 1997. Preferential translation of reovirus mRNA by a sigma3-dependent mechanism. Virology **232:**62-73.

Schnitzer, T.J. 1985. Protein coding assignment of the S genes of avian reovirus S1133. Virology **141:**167-170.

Shapouri, M.R., M. Arella, and A. Silim. 1996. Evidence for the multimeric nature and cell binding ability of avian reovirus sigma 3 protein. J. Gen. Virol. **77:**1203-1210.

Sharp, A.H., and B.N. Fields. 1981. Reovirus inhibition of cellular DNA synthesis: Role of the S1 gene. J. Virol. **38:**389-392.

Shatkin, A.J., and A.J. LaFiandra. 1972. Transcription by infectious subviral particles of reovirus. J. Virol. **10:**698-706.

Shatkin, A.J., and J.D. Sipe. 1968. RNA polymerase activity in purified reoviruses. Proc. Natl. Acad. Sci. USA. **61:**1462-1469.

Shepard, D.A., J.G. Ehnstrom, and L.A. Schiff. 1995. Association of reovirus outer capsid proteins σ3 and μ1 causes a conformational change that renders σ3 protease sensitive. J. Virol. **69:**8180-8184.

Shepard, D.A., J.G. Ehnstrom, P.J. Skinner, and L.A. Schiff. 1996. Mutations in the zinc-binding motif of the reovirus capsid protein delta 3 eliminate its ability to associate with capsid protein mu 1. J. Virol. **70:**2065-2068.

Shing, M., and K.M. Coombs. 1996. Assembly of the reovirus outer capsid requires mu 1/sigma 3 interactions which are prevented by misfolded sigma 3 protein in temperature-sensitive mutant tsG453. Virus Res. **46:**19-29.

Shmulevitz, M., Z. Yameen, S. Dawe, J. Shou, D. O'Hara, I. Holmes, and R. Duncan. 2002. Sequential partially overlapping gene arrangement in the tricistronic S1 genome segments of avian reovirus and nelson bay reovirus: implications for translation initiation. J. Virol. **76:** 609-618.

Skehel, J.J., and W.K. Joklik. 1969. Studies on the *in vitro* transcription of reovirus RNA catalyzed by reovirus cores. Virology **39:**822-831.

Silverstein, S.C, J.K. Christman, and G. Acs. 1976. The reovirus replicative cycle. Annu. Rev. Biochem. **45:**375-408.

Smith, J.A., S.C. Schmechel, B.R. Williams, R.H. Silverman, L.A. Schiff. 2005. Involvement of the interferon-regulated antiviral proteins PKR and Rnase L in reovirus-induced shutoff of cellular translation. J. Virol. **79:**2240-2250.

Southern, J.A., D.F. Young, F. Heaney, W. Baumgartner, and R.E. Randall. 1991. Identification of an epitope on the P and V proteins of Simian Virus 5 that distinguishes between two isolates with different biological characteristics. J. Gen. Virol. **72:**1551-1557.

Spandidos, D.A., and A.F. Graham. 1976. Physical and chemical characterization of an avian reovirus. J. Virol. **19:** 968-976.

Stanley, N.F., D.C. Dorman, and J. Ponsford. 1953. Studies on the pathogenesis of a hitherto undescribed virus (hepato-encephalomyelitis) producing unusual symptoms in suckling mice. Aust. J. Exp. Biol. Med. Sci. **31:**147-159.

Stehle, T. and T.S. Dermody. 2003. Structural evidence for common functions and ancestry of the reovirus and adenovirus attachment proteins. Rev. Med. Virol. **13:**123-132.

Strong, J.E., G. Leone, R. Duncan, R.K. Sharma, P.W. Lee. 1991. Biochemical and biophysical characterization of the reovirus cell attachment protein σ1: evidence that it is a homotrimer. Virology **184:**23-32.

Tai, J.H., J.V. Williams, K.M. Edwards, P.F. Wright, J.E. Crowe, and T.S. Dermody. 2005. Prevalence of reovirus-specific antibodies in young children in Nashville, Tennessee. J. Infect. Dis. **191:**1221-1224.

Tardieu, M., M.L. Powers, H.L. Weiner. 1983. Age-dependent susceptibility to reovirus type 3 encephalitis: role of viral and host factors. Ann. Neurol. **13:**602–607.

Theophilus, M.B., J.-A. Huang, I.H. Holmes. 1995. Avian reovirus σC protein contains a putative fusion sequence and induces fusion when expressed in mammalian cells. Virology **208:**678-684.

Tillotson, L., and A.J. Shatkin. 1992. Reovirus polypeptide σ3 and N-terminal cleavage myristoylation of polypeptide μ1 are required for site-specific cleavage to μ1C in transfected cells. J. Virol. **66:**2180-2186.

Tourís-Otero, F., J. Martínez-Costas, V.N. Vakharia, and J. Benavente. 2005. Characterization of the nucleic acid-binding activity of the avian reovirus non-structural protein sigma NS. J. Gen. Virol. **84**:1159-1169.

Tourís-Otero, F., M.C.-S. Martín, J. Martínez-Costas, and J. Benavente. 2004a. Avian reovirus morphogenesis occurs within viral factories and begins with the selective recruitment of σNS and λA to μNS inclusions. J. Mol. Biol. **341:**361-374.

Tourís-Otero, F., J. Martínez-Costas, V.N. Vakharia, and J. Benavente. 2004. Avian reovirus nonstructural protein μNS forms viroplasm-like inclusions and recruits protein σNS to these structures. Virology **319:**94-106.

Tyler, K.L. 2001. Mammalian reoviruses. *In:* Fields Virology. 4th ed. Eds. Knipe, D.V. and P.M. Howley. Lippincott Williams and Wilkins, Philadelphia, PA, pp.1729-1745.

Tyler, K.L., E.S. Barton, M.L. Ibach, C. Robinson, J.A. Campbell, S.M. O'Donnell, T. Valyi-Nagy, P. Clarke, J.D. Wetzel, and T.S. Dermody. 2004. Isolation and molecular characterization of a novel type 3 reovirus from a child with meningitis. J. Infect. Dis. **189:**1664-1675.

Tyler, K.L., P. Clarke, R.L. DeBiasi, D. Kominsky, and G.J. Poggioli. 2001. Reoviruses and the host cell. Trends Microbiol. **9:**560-564.

Tyler, K.L., D.A. McPhee, and B.N. Fields. 1986. Distinct pathways of viral spread in the host determined by reovirus S1 gene segment. Science **233:**770–774.
van der Heide, L. 1977. Viral arthritis/tenosynovitis: a review. Avian Pathol. **6:**271-284.

Varela, R., and J. Benavente. 1994. Protein coding assignment of avian reovirus strain S1133. J. Virol. **68:**6775-6777.

Wiebe, M.E., and W.K. Joklik. 1975. The mechanism of inhibition of reovirus replication by interferon. Virology **66:**229-240.

Weiner, H.L., and W.K. Joklik. 1987. Comparison of the reovirus serotype 1, 2, and 3 S3 genome segments encoding the nonstructural proteins sigma NS. Virology **161:**332-339.

Weiner, H.L., K.A. Ault, and B.N. Fields. 1980a. Interaction of reovirus with cell surface receptors. I. Murine and human lymphocytes have a receptor for the hemagglutinin of reovirus type 3. J. Immunol. **124:**2143–8.

Weiner, H.L., D. Drayna, D.R. Averill Jr., and B.N. Fields. 1977. Molecular basis of reovirus virulence: role of the S1 gene. Proc. Natl. Acad. Sci. USA. **74:**5744–5748.

Weiner, H.L., M.L. Powers, and B.N. Fields. 1980. Absolute linkage of virulence and central nervous system tropism of reoviruses to viral hemagglutinin. J. Infect. Dis. **141:**609–616.

Wolf, J.L., D.H. Rubin, R. Finberg, R.S. Kauffman, A.H. Sharpe, J.S. Trier, and B.N. Fields. 1981. Intestinal M cells: a pathway of entry of reovirus into the host. Science **212:**471–472.

Wong, C.J., Z. Price, and D.A. Bruckner. 1984. Aseptic meningitis in an infant with rotavirus gastroenteritis. Pediatr. Infect. Dis. **3:**244–246.

Xu, P., S.E. Miller, and W.K. Joklik. 1993. Generation of reovirus core-like particles in cells infected with hybrid vaccinia viruses that express genome segments L1, L2, L3, and S2. Virology **197:**726-731.

Xu, W. 2004. Characterization of avian reovirus temperature-sensitive mutants. M.Sc. Thesis. University of Manitoba, Winnipeg.

Xu, W., M.K. Patrick, P.R. Hazelton, and K.M. Coombs. 2004. Avian reovirus temperature-sensitive mutant tsA12 has a lesion in major core protein sigma and is defective in assembly. J. Virol. **78:**11142-11151.

Xu, W., A.T. Tran, M.K. Patrick, and K.M. Coombs. 2005. Assignment of avian reovirus temperature-sensitive mutant recombination groups B, C, and D to genome segments. Virology **338:**227-235.

Yin, H.S., Y.P. Su, and L.H. Lee. 2002. Evidence of nucleotidyl phosphatase activity associated with core protein σA of avian reovirus S1133. Virology **293:**379-385.

Yue, Z., and A.J. Shatkin. 1997. Double-stranded RNA-dependent protein kinase (PKR) is regulated by reovirus structural proteins. Virology **234:**364-371.

Yue, Z., and A.J. Shatkin. 1996. Regulated, stable expression and nuclear presence of retrovirus double-stranded RNA-binding protein sigma3 in HeLa cells. J. Virol. **70:**3497-3501.

Yuwen, H., J.H. Cox, J.W. Yewdell, J.R. Bennink, and B. Moss. 1993. Nuclear localization of a double-stranded RNA-binding protein encoded by the vaccinia virus E3L gene. Virology **195:**732-744.

Zarbl, H., and S. Millward. 1983. The reovirus multiplication cycle. *In:* The Reoviridae. Ed. Joklik, W.K. Springer, Plenum, NY, pp 197-228.

Zhang, X., J. Tang, S.B. Walker, D. O'Hara, M.L. Nibert, R. Duncan, and T.S. Baker. 2005. Structure of avian orthoreovirus virion by electron cryomicroscopy and image reconstruction. Virology **343:**25-35.

Zou, S., and E.G. Brown. 1996. Stable expression of the reovirus mu2 protein in mouse L cells complements the growth of a reovirus ts mutant with a defect in its M1 gene. Virology **217:**42-48.